Discovery and demonstration of functional type IV pili production and post-translational modification by a medically relevant *Acinetobacter* species

DISSERTATION

Presented in Partial Fulfillment of the Requirements for the Degree Doctor of Philosophy in the Graduate School of The Ohio State University

By

Christian Michael Harding

Graduate Program in Biomedical Sciences.

The Ohio State University

2015

Dissertation Committee:

Daniel Wozniak, Ph.D., Advisor

Amal Amer, M.D., Ph.D.

Larry Schlesinger, M.D.

Kevin Mason, Ph.D.

Abstract

Acinetobacter nosocomialis is a member of the *Acinetobacter calcoaceticus-baumannii* complex, which are Gram-negative opportunistic pathogens of increasing relevance worldwide. Medically relevant *Acinetobacter* species form biofilms, are resistant to desiccation, and easily acquire antibiotic resistance genes, all of which contribute to its ability to cause disease. Despite many reports on the epidemiology and antibiotic resistance phenotypes of *Acinetobacter*, there are limited reports characterizing the virulence mechanisms of these important nosocomial pathogens. Type IV pili (Tfp) are transenvelope protein complexes that can act as surface appendages mediating many bacterial processes. Analysis of the genomes of fully sequenced medically relevant *Acinetobacter* strains reveals the presence of genes that encode proteins predicted to be involved with the biogenesis of Tfp. Furthermore, many medically relevant *Acinetobacter* species have been shown to exhibit twitching motility and natural transformation, two classical Tfp-associated phenotypes. Therefore we utilized mutagenesis strategies to selectively delete genes encoding proteins predicted to be involved in Tfp biogenesis and probed for Tfp functionality. In our analysis we determined that *A. nosocomialis* strain M2 did produce functional Tfp, which were required for natural transformation and twitching motility. During the course of our studies we also identified that the major pilin subunit, PilA, of the Tfp fiber was

post-translationally modified. Subsequently we determined that PilA was glycosylated by the pilin-specific oligosaccharyltransferase, TfpO, at the carboxy-terminal serine. Lastly, we demonstrated that many *Acinetobacter* species encode two functional oligosaccharyltransferases, one devoted exclusively to pilin glycosylation and the other to general protein glycosylation. This study is the first to describe the production of functional Tfp production by a medically relevant *Acinetobacter* species and also demonstrated that the pilin glycosylation system shares a common pathway with the general protein glycosylation pathway.

Dedication

To Robert S. Munson, Jr.

Acknowledgments

First and foremost, I want to thank my family. Simon and Ian, you are the best brothers and I'm so proud of you. Dad, thanks for supporting me anytime I needed help and even when I didn't. Mom, thanks for being eternally loving. Ashley, I love you endlessly and could not have done this without you.

I want to thank my undergraduate mentor, Pamela Riggs-Gelaso, Ph.D., for giving me my first opportunity to work in a research lab. You believed in me and that provided me with the confidence I needed to pursue graduate school.

Thanks to my committee, Amal Amer, Larry Schlesinger, and Dan Wozniak for not sugar coating my project and its problems. I will not forget the simple advice of focus and the impact that it had.

I want to thank Beth Baker, Michael Carruthers, Erin Grundy, Alistair Harrison, and Estevan Santana for teaching me to clone. These are skills I will never forget. Lastly, I want to thank Robert Munson for molding me into a scientist, a critical thinker, and an honorable man. You truly will always be a mentor to me.

Vita

2009 .....B.S. Biology, College of Charleston

2009-2010 .....Chemical Stock Room Manager, College of Charleston

2010 to present .....Graduate Research Associate, Department of Pediatrics, The Ohio State University

Publications

Harding CM, Tracy EN, Carruthers MD, Rather PN, Actis LA, Munson RS, Jr. 2013. *Acinetobacter baumannii* strain M2 produces type IV pili which play a role in natural transformation and twitching motility but not surface-associated motility. mBio 4(4):e00360-13. doi:10.1128/mBio.00360-13.

Carruthers MD, Harding CM, Baker BD, Bonomo RA, Hujer KM, Rather PN, Munson RS, Jr. 2013. Draft genome sequence of the clinical isolate *Acinetobacter nosocomialis* strain M2. Genome Announc. 1(6):e00906-13. doi:10.1128/genomeA.00906-13.

Harding CM, Nasr MA, Kinsella RL, Scott NE, Foster LJ, Weber BS, Fiester SE, Actis LA, Tracy EN, Munson RS, Jr, Feldman, MF. 2015. *Acinetobacter* strains carry two functional oligosaccharyltransferases, one devoted exclusively to type IV pilin, and the other one dedicated to *O*-glycosylation of multiple proteins. Molecular Microbiology. DOI: 10.1111/mmi.12986.

Fields of Study

Major Field: Biomedical Sciences

Specialization: Microbial Pathogenesis

Table of Contents

List of Tables

List of Figures

Chapter 1: Introduction

1.1 *Acinetobacter* background

The genus *Acinetobacter* comprises a group of Gram-negative coccobacilli within the *Moraxellaceae* family first described by Brisou and Prevot (1). Bacteria within the genus *Acinetobacter* are classified as strictly aerobic, catalase-positive, and oxidase-negative. *Acinetobacter* species are capable of growing in minimal media with acetate as the sole carbon source and ammonia as the sole nitrogen source (2). Early attempts to assign bacteria to the genus utilized a transformation assay, where, DNA extracts from Gram-negative, oxidase-negative bacteria were purified and used as a source of donor DNA to transform auxotrophs of a competent *Acinetobacter* strain into a prototrophic strain (3). The etymology of the genus name *Acinetobacter* roughly translates to “non-motile rod,” however, some species and strains from the *Acinetobacter* genus are capable of bacterial locomotion such as type IV pili-dependent twitching motility; additionally, some species and strains exhibit a flagella-independent, type IV pili-independent surface-associated motility on semi-solid media (2, 4-6).

As of 1986, only *A. calcoaceticus* and *A. lwoffi* were recognized by the *Approved Lists of Bacterial Names* as species with the *Acinetobacter* genus; thus,

prompting the delineation of the genus into groups and species. Due to insufficient criteria for species delineation and the difficulty separating species phenotypically, DNA-DNA hybridization assays comparing DNA relatedness between *Acinetobacter* species were established as the standard for species grouping (7-9). Using 85 *Acinetobacter* strains, Bouvet and Grimont defined twelve DNA groups, designated as genomic species one through twelve. Within the genomic species hierarchy, the two original *Acinetobacter* species, *A. calcoaceticus* and *A. lwoffi*, were designated as genomic species 1 and genomic species 8, respectively. Four additional genomic groups were assigned officially as *A. baumannii* (genomic species 2), *A haemolyticus* (genomic species 4), *A. junii* (genomic species 5), and *A. johnsonnii* (genomic species 7) (8). Tjernberg and Ursing extended the use of DNA-DNA hybridization for *Acinetobacter* genomic grouping and further identified three additional genomic groups designated 13TU, 14TU, and 15TU (10). Although the DNA-DNA hybridization methodologies established distinct genomic species, DNA groups 1, 2, 3, and 13TU were biochemically very similar and were grouped together as the *Acinetobacter calcoaceticus-A. baumannii* (Acb) complex (9). In 2011, Nemec and colleagues genotypically and phenotypically characterized the two remaining unnamed species of the Acb complex and proposed the formal species designation of *A. pittii* (formerly *Acinetobacter* genomic species 3) and *A. nosocomialis* (formerly *Acinetobacter* genomic species 13TU) (11). Recently, the diesel-oil and *n*-hexadecane-degrading *A. oleivorans* DR1 was identified as a

member of the Acb complex due to its genetic relatedness to other Acb members (12, 13). Today, the Acb complex comprises these five species, of which, *A calcoaceticus* and *A. oleivorans* are typically environmental isolates found in soil and water that rarely cause disease in humans, while, *A. baumannii*, *A. pittii*, and *A. nosocomialis* are considered opportunistic pathogens typically isolated from patients and health care facilities.

1.2 *A. baylyi* ADP1 background

Although studies led by Bouvet and Grimont as well as Tjernberg and Ursing firmly established DNA groupings for *Acinetobacter* genomic speciation based on DNA-DNA hybridization, some strains of *Acinetobacter* failed to match to any specific DNA group (8, 10, 14). These environmental isolates, mainly isolated from activated sludge, were further characterized and speciated based on unique 16s rDNA sequences coupled with DNA-DNA hybridization analyses described by Carr and colleagues (14). Seven new species were identified as a result of their studies, of particular interest, was the identification of the novel species *A. baylyi*.

Despite not officially being recognized as a species until 2003, *A. baylyi* strains have widely been used in *Acinetobacter* studies due to their genetic tractability and broad metabolic growth capacity (15). Specifically, *A. baylyi* ADP1 has been the choice of model organism to study *Acinetobacter* biology and has since been

adapted to study mechanisms that may promote virulence in the medically relevant *Acinetobacter* species. *A. baylyi* ADP1 is a derivative of the soil isolate, *Acinetobacter* species (sp.) BD4. *Acinetobacter* sp. BD4 was originally studied for its robust ability to form a thick polysaccharide capsule consisting of rhamnose and glucose (16-19). Later, Juni and Janick discovered that *Acinetobacter* sp. BD4 was highly transformable, i.e. able to uptake foreign DNA and recombine that DNA into the host cell chromosome. During these pivotal studies, Juni and Janick found that a microencapsulated derivative of *Acinetobacter* sp. BD4, defined as *Acinetobacter* sp. BD413, was much more amenable to laboratory manipulation and was thus used as the background for development of the auxotrophic strains utilized in the classical transformation assay defining Gram-negative, oxidase negative coccobacilli as belonging to the genus *Acinetobacter* (3, 20). In 1975, Patel and colleagues utilized *Acinetobacter* sp. BD413 for studies revolving around β-ketoadipate enol-lactone hydrolases I and II production and formally changed the designation from *Acinetobacter* sp. BD413 to *Acinetobacter* sp. strain ADP1 (21). Finally in 2006, Vaneechoutte and colleagues identified that *Acinetobacter* sp. strain ADP1 actually belonged to the genus *A. baylyi* previously defined in 2003 (14, 22).

1.3 *Acinetobacter* medical relevance

Acinetobacter species have been isolated from clinical specimens and identified as the source of hospital outbreaks for decades (10, 23). Members of the Acb

complex are by far the most common isolates obtained from clinical specimens and hospital outbreaks are most frequently caused by *A. baumannii*, *A. pittii*, or *A. nosocomialis*; however, many *Acinetobacter* species have been associated with clinical disease (10, 24-26). *A. baumannii* is considered to be the most commonly isolated species causing human infections; however, due mainly to technical difficulties, members of the Acb are unreliably differentiated by clinical laboratories leading to an overestimation of *A. baumannii* induced infections and to the limited reports regarding *A. pittii* and *A. nosocomialis* (25, 27, 28). Typically, members of the Acb complex cause disease in the immuno-compromised patient population with severe hospital outbreaks associated with intensive care units; however, episodes of community-acquired *Acinetobacter* infections have been documented, although most reported cases of community-acquired *Acinetobacter* infections occurred in people with underlying conditions such as diabetes, alcoholism, and chronic obstructive pulmonary disorder (23).

Acinetobacter induced infections typically occur in the respiratory tract; however, bloodstream, urinary tract, skin and soft tissue, and intra-abdominal infections can occur (29). Hospital-acquired pneumonia (HAP) is considered the most common clinical manifestation of *Acinetobacter* induced infections with the majority of HAP occurring in mechanically ventilated patients (23, 30). It is believed that environmental exposure from health care worker hands and/or contaminated surfaces primes the immuno-compromised patient for colonization

during intubation, at which point, a relay series between an infected patient to other susceptible patients is established leading to outbreaks within hospital wards (23, 26, 31-33).

1.4 Mechanisms of *Acinetobacter* antibiotic resistance

The emergence of *Acinetobacter* as severe opportunistic pathogen can be partially attributed to the rapid evolution of multiply drug resistant (MDR) strains; so much so, that the Center for Disease Control and Prevention (CDC) has listed MDR *Acinetobacter* as a serious threat (34). Medically relevant *Acinetobacter* species, particularly *A. baumannii*, *A. pittii*, and *A. nosocomialis*, have amassed an armamentarium of genetic elements encoding proteins that have been shown to facilitate resistance to many clinically relevant antibiotics. Although the overwhelming majority of published literature revolves around the mechanisms of antibiotic resistance of *A. baumannii*, it is important to note that clinical labs worldwide currently do not differentiate between *A. baumannii*, *A. pittii*, *A. nosocomialis*, *A. oleivorans*, and *A. calcoaceticus*; therefore, many publications may in fact be referring to all five species in the *A. calcoaceticus-A. baumannii* complex when specifically referencing *A. baumannii* alone (35).

Inherent to members of the Acb complex is a chromosomally encoded *Acinetobacter* derived cephalosporinase (36, 37). Although Acb complex members encode these AmpC-like β-lactamases (*bla*), the native expression

levels are so low as to not confer clinically relevant levels of resistance; however, introduction of an insertion sequence, designated IS*Aba1*, leads to overexpression of the *Acinetobacter* derived cephalosporinase, thus, conferring resistance to penicillins and cephaloporins (38). Recently, insertion sequence, IS*Aba125*, has emerged as another mechanism for driving expression of *Acinetobacter* derived cephalosporinases (39). As with *Acinetobacter* derived cephalosporinases, many Acb members endogenously encode a carbapenem-hydrolyzing class D β-lactamase, termed OXA-51; however, its native transcriptional levels are too low to confer resistance. As with *Acinetobacter* derived cephalosporinases, clinically relevant carbepenem resistance is gained after acquisition of IS*Aba1* or IS*Aba9* (40, 41). *Acinetobacter* species have also been observed to horizontally acquire extended-spectrum β-lactamases (ESBL) including TEM-1, TEM-2, and CARB-2 conferring resistance to cephalosporins (42). Alarming rates of acquired resistance to carbapenems are also on the rise primarily mediated by horizontal acquisition of the carbapenemases, OXA-23, OXA-24, and OXA-54 (43, 44).

Acinetobacter species have also been observed to express efflux pumps responsible for conferring resistance to many antibiotics. The AdeABC efflux pump belonging to the resistance-nodulation-division family of efflux pumps has been observed to confer resistance to aminoglycosides, beta-lactams,

fluroquinolones, tetracyclines, tigecycline, macrolides, chloramphenicol, and trimethoprim (45).

As a result of increased antibiotic resistance mechanisms acquired by medically relevant *Acinetobacter* species, many clinicians are returning to older, more toxic antibiotics to treat recalcitrant MDR *Acinetobacter* infections. Polymixin derivatives are utilized as a last line of treatment options; however, *Acinetobacter* species are developing sophisticated mechanisms of polymyxin resistance. Mutations in *lpxA*, *lpxC*, and *lpxD* have been observed, resulting in complete loss of lipopolysaccharide (LPS) production depriving polymixins of their target (46). Modifications in the lipid A component of LPS have also been observed as a result of mutations in the *pmrAB* two component signaling pathway involved in lipid A biosynthesis (47). Lastly, *in vivo* emergence of colistin resistance has been observed in clinical isolates during colistin treatment demonstrating the ability of medically relevant *Acinetobacter* species to adapt to their clinical environment (48).

1.5 Virulence mechanisms in *Acinetobacter*

1.5.1 Virulence introduction

Although our understanding of the mechanisms of antibiotic resistance utilized by medically relevant *Acinetobacter* species has been thoroughly studied, the

antibiotic resistant-independent molecular mechanisms employed by *Acinetobacter* to cause disease are just beginning to be characterized. Within the last 15 years significant strides have been made in our understanding of *Acinetobacter* pathogenicity; for example, outer membrane protein A (OmpA) has been identified as virulence factor mediating adherence to biotic and abiotic surfaces, epithelial toxicity, and resistance to serum (49-52). Other characterized virulence factors include the ability of *Acinetobacter* species to form biofilms, produce capsular polysaccharides, and scavenge iron via siderophore acquisition systems (53-56).

In 2007 the first *A. baumannii* genome was made publically available, enabling investigators to identify genes or gene clusters predicted to encode proteins known to be virulence factors in other Gram-negative bacteria (57). Multiple large gene clusters associated with the production of oligosaccharides were identified as well as putative systems for transferring the oligosaccharides to the cell surface or protein acceptors. Furthermore, gene clusters predicted to encode proteins required for the biogenesis of a type IV pili system were identified in many *Acinetobacter* species, which, was expected given that many *Acinetobacter* species were previously observed to exhibit twitching motility, a type IV pili-dependent form of bacterial locomotion (5).

1.5.2 Type IV pili biogenesis and functions

Type IV pili (Tfp) are bacterial surface appendages produced by an array of both Gram-negative and Gram-positive bacteria (58, 59). Type IV pili systems span both the inner and outer membranes of Gram-negative bacteria and are reliant upon four protein complexes: the pilus fiber itself, a motor protein complex, an alignment protein complex, and an outer membrane complex (60). The first protein complex is the pilus fiber itself, which is composed predominately of a major pilin subunit, so named for its abundance within the fiber itself (61, 62). Assembly of the major pilin subunit into the Tfp fiber first requires post-translational processing by a dedicated prepilin peptidase. All type IV pilin subunits have a leader peptide sequence that contains an N-terminal type III signal sequence, which is recognized by the prepilin peptidase. Type IV major pilin processing by the prepilin peptidase involves cleavage of a small N-terminal leader peptide, which, can also be coupled with mono-methylation of the new N-terminal phenylalanine at the α-amino group (63, 64). Other less abundant constituents of the pilus fiber include minor pilins, which also contain an N-terminal type III signal sequence and require processing by the prepilin peptidase; however, minor pilins only contribute a small proportion of pilin subunits to the fiber itself (65, 66). Processed pilins are then shuttled to the motor protein complex, where, polymerization is mediated through ATP hydrolysis by an ATPase of the large VirB11 family (67). Polymerized pilin subunits forming the nascent pilin fiber are oriented to the outer membrane protein complex by the

alignment protein complex consisting of periplasmic and inner membrane proteins (60). Pilus extrusion through the outer membrane is mediated by the outer membrane complex consisting of a dodecamer of secretin monomers forming a channel for pilus fiber exit (68, 69). Pilus retraction is again mediated through the motor protein complex in a manner analogous to pilus polymerization, where ATP hydrolysis by ATPases orthologous to the assembly ATPase powers pilus retraction (70).

When Tfp are functioning, repeated rounds of pilus extension, pilus association with surfaces, and subsequent retraction can occur generating forces around 100 pN (71, 72). These repeated cycles and the forces generated associated with each cycle allow for Tfp to act as bacterial grappling hooks mediating many adherent dependent processes, such as, twitching motility, biofilm formation and maintenance, cell association, and natural transformation (71, 73-75). Some phenomena associated with Tfp, such as, biofilm formation and cell association are not exclusively dependent on Tfp; however, are enhanced or partially dependent on functioning Tfp. Both natural transformation and twitching motility, two of the most well characterized Tfp-dependent phenotypes in Gram-negative bacteria, however are completely dependent on functioning Tfp (71, 76).

Natural transformation is defined as the ability of a bacteria to uptake exogenous DNA and homologously recombine the DNA into the host cell chromosome,

resulting in heritable transmission of the DNA to daughter cells. Type IV pili alone are not sufficient for natural transformation; however, Tfp mediate the pivotal first steps of cellular association with the exogenous DNA (76). Disrupting the function of one of the four protein complexes of the Tfp can dramatically reduce the natural transformability of an organism. Although the dependency of Tfp for natural transformation has been studied for decades, it has just recently been shown that a conserved minor pilin of *Neisseria* mediates DNA binding through an electropositive stripe that is predicted to be surface exposed on the Tfp fiber (76). It has also been shown that Tfp retraction deficient mutants lose their ability to undergo natural transformation, indicating that DNA binding to the fiber is not sufficient for DNA uptake (77, 78).

Twitching motility is described as the jerky bacterial locomotion exhibited at the interface of a solidified growth medium and the substratum (79). Although Tfp were known to be required for twitching motility, studies utilizing optical tweezers were required to unequivocally demonstrate that Tfp retraction mediated bacterial cell translocation (72). In its simplest form, twitching motility is regarded as a form of bacterial locomotion facilitating the translocation of a bacterium in order to explore its environment. Twitching motility has also been implicated in biofilm formation and maintenance; for example, mutations in the retraction ATPase of *P. aeruginosa* resulted in flat, mat like biofilm, while wild-type bacteria were able to form both the mat like biofilm and mushroom towers. The bacteria associated

with the mushroom towers required functioning Tfp to build, climb, and maintain the tower (80).

1.5.3 *Acinetobacter* and type IV pili associated phenotypes

Many *Acinetobacter* species and strains contain the genes predicted to encode the necessary proteins for all four subsystems of a functioning Tfp system (81). Although twitching motility and natural transformation, two classically associated Tfp-associated phenotypes, have been observed in *Acinetobacter* species, only a handful of reports attempted to characterize the molecular components mediating these processes across *Acinetobacter* species. The system of natural transformation in *A. baylyi* ADP1 is the most comprehensively characterized system to date (15, 82-84). Natural competence in *A. baylyi* ADP1 only requires free DNA, which can be found in any of the following forms: PCR products, linear plasmids, circular plasmids, cell lysates, or whole cells that release DNA as they die, making *A. bayyi* ADP1 one of the most promiscuously competent bacterium characterized (15, 82, 85). Not only is *A. baylyi* ADP1 highly competent to uptake exogenous DNA, but it also has intrinsic factors allowing for efficient recombination into the host cell chromosome; thus, allowing for systems studying gene duplication and amplification, incorporation of foreign DNA, and metabolic engineering (15). To demonstrate *A. baylyi* ADP1's versatility as a model organism, a single-gene deletion collection for all dispersible genes has been constructed allowing for the exploration of gene function (86).

The ability of *A. baylyi* ADP1 to uptake exogenous DNA resembles natural transformation systems dependent on Tfp. The *comP* gene, encoding the pilin-like factor ComP, is homologous to the major pilin subunit, PilA, of Tfp systems and was the first gene found to be required for natural transformation in an *Acinetobacter* species (87, 88). ComP displays significant similarities to type IV pilins as it has a typical leader sequence containing a type III N-terminal signal sequence and an extended N-terminal hydrophobic alpha helix domain; however, no pilin-like structure associated with ComP has been observed, prompting the conservative designation as type IV pilin-like to describe the natural transformation system in *A. baylyi* ADP1. Another gene cluster associated with natural transformation was subsequently identified, which contained genes predicted to encode minor pilins, designated as ComE and ComF, and the predicted tip associated protein, designated ComC (89, 90). Deletion of the predicted minor pilin genes, *comE* and *comF*, both decreased the transformability of ADP1, however, at varying levels. A *comE* mutant had a 10-fold decrease in transformability as compared to the parental strain, whereas, the *comF* mutant had a 1000-fold decrease. Interestingly, the mutant lacking the predicted tip-associated protein, ComC, did not exhibit any detectable transformation levels.

Genotypes and phenotypes associated with Tfp systems have also been observed in members of the Acb complex. Many research groups identified the presence of genes encoding proteins predicted to be required for the biogenesis

of Tfp in *A. baumannii* (5, 81, 91). Additionally, studies led by Philip Rather identified that the predicted Tfp retraction ATPase, PilT, was partially required for surface-associated motility by the clinical isolate *A. nosocomialis* strain M2 (92). In Chapter 2, in collaboration with Philip Rather, we provided the genome sequence of *A. nosocomialis* strain M2, allowing us to also identify genes predicted to encode proteins required for the biogenesis of Tfp (93). Furthermore, many Acb clinical isolates were shown to be able to exhibit twitching motility. Lastly, recent work has demonstrated that *A. baumannii* ATCC 17978 requires the *pilT* gene, encoding for the putative retraction ATPase of Tfp, for optimal biofilm formation and/or maintenance; however, these experiments did not contain a complemented *pilT* strain and need further characterization to conclusively link Tfp and biofilm formation in *Acinetobacter* (94).

Natural transformation has also been observed in a medically relevant *Acinetobacter* species; specifically, *A. baumannii* A118, a blood isolate from an intensive care patient, was found to be naturally competent in the uptake of plasmid DNA and oligodeoxynucletotide analogs (95).

Although observations of Tfp have been associated with members of the Acb complex, no definitive experimental evidence unequivocally demonstrated the ability of these species to produce functional Tfp. In Chapter 3, we describe the discovery and demonstration of functional Tfp production by *A. nosocomialis*

strain M2, which, were required for natural transformation and twitching motility, but not the unique surface-associated motility exhibited by many *Acinetobacter* clinical isolates.

1.5.4 General *O*-glycosylation systems

Glycosylation, or the covalent attachment of a carbohydrate moiety to an amino acid, is the most abundant form of post-translational modification and has been identified in all three domains of life (96, 97). Covalent attachment of carbohydrate moieties has been identified as either *N*- or *O*-linked depending on which functional group the carbohydrate is attached to. *O*-linked glycosylation occurs when a carbohydrate moiety is covalently attached to the hydroxyl oxygen of threonine or serine residues. *O*-glycosylation in bacteria has been characterized as oligosaccharyltransferase (OTase) independent and OTase dependent, where the latter has only been identified in bacteria (98).

OTase independent glycosylation of proteins is mediated through a sequential transfer method, where, glycosyl-transferases enzymatically transfer a monosaccharide from a nucleotide-activated precursor directly to a protein acceptor located in the cytoplasm. Glycosylation via OTase independent systems have been extensively studied for flagellin subunits of *Pseudomonas*, *Campylobacter*, and *Clostridium* species as well as for adhesins, such as, the HMW1 adhesin of *Haemophilus influenzae* (99-102).

OTase dependent glycosylation is characterized as a block transfer system, where, an OTase transfers an assembled oligosaccharide from a lipid carrier to a protein acceptor (96). OTase dependent glycosylation is reliant upon the biosynthesis of a lipid-linked oligosaccharide, requiring the coordinated activities of sequential glycosyl-transferases to assemble a glycan chain onto a lipid carrier. At the inner leaflet of the inner membrane, OTase dependent glycosylation is initiated by an initial glycosyl-transferase, which transfers a nucleotide-activated monosaccharide to an undecaprenyl phosphate (Und-P) lipid (103). Glycosyl-transferases then transfer the remaining sugars to the growing lipid-linked oligosaccharide. The fully assembled lipid-linked oligosaccharide is then flipped from the inner leaflet of the inner membrane to the outer leaflet of the inner membrane making the glycan available to periplasmic proteins (103). A dedicated OTase then transfers the glycan from the lipid carrier to a protein acceptor for protein glycosylation or can be further processed and polymerized into chains, which can be shuttled to the outer membrane and anchored to form a polysaccharide capsule (104). OTase dependent *O*-glycosylation systems have been identified in many bacteria species; including, *A. baumannii*, *Bacteroides fragilis*, *Burkholderia cenocepacia*, *Francisella tularensis, Neisseria* spp.*,* and *Porphyromonas gingivalis* (105-109).

1.5.5 *O*-glycosylation in *Acinetobacter*

The general *O*-glycosylation system from *A. baumannii* ATCC 17978 is hypothesized to be mechanistically similar to the OTase dependent system in *Neisseria* spp. where a lipid linked oligosaccharide is assembled on an Und-P precursor at the inner leaflet of the cytoplasmic membrane, flipped to the periplasm, and the glycan transferred by an OTase to target proteins (98). As with *Neisseria*, an *Acinetobacter* OTase was identified and found to be responsible for the glycosylation of at least seven membrane associated proteins. The OTase, $PglL_{Ab}$, was found to transfer a pentasaccharide β-GlcNAc3NAcA4OAc-4-(β-GlcNAc-6-)-α-Gal-6-β-Glc-3-β-GalNAc- to peptide regions of low complexity rich in serine, proline, and alanine. Loss of the $PglL_{Ab}$ OTase resulted in a diminished ability of *A. baumannii* ATCC 17978 to form biofilms in a flow chamber system and attenuated its *in vivo* virulence in a *Dictyostelium discoideym*, *Galleria mellonella*, and a murine peritoneal sepsis model (105). Interestingly, the same pentasaccharide was identified as the repeat subunit for the capsule of *A. baumannii* ATCC 17978 indicating a common pathway for *O*-linked protein glycosylation and capsule synthesis (55).

Although *Acinetobacter* spp. and *Neisseria* spp. utilize similar systems for lipid-linked oligosaccharide biosynthesis and glycan transfer to proteins, the glycan diversity of *Acinetobacter* species is far greater. Although extensive glycan diversity was found with the genus *Acinetobacter*, similar proteins were found to

be glycosylated in similar peptide regions indicating a conserved system for transferring glycans to proteins. *Acinetobacter* spp. were also found to glycosylate proteins with dimeric glycan chains, increasing the repertoire of glycan-protein states. Lastly, a diverse *O*-glycosylation system has been identified in *A. baylyi* ADP1, with two separate systems for each protein glycosylation and capsule biosynthesis (110, 111).

1.5.6 Pilin glycosylation

As mentioned above, polymerization of the major pilin subunit into the TFP fiber first requires post-translational processing by a dedicated prepilin peptidase; however, type IV major pilins are not limited to post-translational modification by the prepilin peptidase, in fact, many Tfp producing Gram-negative bacteria are capable of furthering modifying their respective major pilin subunits with phosporylcholine, phosphorylethanolamine, and/or glycan subunits (62).

Glycosylation of a major pilin subunit has been identified as one of the most prominent pilin post-translational modifications secondary to prepilin processing. Many Gram-negative bacteria including, *Neisseria* species, *Pseudomonas* species, *Francisella* species, and *Dicholebacter nodosus* are able to glycosylate their respective major type IV pilin subunits (112-116). Glycosylation of pilin subunits canonically proceeds through a block transfer method where a dedicated *O*-oligosaccharyltransferase (*O*-OTase) transfers a hetero-

oligosaccharide to a single conserved site on a pilin subunit; however, a hybrid block/sequential transfer system does exist where multiple residues of a pilin subunit can be modified with monomers or homopolymers of a sugar (117).

The *Neisseria* pilin glycosylation (pgl) system is the most comprehensively defined system, where a glycan is sequentially assembled on an Und-P carrier at the cytoplasmic surface of the inner membrane generating a lipid-linked oligosaccharide (LLO), which is translocated across the inner member to the periplasm (108). The periplasmic LLO serves as a substrate for the *O*-Otase PglL, which transfers the glycan *en block* to serine 63 on the major pilin subunit PilE. Both *N. gonorrhoeae* and *N. meningiditis* are able to glycosylate their respective pilins at serine 63 (118). Although pilin glycosylation is highly conserved between the two species, the glycans synthesized by each species can differ due to phase variation of *pglE* and allelic variation of *pglB* (119, 120).

At least two different systems for pilin glycosylation have been identified in *P. aeruginosa.* The first characterized *P. aeruginosa* pilin glycosylation system is a product of a bifurcation in the O-antigen synthesis pathway; whereby, the dedicated pilin-specific OTase, PilO (also known as TfpO), transfers a single subunit of the lipopolysaccharide (LPS) O-antigen repeat unit *en block* to the conserved carboxy-terminal serine on group I pilins ($PilA_I$) (113, 121, 122). The second characterized *P. aeruginosa* pilin glycosylation system was defined by TfpW-dependent glycosylation of group IV pilins ($PilA_{IV}$) with monomers or

homopolymers of the rare D-arabinofuranose (D-Ara*f*) unit on multiple serine and threonine residues in the predicted *αβ*-loop and *β*-sheet regions of PilA (114, 117). The latter, unconventional system has not been fully defined in regards to whether TfpW has only glycosyl-transferase activity sequentially adding monomers of D-Ara*f* to the pilin subunit or both glycosyl-transferase and oligosaccharyl-transferase activities acting in both a sequential and block transfer mechanism to add monomers and homopolymers of D-Ara*f* to the pilin subunit, respectively (123).

During the initial studies describing the mechanisms of natural transformation in *A. baylyi* APD1, the pilin-like factor ComP was shown to exist in two molecular forms, indicating, that ComP was able to be post-translational modified; however, it wasn't until 13 years later that evidence was presented linking the post-translational modification of ComP to a glycosylation event (88, 110). In their study, Schulz and colleagues demonstrated that deletion of a gene predicted to encode an OTase resulted in the increased electrophoretic mobility of ComP as compared to ComP from the parental strain; even still, their evidence did not definitively demonstrate glycosylation of ComP. In Chapter 4, we describe the identification of *Acinetobacter* strains that carry two functional OTases, one devoted exclusively to type IV pilin, and the other one dedicated to *O*-glycosylation of multiple proteins. Furthermore, we also demonstrated that pilin

glycosylation also shares a common pathway with general *O*-glycosylation and capsule production.

1.6 Summary

Acinetobacter species are ubiquitously distributed, metabolically diverse, resilient bacteria broadly known for their ability to degrade and utilize many carbon sources; however, some *Acinetobacter* species have recently emerged as opportunistic human pathogens capable of causing severe disease. Compounding the issue is an alarming rise in antibiotic resistant *Acinetobacter* strains and an increased *Acinetobacter* hospital persistence, making these infections and outbreaks difficult to manage and treat.

Previous reports identified genes predicted to encode proteins required for the biogenesis of a type IV pili system as well as a glycosylation system, both of which have been described as virulence factors in other Gram-negative bacteria. Herein, we present work revolving around the discovery and demonstration of functional Tfp production and post-translational modification by a medically relevant *Acinetobacter* species; moreover, we couple these findings with the identification of a novel pilin-specific glycosylation system, which, is independent from the general *O*-glycosylation system.

Chapter 2: Draft genome sequence of the clinical Isolate *Acinetobacter nosocomialis* Strain M2

2.1 Abstract

We report the 3.78 Mbp high-quality draft assembly of the genome from a clinical isolate of *Acinetobacter nosocomialis* called strain M2 (previously known as *A. baumannii* strain M2).

2.2 Genome Announcement

Acinetobacter nosocomialis is a member of the *Acinetobacter calcoaceticus – Acinetobacter baumannii* (Acb) complex, which is comprised of *A. calcoaceticus, A. baumannii, A. pittii* (formerly genomic species 3) and *A. nosocomialis* (formerly genomic species 13TU) (11). Except for *A. calcoaceticus*, members of the Acb complex are opportunistic pathogens that pose a significant threat to human health through their ability to cause potentially severe infections. This threat is compounded by both the high incidence of Acb complex infections in critically ill patients and prevalence of antibiotic resistance exhibited by members of the Acb complex (43).

Acinetobacter nosocomialis strain M2, isolated in 1996 from a hip infection of a patient at Cleveland MetroHealth systems (Cleveland, OH,) has been studied in several laboratories. An acyl homoserine lactone autoinducer synthase from strain M2 has been isolated and characterized (124). Non-native acyl homoserine lactones have been shown to attenuate strain M2 quorum sensing (125). A novel mechanism of fluoroquinolone resistance has been discovered through mutagenesis of strain M2 (126). Twitching motility exhibited by strain M2 is mediated by a Tfp system, which also mediates strain M2's natural transformation phenotype (6). Strain M2 is also motile on the surface of agar plates through an unknown (92), Tfp-independent mechanism (6). In addition, strain M2 is able to out-compete other bacteria using a type VI secretion system (127).

Genomic DNA was prepared using the Qiagen DNA Purification kit. Genome sequencing was performed using the Illumina Hi-Seq and MiSeq maintained at The Research Institute at Nationwide Children's Hospital Biomedical Genomics Core (genomics.nchresearch.org). A total of 4 million paired-end MiSeq reads (300 bp insert size) trimmed to 200 bp and 4 million mate-pair Hi-Seq reads (3 kb insert size) trimmed to 35 bp were assembled *de novo* using Seqman NGen (v4.1.2, DNAstar, Madison, WI). Post-assembly manipulation was performed using SeqMan Pro (DNAstar). This genome assembly yielded 11 contigs comprising a total genome length of 3,782,411 bp, a N50 of 556 kb, with 163-fold

average coverage. Genome annotation using the NCBI Prokaryotic Genomes Automatic Annotation Pipeline (v2.0) predicted a total of 3,487 open reading frames.

Previously, strain M2 was classified by multi-locus sequence typing (MLST) as belonging to the *baumannii* species (R.A. Bonomo, unpublished). Two currently available MLST schemes were used to re-type strain M2. Four of seven genes required for MLST using the “Oxford” scheme (http://pubmlst.org) were identified in the M2 genome. Based upon this analysis, strain M2 is most closely related to an *Acinetobacter* spp. 13TU isolate from Brazil. Five of eight genes required for MLST using the “Pasteur” scheme (www.pasteur.fr/mlst) were identified in the strain M2 genome. Analysis of these alleles indicates that strain M2 is most closely related to *Acinetobacter* gen. sp. 13TU strain RUH 2210. Based on this evidence we recommend that *A. baumannii* strain M2 should be referred to as *Acinetobacter nosocomialis* strain M2.

2.3 Nucleotide Sequence Accession Number

This Whole Genome Shotgun project has been deposited at DDBJ/EMBL/GenBank under the accession AWOW00000000. The version described in this paper is version AWOW01000000.

Chapter 3: Demonstration of type IV pili production by *Acinetobacter baumannii* and their role in natural transformation, twitching motility and surface-associated motility

3.1 Introduction

Acinetobacter baumannii is an aerobic Gram-negative, non-flagellated opportunistic pathogen; of late, some strains have developed resistance to most antimicrobial therapies (128). Hospital-acquired pneumonia is the most common clinical manifestation of *A. baumannii* infections; moreover, these infections frequently occur in mechanically ventilated patients, suggesting that environmental exposure to *A. baumannii* followed by subsequent accidental inoculation associated with the endotracheal tube may lead to infection (23). Interestingly, we now know that *A. baumannii* is not ubiquitous in nature, but actually is isolated primarily within hospital settings on medical equipment, hospital workers and patients and should not be considered just an environmental contaminant (129). Key to *A. baumannii*'s persistence in hospital environments is its ability to resist desiccation, surviving on surfaces including bed rails, bedside tables, surfaces of ventilators and even mattresses (130, 131). From 1993 to 2004, multi-drug resistant (MDR) *Acinetobacter* spp. infections increased 23% in intensive care units, more than double any other Gram-

negative bacillus (132). *A. baumannii* has gained attention as an “ESKAPE” pathogen, one of a cohort of microorganisms that causes the majority of MDR nosocomial infections within the United States, aptly named for their ability to escape the effects of modern antimicrobial therapies (133). Furthermore, the competency of *A. baumannii* to acquire antibiotic resistance genes has now resulted in strains that are characterized as extensively drug-resistant (XDR) and pan drug-resistant (PDR), prompting the suggestion we may be nearing the end of antibiotic era for this important Gram-negative pathogen (134, 135). In addition, the prevalence of MDR *A. baumannii,* an increase of infection incidence and its recalcitrance to desiccation signifies the clinical importance of this opportunistic pathogen.

Although *A. baumannii* has earned global recognition for its ability to infect the immune-compromised patient population, little is actually known about how *A. baumannii* causes disease. Recent characterization of *A. baumannii* indicates that a handful of molecular factors are required for virulence in models that partially recapitulate human disease, including but not limited to, outer membrane protein A (OmpA), phospholipase D, biofilm-associated protein (Bap), an *O*-glycosylation system, the *Acinetobacter* trimeric autotransporter (Ata), the Csu chaperone-usher type pilus, the acinetobactin-mediated iron acquisition system and a secreted serine protease (49, 52, 105, 136-141). Despite these significant

findings, there is still a clear need to better define the bacterial determinants that facilitate colonization and subsequent disease.

Type IV pili (Tfp) are multi-protein bacterial surface appendages assembled by many Gram-negative bacteria (142, 143). Due to their dynamic nature, Tfp are able to be rapidly assembled and dissembled participating in processes such as natural transformation, twitching motility, as well as adherence to abiotic and biotic surfaces. Natural transformation, or the ability of an organism to acquire exogenous DNA in a horizontal fashion, is a multi-step processes involving the uptake of DNA, processing of DNA and ensuing homologous recombination (144). Tfp-associated genes and their products are linked to DNA uptake; however, Tfp alone are not sufficient for natural transformation. Tfp also mediate a unique form of flagella-independent motility termed twitching motility. Twitching motility involves the assembly of Tfp, attachment and subsequent retraction of the pilus facilitating the translocation of the cell body towards the point of attachment (60). Interestingly, the term twitching motility was coined in 1965 by Lautrop to describe the jerky locomotion exhibited by *Acinetobacter calcoaceticus*, thereby laying the roots early for a link between *Acinetobacter* spp. and Tfp (79).

Recently, Smith *et al*. sequenced the genome of *A. baumannii* strain ATCC 17978 and described several genes whose products might play a role in

transformation; some of these were predicted to encode components of a Tfp-like system (57). Furthermore, a recent analyses of the published *A. baumannii* genomes has revealed many genes whose products have homology to proteins required for the biogenesis of Tfp found in other Gram-negative bacteria; thus, it appears that some *A. baumannii* strains contain the coding potential required to assemble Tfp (81). In addition to this analysis, Antunes *et al.* demonstrated that *A. baumannii* strain AYE exhibited twitching motility. A complete list of Tfp biogenesis gene homologs in three *A. baumannii* reference strains can be found in the Antunes *et al.* study (81). Eijkelkamp and co-workers simultaneously reported that several genes in *A. baumannii* strain ATCC 17978, which likely encode proteins required for Tfp biogenesis, were slightly down-regulated under low iron growth conditions and surface-associated motility was lost (91). In other organisms, Tfp are associated with numerous phenotypes including natural transformation and/or twitching motility (145, 146). Ramirez *et al.* identified a clinical isolate of *A. baumannii* isolated from blood that was naturally transformable; however, the molecular basis for this phenotype was not explored (95). Also, some *A. baumannii* clinical isolates are capable of twitching motility [reviewed in (147)]. Recently, Eijkelkamp *et al*. reported that all of the international clone I *A. baumannii* clinical isolates tested in their study as well as some clinical strains that did not belong to a currently characterized clonal lineage were capable of twitching motility indicating that these strains may produce functional Tfp (91). It has been speculated that Tfp might play a role in

the unique, flagella independent surface-associated motility displayed by many *A. baumannii* clinical isolates; yet, there is no experimental evidence demonstrating that *A. baumannii* strains produce functional Tfp (91, 92).

In this report, we have demonstrated that *A. baumannii* strain M2, a clinical isolate, was naturally transformable and that natural transformation was dependent on genes which encode orthologs of proteins required for the biogenesis of Tfp found in other Gram-negative organisms. These gene products were also required for twitching motility, another Tfp-associated phenotype. Similar to observations made in other organisms (*Neisseria gonorrhoeae*, *Pseudomonas aeruginosa* and *Dichelobacter nodosus*), strain M2Δ*pilT* mutant exhibited more surface exposed PilA as compared to the wild type strain (49, 148, 149). Tfp were readily visualized by transmission electron microscopy on *pilT* mutant cells but not on *pilA or pilA pilT* double mutant cells. Collectively, we conclude that *A. baumannii* strain M2 produces functional Tfp and that these structures are required for natural transformation and twitching motility. Lastly, we demonstrated that the unique surface-associated motility exhibited by many clinical isolates is not dependent on the production of functional Tfp in strain M2.

3.2 Methods

Strains, plasmids and growth conditions. Bacterial strains and plasmids used for this study are listed in Table 3.1. All bacterial strains were grown on L-agar or

in LB-broth. When appropriate, antibiotics were added to the *A. baumannii* cultures at the following concentrations: 750 µg ampicillin/mL, 20 µg kanamycin/mL, 50 µg streptomycin/mL or 12.5 µg chloramphenicol/mL. When appropriate, *Escherichia coli* cultures were supplemented with antibiotics at the following concentrations: 50 µg ampicillin/mL for *E. coli* strains containing plasmids other than pGEM derivatives, 100 µg ampicillin/mL for *E. coli* strains containing pGEM derivatives, 25 µg streptomycin/mL or 20 µg kanamycin/mL.

Construction of the *pilA, pilD* and *pilT* mutants. Primers for this study were obtained from Integrated DNA Technologies (Coralville, IA) and are listed in Table 3.2. We constructed a mutant deficient in expression of in the *pilA* gene as follows. The *pilA* gene plus approximately 1 kb of DNA 5' and 3' of *pilA* was amplified by PCR using primer set 1. The amplicon was then ligated into pGEM-T-Ez (Promega, Madison, WI) and the ligation products transformed into *E. coli* DH5α. A plasmid with the correct insert was saved as pGEM-*pilA* and the sequence of the insert was verified by sequencing. The *pilA* gene in pGEM-*pilA* was then replaced with a kanamycin resistance cassette flanked by FRT sites from pKD13 using a lambda recombinase-based strategy (150, 151). An amplicon was generated that contained 47 nt of DNA 5' of *pilA* along the translational start, the cassette, the last 21 nt of the *pilA* gene and 29 nt downstream of *pilA* using primer set 2 and pKD13 as template. The amplicon and pGEM-*pilA* were electroporated into *E. coli* strain DY380 that had been heat

shocked at 42˚C for 15 min prior to electroporation to induce expression of the lambda recombinase genes. Clones containing a plasmid with the *pilA* gene replaced by the cassette were identified on L-agar supplemented with kanamycin. Plasmids were isolated and characterized; a plasmid containing FRT-kan-FRT in place of the *pilA* gene was saved as pGEM-Δ*pilA*::kan.

Natural transformation was then used to move the Δ*pilA*::kan insert into M2. The plasmid pGEM-Δ*pilA*::kan and primer set 1 were used to generate an amplicon containing, Δ*pilA*::kan and flanked 1 kb up- and down-stream of *pilA*. An overnight culture of strain M2 was diluted 1:10 in 500 µl of LB-broth and incubated at 37˚C with shaking at 180 rpm for 2 h. Following the 2 h incubation, 1 µg of the amplicon was added to the bacterial culture. Cells were then transferred to an L-agar plate and incubated at 37˚C for 4 h. Cells were collected from the plate, resuspended in 500 µL of LB-broth and dilutions plated on L-agar supplemented with kanamycin at 37˚C. Kanamycin resistant clones were characterized by PCR analysis and sequencing to verify allele exchange. A clone was saved as M2Δ*pilA*::kan. The identical strategy was used to construct M2Δ*pilD*::kan using primer sets 3 and 4.

Since a mutation in *pilT* might be polar on *pilU*, we modified our strategy so as to remove the cassette leaving a short ORF containing the translational start of *pilT*, a small scar left by the excision of the cassette and the last 21 nt of *pilT*. For this

construction, *pilTU* were amplified from M2 genomic DNA with primer set 5 and cloned as above. A clone was saved as pGEM-*pilTU.*

To construct an unmarked mutation in *pilT*, a derivative of pKD13 containing FRT-kan-*sacB*-FRT, pRSM3542, was used as the template in a PCR with primer set 6 (127). The amplicon, along with pGEM-*pilTU*, were electroporated into heat-shocked *E. coli* DY380 as described above. Restriction digest analysis and sequencing was performed on plasmid purified from kanamycin resistant clones. A correct clones was saved as pGEM-Δ*pilT*::[kan-*sacB*]*pilU*. To introduce this mutation into straim M2, an PCR was performed using pGEM-Δ*pilT*::[kan-*sacB*]*pilU* as template and primer set 5. This amplicon was introduced into strain M2 by natural transformation as described above. A kanamycin resistant clone with the correct sequence was saved as M2Δ*pilT*::kan-*sacB*.

A triparental mating strategy was employed to transiently introduce the pFLP2 plasmid, which expresses the FLP recombinase, into M2Δ*pilT*::kan-*sacB* as described by Carruthers *et al* (127). Briefly, 100 µL of stationary culture normalized to an OD_{600} = 2.0 of each of DH5α(pFLP2), HB101(pRK2013) and M2Δ*pilT*::kan-*sacB* were added to 700 µL of warm LB broth. The bacterial suspension was washed twice by centrifugation at 7,000 x *g* followed by re-suspension of the bacterial pellet in 1 mL of 32˚C LB-broth. On the final wash, the bacterial pellet was resuspended in 25 µL of LB-broth and the suspension

was spotted on a pre-warmed L-agar plate and allowed to incubate for 16 h at 32˚C. The plates were then transitioned to 37˚C for 2 h to transiently induce the FLP recombinase. Bacteria were then scraped from the plate and resuspended in 1 mL of LB-broth. Serial dilutions were plated on L-agar containing 10% sucrose and 12.5 µg of chloramphenicol/mL and incubated at 26˚C to select for transconjugants that lost *sacB* and to select against *E. coli* strains. Strain M2 is naturally resistant to chloramphenicol at the concentrations used in this study. Clones demonstrating sucrose resistance were analyzed by PCR to verify loss of the *kan-sacB* cassette. A correct clone was sequenced and saved as M2Δ*pilT*.

Construction of the *pgyA* mutant stain. The pGEM-*pilA* vector was constructed so that it contained the *pilA* gene as well as flanking DNA, which included the *pgyA* gene. Thus, to construct a *pgyA* mutant strain the following strategy was employed. EcoRV, a unique restriction site 64 bp from the 5' end of *pgyA* was used to digest pGEM-*pilA*. The kanamycin cassette from pUC4K was excised with HincII and ligated to the EcoRV linearized pGEM-*pilA*, transformed into DH5α and clones selected for on L-agar supplemented with kanamycin. A clone demonstrating the correct restriction pattern was used to generate a PCR amplicon containing the interrupted *pgyA* gene along with approximately 1 kb of flanking DNA using primer set 1. The resulting amplicon was transformed into strain M2 via natural transformation as described above. Transformants were

selected for on L-agar supplemented with kanamycin. A clone with the correct insertion was verified with colony PCR and sequencing to confirm the mutation.

Construction of complemented mutant strains. A mini-Tn*7* transposon system was used to complement mutations made in strain M2 in single copy, under the control of each gene's predicted promoter. Construction of the mini-Tn*7* containing plasmid, pRSM3510, employed for this study has been described (127).The *pilA* gene along with 430 bp upstream of the start codon was amplified with primer set 7. The forward primer contained a BamHI site on the 5' end while the reverse primer of each primer set contained KpnI on the 3' end. The amplicon was digested with BamHI and KpnI and ligated to pRSM3510 that had been digested with the same enzymes. The ligation mixture was electroporated into *E. coli* EC100D and clones selected on L-agar containing ampicillin. Plasmids containing the *pilA* gene were identified by restriction digestion and verified by sequencing. A clone was saved as pRSM3510-*pilA*. Similarly pRSM3510-*pilTU*, which contains 312 bp upstream of the start codon of *pilT* was constructed using primer set 8 with the following exceptions. The reverse primer did not have a KpnI site on the 3' end and was instead phosphorylated to use in a blunt cloning strategy. pRSM3510 was digested with BamHI and StuI and the *pilTU* amplicon was digested with BamHI, which were subsequently ligated together.

Since *pilD* is the last gene in a cluster of Tfp related genes (Figure 3.1), we assumed *pilD* transcription would be driven from a promoter 5' of *pilB*. Thus, we

constructed a clone containing the putative *pilB* promoter driving expression of *pilD*. Plasmid pGEM-*pilBCD* was generated using primer set 3 and M2 genomic DNA as template as described for pGEM-*pilA*. Inverse PCR using pGEM-*pilBCD* as template and primer set 9 was utilized to create an in-frame deletion of *pilBC,* which left the putative promoter, the start codon of *pilB* and the last 21 bp of *pilC* immediately 5' to the *pilD* gene. This amplicon was self-ligated and electroporated into DH5α. Clones were selected for on L-agar supplemented with ampicillin and a plasmid containing the *pilBC* deletion was saved as pGEM-*pilD*. pGEM-*pilD* was used as a template in a PCR with primer set 10 to produce a amplicon that was cloned into pRSM3510 as described above for pRSM3510-*pilA*. Ligations were electroporated into EC100D and clones selected for on L-agar supplemented with ampicillin. A correct clone was saved as pRSM3510-*pilD*.

Primer set 11 was used to amplify the template, pRSM3510-*pilA,* with a FLAG tag immediately upstream of the stop codon of the *pilA* gene. The amplicon was self-ligated and electroporated into EC100D. Transformants were selected on L-agar supplemented with ampicillin and a correct clone was sequence verified and saved as pRSM3510-*pilA*-FLAG.

Insertion of the mini-Tn7 constructs into the *A. baumannii* mutants. The pRSM3510 derivatives expressing the *pilA*, *pilD* or *pilTU* genes were introduced into the respective *A. baumannii* M2 mutants via a four parental conjugal strategy modified from Kumar *et al* (152). Briefly, 100 µL of stationary cultures normalized to an OD_{600} = 2.0 of the recipient strain (*A. baumannii* mutant), HB101(pRK2013), EC100D(pTNS2) and EC100D containing the appropriate pRSM3510 derivative were added to 600 µL of warm LB broth. Each suspension was washed twice by centrifugation at 7,000 x *g* followed by resuspension of the bacterial pellet in 1 mL of warm LB-broth. On the final wash, the bacterial pellet was resuspended in 25 µL of LB-broth and the suspension was spotted on a pre-warmed L-agar plate and allowed to incubate overnight at 37˚C. The bacteria were scraped from the plate and resuspended in 1 mL of LB-broth, vortexed for 8 sec and serial dilutions plated on L-agar plates supplemented with chloramphenicol to select against *E. coli* strains and ampicillin to select for *A. baumannii* strain M2 exconjugants that received the mini-Tn*7* constructs. To verify that mini-Tn*7* successfully transposed downstream of the *glmS2* gene, primer set 12 (Tn7L forward and downstream *glmS2* reverse) were used to amplify a 400 bp fragment that would only produce a product if mini-Tn*7* had inserted at the predicted *att*Tn*7* in the correct orientation. The four strains were saved as M2Δ*pilA*::kan(*pilA*+), M2Δ*pilD*::kan(*pilD*+), M2Δ*pilT*(*pilTU*+) and M2Δ*pilA*::kan($pilA_{FLAG}^{+}$).

Construction of pGEM-*blsA::strAB*. The *blsA* gene along with 1 kb of upstream and downstream DNA was amplified by PCR with the primer set 13 using *A. baumannii* strain M2 genomic DNA as the template. The amplicon was A-tailed, TA cloned into pGEM-T-Ez and electroporated into DH5α. Transformants were selected on L-agar supplemented with ampicillin and correct clones were verified by restriction digest and sequencing. The *strA* and *strB* genes along with approximately 400 bp of flanking DNA were amplified from *A. baumannii* strain RUH134 with the phosphorylated primer set 14. This PCR product was ligated to an EcoRV digested pGEM-*blsA* and electroporated into DH5α. Clones were selected for on L-agar supplemented with streptomycin. A clone with the correct insertion was saved as pGEM-*blsA*::*strAB*. The interruption in the *blsA* gene is 72 bp downstream of the ATG start.

Construction of the *pilT pilA* mutant. To construct a *pilT pilA* mutant, an insertionally inactivated *pilA* was introduced into the *pilT* mutant strain. Briefly, pGEM-*pilA* was used as template to construct pGEM-Δ*pilA* in which, inverse PCR was performed using primer set 16 to create an in-frame deletion of *pilA*. The resulting amplicon was ligated to a streptomycin cassette (*strAB*), which was PCR amplified from RUH134 using primer set 14, and this ligation product was transformed into *E. coli* DH5α. The resulting plasmid was digested with EcoRI and the region encoding the *pilA* deletion was cloned into pKNOCK-Km. *E. coli* EC100D cells harboring pKNOCK-Δ*pilA*::*strAB*, *E. coli* HB101 harboring

pRK2013 and *A. baumannii* strain M2ΔpilT were used as donor, helper and recipient strains respectively in a triparental conjugation. Transconjugates were selected for on L-agar containing chloramphenicol and streptomycin. Exconjugates were verified by PCR to confirm the *pilA* mutation. A verified clone was saved as M2Δ*pilT*Δ*pilA*::*strAB*.

Construction of the *pilA pilD* mutant. To construct a *pilA pilD* mutant, we introduced a marked deletion of the *pilD* gene into the M2Δ*pilA*::kan (*pilA*$_{FLAG}$+) strain via natural transformation. Briefly, pGEM-*pilBCD* was amplified by inverse PCR using primers set 15 to create an in-frame deletion of the *pilD* gene, in which the ATG start as well as the last 21 nt of the *pilD* gene were left. The streptomycin cassette from *A. baumannii* RUH134 was amplified by PCR using primer set 14 which was 5' phosphorylated. The two amplicons were ligated, electroporated into DH5α and clones selected for on L-agar plates containing streptomycin. A clone demonstrating the correct sequence was used to generate an amplicon encoding the in-frame *pilD* deletion interrupted with the streptomycin cassette as well as 1 kb of flanking DNA. The PCR product was transformed via natural transformation into the *pilA*-FLAG complemented *pilA* mutant as described above. A correct clone was verified by restriction digest and sequencing as M2Δ*pilA*::kanΔ*pilD*::*strAB* (*pilA*$_{FLAG}$+).

Transformation efficiency assays. A single colony, from plates incubated overnight at 37˚C, was used to inoculate 2 mL of LB-broth. After overnight growth at 37˚C, 180 rpm, 50 µL of culture was diluted with 450 µL of fresh LB-broth and grown for 2 h at 37˚C, 180 rpm. One microgram of pGEM-*blsA::strAB,* linearized with PstI, was added to cultures. After 2 h, the bacteria/DNA suspension was spotted on a L-agar plate and incubated for 4 h at 37˚C. Bacteria were removed from the plate, resuspended in 500 µL LB-broth, normalized to an OD_{600} of 50 and serial dilutions were plated on L-agar to enumerate total colony forming units (CFU). In addition, serial dilutions were plated on L-agar supplemented with streptomycin to enumerate CFU of transformants. Transformation efficiency was calculated by dividing the CFU of transformants by the total CFU. Experiments were conducted on at least three separate occasions.

Electron microscopy. M2, the *pilA, pilT* and *pilT pilA* mutant strains were streaked onto L-agar and incubated overnight at 37˚C. One hundred microliters of DPBS was added to isolated colonies to create a slightly turbid bacterial suspension. Twenty microliters of the bacterial suspension was pipetted onto a piece of parafilm and formvar carbon film on 300 square mesh nickel grids (Electron Microscopy Sciences) were placed in each droplet for 5 min. The grids were blotted on filter paper and subsequently incubated in 20 µL of 2% paraformaldehyde in DPBS for 1 h. The grids were washed three times in DPBS and blotted on filter paper, then stained in a 2.0% w/v ammonium molybdate,

2.0% w/v ammonium acetate solution diluted 1:1 with deionized water for 5 min. The grids were blotted dry on filter paper and dried overnight. Images were captured on an FEI Tecnai G2 Spirit transmission electron microscope at the Campus Microscopy and Imaging Facility at The Ohio State University.

Pili shear preparations. M2, the *pilA* and *pilT* mutant strains were each streaked onto 6 L-agar plates each and incubated overnight at 37˚C. In order to purify enough surface exposed protein to visualize by coomassie staining on a polyacrylamide gel, bacteria were collected from agar plates and resuspended in 5 ml volume of phosphate buffered saline containing protease inhibitor cocktail (Roche) yielding a concentrated cell suspension. Appropriate dilutions were made and normalized via absorbance at 600 nm to an optical density of 50. Cells were vortexed at high speed for 1 min, followed by incubation on ice for 1 min. After centrifugtion at 16,000 x *g* for 1 min at 4˚C, resultant supernatants were removed and ammonium sulfate was added to the supernatants to a final concentration of 30%. The preparations were incubated overnight at 4˚C. The precipitated protein was then collected by centrifugation at 20,000 x *g* and resuspended in 100 µL of SDS-PAGE loading buffer. Twenty microliters of each sample was run in duplicate on a 4-20% TGX gel (Biorad) for analysis by silver staining and Coomassie staining. Protein bands were excised and sent off for MALDI-TOF mass spectrometry analysis at the Campus Chemical Instrument Center Mass Spectrometry and Proteomics Facility at The Ohio State University.

Processed and unprocessed PilA-FLAG Western blot. To identify if PilD was the leader peptidase, M2Δ*pilA*::kan (*pilA*$_{FLAG}$*+)* and M2Δ*pilA*::kan Δ*pilD*::*strAB* (*pilA*$_{FLAG}$+) were streaked onto L-agar and incubated for 16-18 hours at 37˚C. The cells were scraped from the plate into DPBS and normalized to OD_{600} of 5.0. Samples were resuspended in 1X loading buffer, boiled for 10 min and then run on a 4-20% TGS gel and transferred to nitrocellulose for western blot analysis with an anti-FLAG antibody (Agilent) following the manufacturers protocol.

Twitching Motility. Twitching motility plates, comprised of 10 g tryptone/L, 5 g NaCl/L and 10 g agarose/L (BP164-100, Fisher) (1.0%) were prepared fresh for each experiment. Each plate was made by pouring 30 mL media into a 150 mm petri-dish and allowing the media to air dry with the lid off for 20 min in a laminar flow hood. Each twitching motility plate was stab inoculated with a colony of bacteria to the agarose/petri plate interface and placed in a 37˚C, humidified incubator for 18 h. To visualize the bacteria at the interface, agarose was removed from each plate and the plates were washed with phosphate buffered saline (PBS) and stained with 0.1% crystal violet (w/v) in water for 5 min. To remove excess crystal violet, each plate was gently washed with PBS and allowed to dry. Twitching motility assays were conducted on at least three separate occasions.

Surface-Associated Motility. Surface motility plates, comprised of 5 g tryptone/L, 2.5 g NaCl/L, and 5 g agarose/L (0.3%) as previously described (147), were prepared fresh for each surface motility experiment. In order to reduce variation between plates, each plate was poured with 30 mL of surface motility media in a laminar flow hood with the lids off. The plates were allowed to dry for 30 min and then promptly used for motility assays. Motility plates were inoculated on the surface with 2 µL of a bacterial suspension normalized to an OD_{600} of 2.0. Each bacterial culture was started in the morning from an isolated colony and incubated to stationary phase at 37˚C with shaking at 180 rpm. Motility plates were incubated for 18h at 37˚C. Surface-associated motility assays were conducted on at least three separate occasions.

3.3 Results

Identification and arrangement of Tfp biosynthesis gene clusters in *A. baumannii* strain M2

Roche 454 and Ion Torrent instruments were employed to obtain raw genomic sequence for strain M2. These data were assembled and the resulting contig sets (R.S. Munson Jr. and P.N. Rather, unpublished data) were queried for genes whose products have homology to proteins required for the biogenesis of Tfp found in other Gram-negative organisms as well as in completed *A. baumannii* genomes. Antunes *et al*, in Table S2 of their manuscript, published a list of putative Tfp-associated genes in three *A. baumannii* genomes (81).

Eijkelkamp and co-workers examined 11 fully sequenced *A. baumannii* genomes and reported that all contained genes likely to encode proteins involved in Tfp biogenesis (91). In the strain M2 genome, we identified homologs of genes whose products are known to be critical in Tfp biogenesis in other organisms. We chose three of these genes for further investigation as our primary goal was to determine whether functional Tfp were produced by strain M2. The Tfp biogenesis-related gene clusters were arranged similarly to the gene clusters identified in other *A. baumannii* strains (81). One gene cluster was identified that contains genes that encode a putative traffic ATPase (PilB), a putative inner-membrane platform protein (PilC) and a putative prepilin peptidase (PilD) (Fig. 1). A second gene cluster contains genes that encode homologs of the Tfp retraction ATPases PilT and PilU. A third locus contains a gene that encodes the putative major pilin subunit, PilA. PilA has a predicted six amino acid leader peptide, an N-terminal hydrophobic region and a processed length of 138 aa (91). The protein has two cysteines, which are predicted to form one disulfide bridge. Together, these data indicate that strain M2 encodes a type IVa pilus system (58). The gene directly downstream of the *pilA* gene in strain M2 is predicted to encode a 436 aa hypothetical protein that contains a conserved Wzy_C domain found in the O-antigen ligase-like protein family. A gene encoding a member of the O-antigen ligase-like protein family is found immediately downstream of the *pilA* gene in some strains of *P. aeruginosa*. This Wzy_C domain-containing protein, in *P. aeruginosa* is a pilin glycosylase (113). However, in the absence of

functional data we have designated the gene encoding this Wzy_C domain containing protein in strain M2 as *pgyA* for putative glycosylase A.

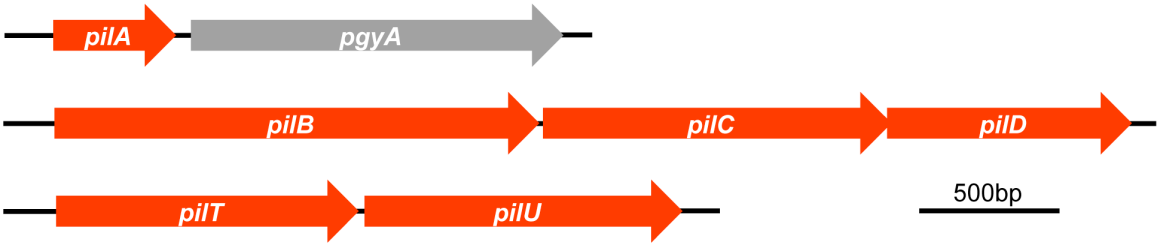

Figure 3.1 The *pil* gene loci in *A. baumannii* strain M2 employed in this study

Genes predicted to encode subunits of a Tfp system in *A. baumannii* strain M2. We identified a *pilA* gene predicted to encode the major pilin subunit followed by *pgyA* possibly coding for a type IV pili O-glycosylase. Two other *pil* gene clusters were identified, a *pilBCD* gene cluster encoding a putative traffic ATPase (*pilB*), a putative inner membrane platform protein (*pilC*) and a putative prepilin peptidase (*pilD*) as well as a *pilTU* gene cluster encoding two putative retraction ATPases.

The *pil* gene products were required for natural transformation

In addition to the identification of Tfp-encoding genes, we observed that strain M2 was naturally transformable; a phenotype associated with the production of Tfp in other naturally transformable Gram-negative organisms. We constructed strains containing mutations in the *pilA*, *pilD* or *pilT* genes and then determined the transformation efficiency of each strain. As shown in Figure 3.2, the transformation efficiency for all mutant strains was below the level of detection in our assay. Each mutation was complemented by cloning the parental gene under the control of its predicted native promoter into a mini-Tn*7* element, which was then transposed into the *att*Tn*7* site downstream of the *glmS*2 gene in the strain M2 chromosome. Transformation, similar to parental levels, was observed in the complemented *pilA* and *pilD* mutants. In contrast, we were unable to complement the *pilT* mutation with the parental *pilT* allele. In *A. baumannii*, *pilT* and *pilU* are contiguous on the chromosome as in they are in *P. aeruginosa* (Figure 3.1). However in *P. aeruginosa*, *pilT* and *pilU* are independently transcribed indicating that the promoter for *pilU* may be within the *pilT* open reading frame (149). Thus, it is likely that our inability to complement the *pilT* mutation was due to polar effects on *pilU*. We therefore reintroduced a complete *pilTU* gene cluster, using the mini-Tn7 system, into the *pilT* strain; the natural transformation phenotype was restored suggesting that we may have affected transcription of *pilU* in the *pilT* mutant. In addition, we introduced an empty mini-Tn*7* element into the *pilA* mutant and demonstrated that this strain did not have detectable levels of

transformation, indicating that the mini-Tn*7* alone does not restore the transformation phenotype (R.S. Munson, data not shown). We also generated a strain containing a deletion of the *pgyA* gene. This mutant was naturally transformable.

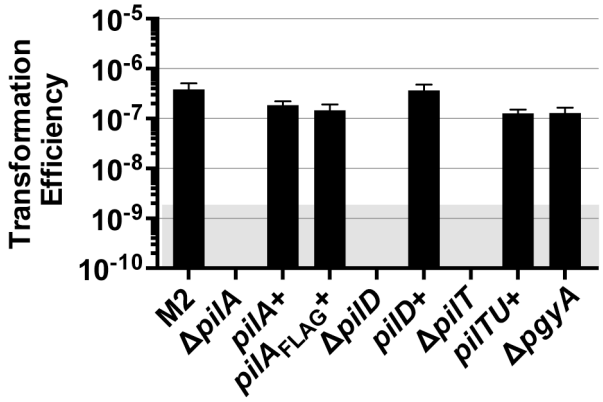

Figure 3.2 Strain M2 natural transformation was reliant upon *pil* gene products

Strain M2, the *pilA*, *pilD*, *pilT* isogenic mutants and their respective complemented strains including a ∆*pilA* strain complemented with the *pilA* gene fused to a FLAG tag were tested for their transformation efficiency. The *pilA*, *pilD* and *pilT* mutants had transformation efficiencies below our level of detection, but the complemented strains regained the natural transformation phenotype. The *pgyA* mutant retained parental levels of transformation. The gray shaded area represents the level of detection of the assay. Transformation efficiency was calculated as the ratio of transformants/mL divided by the total CFU/mL for a given reaction. Bars represent mean of three independent experiments with two technical replicates each and error bars represent the standard error of the mean.

Tfp-like structures were observed on the surface of strain M2

Type IV pili are long, narrow fibers, generally less than 8 nm in diameter that can be readily visualized on the surface of many Gram-negative bacteria including *Neisseria* species and *P. aeruginosa* (58). We failed to observe Tfp-like structures when whole cells of strain M2 were examined by transmission electron microscopy (TEM). However, the inability to detect Tfp by EM is similar to what we observed with Tfp in *H. influenzae*; that is, unless the Tfp regulon was overexpressed, Tfp were not observed by EM (145). Others have demonstrated that strains containing mutations in the *pilT* gene *of N.* gonorrhoeae*, P.* aeruginosa *and D. nodosus* are hyper-piliated as compared to the parental strain (49, 148, 149). We readily observed Tfp-like structures on the *pilT* mutant by TEM (Figure 3.3). Moreover, we did not observe Tfp-like structures on the *pilA* mutant (R.S. Munson Jr., unpublished data). To verify that these structures were in fact Tfp, we constructed a double *pilT pilA* mutant strain and examined for the loss of Tfp-like structures. This strain was devoid of Tfp-like structures, albeit, for one cell out of the >1000 viewed which displayed a structure with similar dimensions to Tfp. These data are consistent with the observed transformation phenotype in that both data sets reaffirm the conclusion that Tfp are produced by strain M2.

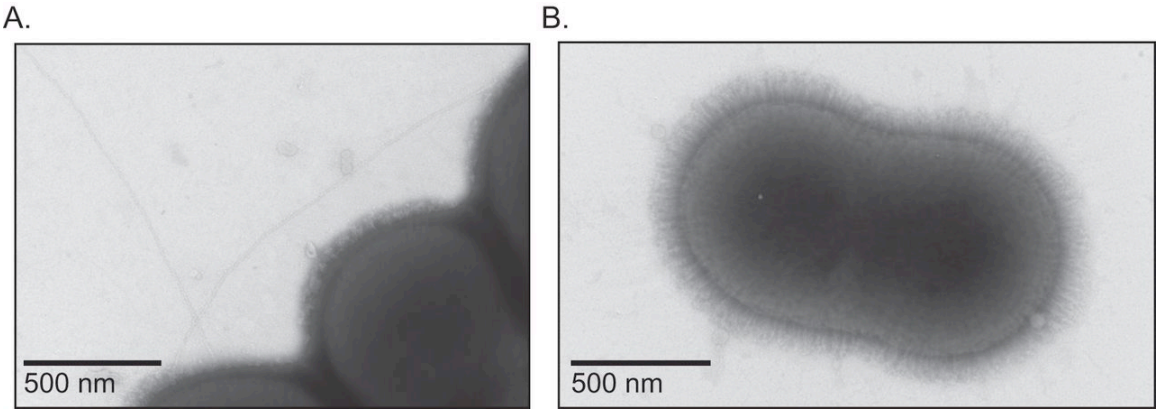

Figure 3.3 Observation of Tfp on the Δ*pilT* mutant.

A) Type IV pili-like appendages were readily observed on the surface of the Δ*pilT* mutant. Bacteria were prepared for electron microscopy on three independent experiments and a representative image is shown. B.) Type IV pili-like appendages were not observed on the surface of a Δ*pilT*Δ*pilA*::*strAB* mutant.

The major pilin subunit, PilA, was surface exposed

Type IV pili are polymers composed predominately of the major pilin subunit, PilA, and minor pilins so named for their relative abundance within the pilus fiber. By shearing pili from the surface of bacteria, the fiber can be separated from whole cells (153, 154), disassembled into its components, separated by SDS-PAGE analysis and protein composition determined via mass spectrometry. Cells of the parental M2 strain as well as the isogenic *pilA* and *pilT* mutant strains were vortexed to shear off surface structures. Whole cells were separated from the sheared protein fraction by centrifugation. The sheared protein fractions from each strain were then analyzed by SDS-PAGE. Selected bands were excised and the proteins were identified by mass spectrometry. As shown in Figure 3.4, when the sheared protein fractions were examined on a silver-stained SDS-PAGE, a band was present in the parental fraction slightly above the predicted mass of PilA (13.9 kDa). This band was absent in the fraction prepared from the *pilA* mutant. When preparations from the *pilT* mutant were characterized, a band was observed which had the same mobility as the band in the parental fraction. In addition, a band with a lower apparent molecular weight was present. The regions where the bands were present were excised from a Coomassie-stained SDS-PAGE gel, trypsinized and subjected to MALDI-TOF mass spectrometry. As expected, the upper band present in the both the parental and *pilT* mutant fraction was identified as PilA. The PilA protein was not found in this region of the preparation from the *pilA* mutant. Interestingly, the lowest band in the *pilT* mutant

fraction was also identified as PilA protein. These data taken together with the TEM images provide additional evidence that strain M2 produced Tfp and that PilA is the major pilin subunit.

Lastly, a band running at an intermediate molecular weight between the upper and lower bands of the *pilT* mutant fraction was observed in all three samples. This band was identified as a protein containing a spore coat domain by Blast; however, structural prediction analysis [PHYRE2, (155)] of the primary amino acid sequence revealed that this protein may be a pilin of a chaperone usher pilus system that is not yet characterized in *A. baumannii*. This protein is highly homologous to a putative biofilm synthesis protein (NCBI Accession Number YP_001713377) found in *A. baumannii* strain AYE. We are currently investigating the role of this putative type I pilin in the biology of *A. baumannii*.

A.

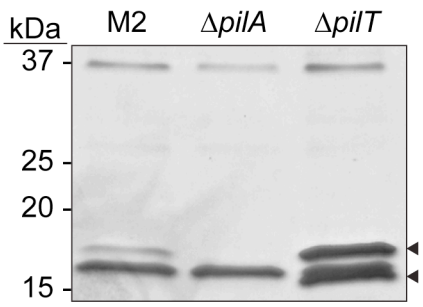

B.

MNAQK GFTLIELMIVVAIIFILAAIAIPAY
QNYIAK SQASEAFTLADFLK TTINTNLQAQ
TCFAGGATAVTAADK VSGKYGDAEIGGTAP
NCTITYTFK SSGVSNKLTSTK IVMNVSETG
ILK NSGTDTPVELLPQSFVAS

Figure 3.4 PilA, the major pilin subunit, was surface exposed

A) The parental strain, the *pilA* and *pilT* mutant strains were resuspended in DPBS from L-agar plates and vortexed to remove surface appendages. The sheared proteins were separated by SDS-PAGE, excised and examined by MALDI-TOF mass spectrometry. The upper band in both the parental and *pilT* mutant fraction was identified as PilA. Interestingly the lowest band present in the *pilT* mutant fraction was also identified as PilA. PilA was not identified in the *pilA* mutant fraction. B) The primary amino acid sequence of the unprocessed prepilin, PilA, is shown. Predicted tryptic peptides are separated by a space and shown in alternating colors for clarity. Underlined peptides were identified in both samples analyzed from the *pilT* mutant. The predominant band in the sample from the *pilA* mutant strain (also seen in the other preparations) is a predicted pilin produced by a chaperone/usher system. This is 87% identical to a putative biofilm synthesis protein (YP_001713377) in *A. baumannii* strain AYE.

The strain M2 PilD homolog was required for processing of PilA

Based on homology, we predicted that *pilD* encodes the prepilin peptidase, a protein required in other Tfp systems that acts by cleaving an N-terminal leader peptide from immature PilA. To test this prediction, we compared the molecular mass of PilA produced in *pilD*$^{+}$ and *pilD*$^{-}$ backgrounds. As we do not currently have an antiserum that recognizes strain M2's PilA, we constructed a mini-Tn*7* element carrying sequence that encoded PilA with a C-terminal FLAG tag. Strains containing the *pilA*$_{FLAG}$ gene in a *pilA* mutant and a double *pilA pilT* mutant background were constructed. We then compared whole cell lysates of the two strains by Western blot analysis, probing with an anti-FLAG antibody. In Figure 3.5, we show that PilA$_{FLAG}$ was detected in both strains; however, PilA from the double *pilA pilD* mutant strain migrated as a higher molecular mass protein when compared to PilA produced in the *pilA* mutant background. These results are consistent with our hypothesis that PilD is the prepilin peptidase involved in processing of strain M2's major pilin, PilA.

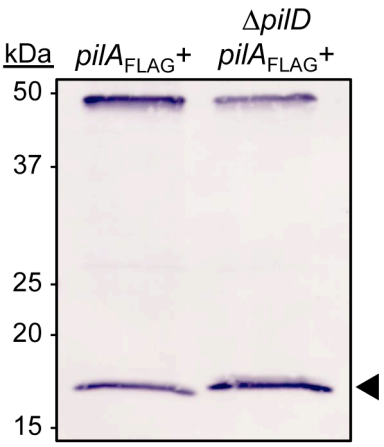

Figure 3.5 The strain M2 PilD homolog acted as a prepilin peptidase

Whole cell lysates of the M2Δ*pilA*::kan (*pilA*$_{FLAG}$*+)* and M2Δ*pilA*::kan Δ*pilD*::*strAB* (*pilA*$_{FLAG}$+) strains were examined by Western blot analysis for processed and unprocessed PilA$_{FLAG}$. The non-specific band around 50 kDa was included to demonstrate equal migration of proteins. PilA$_{FLAG}$ from the M2Δ*pilA*::kan (*pilA*$_{FLAG}$*+)* migrated to slightly lower position compared to PilA$_{FLAG}$ from M2Δ*pilA*::kan Δ*pilD*::*strAB* (*pilA*$_{FLAG}$+). The leader peptide of M2's PilA is predicted to be six amino acids. Western blot analysis was conducted on three separate occasions and a representative blot is shown.

The *pilA*, *pilD* and *pilTU* gene products were required for twitching motility, but not surface-associated motility

Twitching motility, a Tfp-dependent phenotype, is generally observed at the interphase of the petri dish and an agar or agarose surface. Classically, twitching motility assays have been conducted with medium containing 1% of the solidifying agent agar; however, agarose may be substituted. Given that transformation of strain M2 was dependent on Tfp, we hypothesized that strain M2 would be capable of twitching motility. As shown in Figure 3.6, strain M2 exhibited twitching motility. In contrast, the *pilA*, *pilD*, and *pilT* mutants did not exhibit twitching motility. Parental levels of twitching motility were observed when the complemented mutants were tested. The *pilA* mutant containing an empty mini-Tn*7* element did not exhibit twitching motility (R.S. Munson, data now shown). The *pgyA* mutant strain retained parental levels of twitching motility.

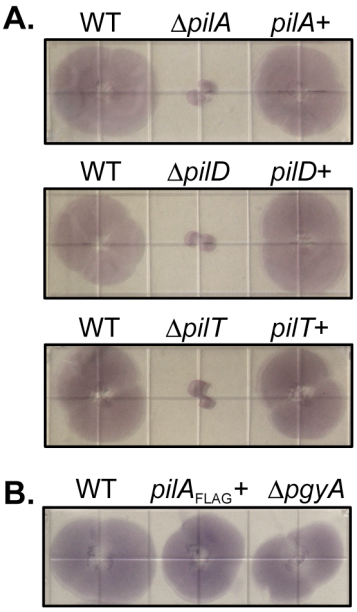

Figure 3.6 Twitching motility was reliant upon the *pil* gene products.

A) Twitching motility was observed at the agarose/plastic interface for strains M2, and the complemented mutants but not observed with the *pilA*, *pilD* and *pilT* mutants. Each strain was inoculated by stabbing through the agarose to the surface of a plastic petri dish followed by incubation at 37˚C for 18 h. The agarose was removed and the non-adherent bacteria were removed by washing with PBS. The adherent bacteria were visualized by staining with 0.1% crystal violet. Each square grid on the plate is 13 mm wide. Twitching motility was performed on three independent occasions a representative image is shown. B) The C-terminal FLAG tag on PilA did not impede twitching motility. The *pgyA* mutant retained the twitching motility phenotype.

Some *A. baumannii* isolates are also capable of a flagella-independent surface-associated motility exhibited on semi-solid media (156, 157). Clemmer *et al.* demonstrated that strain M2 was capable of surface-associated motility (92). In their study, surface-associated motility was impaired but not absent in a *pilT* mutant. To further explore the role of Tfp in *A. baumannii* strain M2 surface-associated motility, we assessed the isogenic Tfp mutant strains for their ability to translocate across the surface of semi-solid media. Interestingly, the surface-associated motility of the *pilA*, *pilD* and *pilT* mutants were similar to that of the parental M2 strain (Figure 3.7).

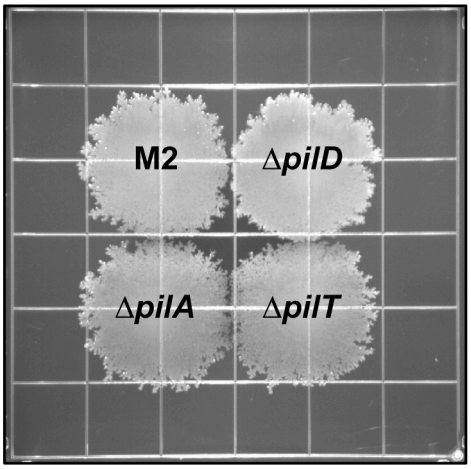

Figure 3.7 The *pil* gene products were not required for surface-associated motility

Strain M2, the *pilA, pilD* and *pilT* mutants were inoculated on the surface of a semi-solid agarose plate (0.5%) and incubated for 18 h at 37˚C. The *pilA, pilD* and *pilT* mutant strains demonstrated no defect in surface-associated motility as compared to the parental strain. Each grid is 13mm^2. Surface-associated motility experiments were performed on three separate occasions and a representative image is shown.

3.4 Discussion

Several investigators have noted that *A. baumannii* genomes contain genes that likely encode proteins required for the biogenesis of Tfp and it has been suggested that Tfp might be involved in the surface-associated motility phenotype demonstrated by some *A. baumannii* isolates (92). We sought to definitively demonstrate the production of Tfp in an *A. baumannii* clinical isolate and determine whether the classically defined Tfp-associated phenotypes, transformation and twitching motility, required *A. baumannii* Tfp.

In *A. baummanii* strain M2, we identified several genes whose products were known to be involved in Tfp biogenesis in other organisms (145, 158). We demonstrated that strain M2 was naturally transformable and exhibited twitching motility; both phenotypes were absent in the *pilA, pilD* and *pilT* mutants. The *pilA*, *pilD* and *pilT* mutations were then complemented, restoring the Tfp-dependent phenotypes.

Major and minor Tfp pilins are processed prior to being polymerized into a fiber by the removal a leader peptide by a dedicated prepilin peptidase, PilD (63). We tested for the predicted PilD activity by constructing strains that expressed C-terminal flag-tagged PilA in a *pilA* mutant and a double *pilA pilD* mutant background. When examined by Western blot the PilA-Flag protein produced in the *pilA pilD* mutant ran with a slightly higher apparent molecular weight

compared to the protein produced in the *pilD*$^{+}$ strain, consistent with cleavage of the predicted six amino acid leader peptide.

Downstream of the *pilA* gene is a gene encoding a hypothetical protein containing an O-antigen ligase (Wzy_C) domain. This gene is found in a subset of genomes of the clinical isolates that have been sequenced. These include *A. baumannii* strain ACICU (Accession CP000863), TYTH-1 (Accession CP-003856), MDR-TJ (Accession CP003500), MDR-ZJ06 (Accession CP001937), TCDC-AB0715 (Accession CP002522), and 1656-2 (Accession CP001921). It is possible that PgyA is a pilin glycosylase as PilO produced by *P. aeruginosa* 1244 also contains a Wzy_C domain, and catalyzes the addition of a trisaccharide to serine 148 of PilA (122). Eleven serine residues are present in the M2 PilA; however, the location of serines within the strain M2 protein are not the same as those identified as glycosylation targets in the *P. aeruginosa* 1244 pilin. Additional studies are required to determine the activity of PgyA.

The *pygA* gene is not to be confused with the recently characterized *pglL* gene identified in *A. baumannii* ATCC 17978 although the *pglL* gene is present downstream of the *pilA* gene in strain ATCC 17978. In strains whose genomes contain the *pgyA* gene, the *pglL* gene is found immediately downstream of *pgyA*, as is the case in strain M2. In strain ATCC 17978, the *pglL* gene product is required for the O-glycosylation of several proteins of unknown function (105).

Type IV pili are surface appendages that have diameters ranging from 5-8 nm and can measure several microns in length. Tfp have been visualized on, and purified from, many Gram-negative organisms (58). We employed numerous strategies to visualize Tfp on the surface of strain M2, including using immuno-gold labeling and TEM to view pili on M2 strains expressing $PilA_{FLAG}$. These attempts were unsuccessful. However, when we examined the *pilT* mutant strain by negative stain transmission electron microscopy we were able to visualize structures emanating from the surface of the outer-membrane that resembled Tfp. These structures were present on a subset of the cells in the *pilT* mutant population, rarely on the parent but were absent in a double *pilT pilA* mutant, indicating that these structures are most likely Tfp. Although these Tfp-like structures were absent from the double *pilT pilA* mutant cells observed by TEM, one cell out of the >1000 viewed contained a structure with a similar diameter to Tfp; however, its length was substantially shorter than any Tfp observed on the *pilT* mutant. Nevertheless, these observations are expected given the increase in relative abundance of surface exposed PilA on the *pilT* mutant as compared to the parental M2 strain.

Enrichment for bacterial extracellular appendages by shearing bacteria in suspension without excessive cell lysis has been demonstrated for many organisms including *P. aeruginosa* and nontypeable *H. influenzae* (145, 159). Therefore, sheared cell supernatants from the parental M2 as well as the *pilA*

and *pilT* mutant strains were examined by Coomassie stained SDS-PAGE. Multiple bands were present in the fraction from strain M2 when compared to the fraction from the *pilA* mutant and these same bands were greatly enhanced when examined in the fraction from the *pilT* mutant. Our observation was concordant with those by Han *et al.*, where a *pilT* mutant in *D. nodosus* demonstrated an increase in surface exposed PilA as compared to the parental strain (49). The upper band present in the fraction from the parent and the *pilT* mutant contained PilA when analyzed by MALDI-TOF mass spectrometry confirming that strain M2 is able to export PilA to the surface of the cell and by inference, assemble Tfp. Interestingly, the lowest band in the fraction from the *pilT* mutant contained PilA. We hypothesized that PilA in the lower band could simply be truncated or a proteolysis product; however, when we analyzed the mass spec data for differential peptide identification, we found that the same peptides were present in both fractions. All peptides, with the exception of the hydrophobic amino terminal peptide, were present.

Genes predicted to encode Tfp biogenesis proteins have been identified in all of the fully sequenced genomes of *A. baumannii* clinical isolates; however, most of the *A. baumannii* clinical isolates do not exhibit twitching motility (91), a classic phenotype associated with functional Tfp. Additional work will be required to determine if the Tfp-associated genes in these genomes are transcribed and under what conditions.

Recently, Eijkelkamp and co-workers reported that surface-associated motility and twitching motility were not always observed together and concluded that there are different mechanisms accounting for the different motility phenotypes displayed by *A. baumannii* clinical isolates (91). Twitching motility is a form of bacterial motility independent of flagella that requires the Tfp to assemble, bind to a substratum and then dissemble resulting in movement of the cell body towards the point of attachment (60). Twitching motility was observed with strain M2 and this phenotype was dependent on the *pilA*, *pilD* and *pilT* gene products, as twitching motility was absent in the mutant strains but restored to parental levels in the complemented strains. Eijkelkamp *et al.* demonstrated that there is sequence conservation between the PilA protein of *A. baumannii* clinical isolates within the same clonal lineage and that strains within the same clonal lineage exhibited similar motility patterns. Thus, their data suggested that specific PilA sequences might partially influence the ability of a strain to exhibit twitching motility. However, when we compared the sequence of strain M2's PilA to those identified in the Eijkelkamp study, we found that M2's PilA sequence had a 92% identity to *A. baumannii* strain 19606, a clinical isolate that did not exhibit twitching motility. Thus it appears that PilA sequence does not correlate with ability of a particular strain to exhibit twitching motility.

Many strains of *A. baumannii* have also been shown to exhibit a unique surface-associated motility on semi-solid media that resembles swarming motility of *P.*

aeruginosa; however, swarming motility, as defined by Henrichsen, is flagella coordinated movement of groups of cells across a solid surface (160). *Acinetobacter baumannii* surface-associated motility is a flagella-independent, multi-factorial, complex process that is partially dependent on 1,3-diaminopropane synthesis, quorum sensing, iron concentration, the composition of lipopolysaccharide and is sensitive to blue light when cells are grown at 24˚C (92, 147, 156, 157). It has been speculated that Tfp might be involved in the surface-associated motility of this bacterium. Recently, Clemmer *et al.* demonstrated, in strain M2, that a mutant deficient in expression of the PilT protein was partially impaired with respect to surface-associated motility (92). In contrast, the *pilT* mutant we characterized as well as the *pilA* and *pilD* mutants exhibited parental levels of surface-associated motility. Occasionally, the *pilD* mutant exhibited a variable motility as compared to the parental strain as well as the other mutant strains. Rather and coworkers (unpublished data) have observed two subtle but distinct colony morphologies, opaque and translucent, when M2 is streaked on 1% LB agar. These colony morphologies are independent of the Tfp phenotype. When a translucent clone, containing the *pilT* mutation was tested, surface-associated motility of the *pilT* mutant was impaired. In contrast, an opaque clone containing a *pilT* mutation retained parental levels of surface-associated motility. When streaked on a plate, colonies of the *pilT* mutant described by Clemmer *et al.* are primarily translucent (92). Colonies of the *pilT* mutant described herein were primarily opaque, which partially explains

the discrepant results. Overall, however, it is clear that surface-associated motility is not strictly dependent on the expression of Tfp in the opaque form. A complete understanding of the basis for the surface-associated motility will, in part, depend on the identification of the molecular basis for the translucent and opaque colony types.

Herein, we have provided genetic evidence that twitching motility and surface-associated motility are distinct phenotypes confirming and extending the observations of Eijkelkamp and co-workers (91). We also have demonstrated that PilA sequence does not correlate with the ability to exhibit twitching motility. Importantly, we have provided the first visual evidence of Tfp production by an *A. baumannii* strain through the observation of Tfp on the surface of the strain M2 *pilT* mutant, a phenotype that is dependent upon the *pilA* gene product. In addition, we demonstrated that PilA is a major surface exposed protein and taken together with the TEM images, we conclude that PilA is the major pilin subunit. Natural transformation and twitching motility were dependent on expression of Tfp, while the mechanisms responsible for surface-associated motility remain to be determined; however, our data emphatically illustrate that Tfp were not required for surface-associated motility of strain M2. Importantly, our study demonstrated that Tfp are produced by and have a role in the biology of an *A. baumannii* clinical isolate. Future studies will be directed at defining the

conditions that promote Tfp expression and determining the role Tfp in the virulence of this emerging pathogen.

Plasmid or strain	Relevant characteristic(s)	Reference/ Source
Plasmids		
pFLP2	Encodes FLP recombinase	(152)
pKD13	Contains kanamycin resistance gene from Tn5 flanked by FRT sites	(150)
pRSM3542	pKD13 containing *kan-sacB*	(127)
pGEM-T-Ez	General cloning plasmid	Promega
pGEM-*pilA*	pGEM containing *pilA* with 1 kb flanking DNA	This study
pGEM-*pilA*::kan	pGEM-*pilA* containing *pilA*::kan	This study
pGEM-Δ*pilA*	pGEM containing an in frame deletion of the *pilA* gene	This study
pGEM-Δ*pilA*::*strAB*	pGEM-Δ*pilA* containing *pilA*::*strAB*	This study
pGEM-*pilBCD*	pGEM containing *pilBCD* with 1 kb flanking DNA	This study
pGEM-*pilD*::kan	pGEM-*pilBCD* containing *pilD*::kan	This study
pGEM-*pilD*	pGEM containing the predicted *pilB* promoter, the ATG of *pilB*, the last 21bp of *pilC* and *pilD*	This study
pGEM-*pilTU*	pGEM containing *pilTU* with 1 kb flanking DNA	This study
pGEM-*pilT*::[kan-*sacB*]*pilU*	pGEM-*pilTU* containing *pilT* interrupted with the kan-*sacB* cassette	This study
pRSM3510	pKNOCK derivative with a mini-Tn*7* element containing a multiple cloning site	(127)
pRSM3510-*pilA*	pRSM3510 containing *pilA* with expression driven from the predicted *pilA* promoter	This study
pRSM3510-*pilA*-FLAG	pRSM3510 containing *pilA*-FLAG with expression driven from the predicted *pilA* promoter	This study
pRSM3510-*pilD*	pRSM3510 containing *pilD* with expression driven from the predicted *pilB* promoter	This study
pRSM3510-*pilTU*	pRSM3510 containing *pilTU* with expression driven from the predicted *pilT* promoter	This study
pGEM-*blsA*::*strAB*	pGEM containing *blsA* interrupted with a streptomycin resistance cassette	This study

Continued

Table 3.1 Plasmids and strains used in this study

Table 3.1 Continued

Strains		
Acinetobacter baumannii strain M2	Metro Health Systems Clinical Isolate	(124)
M2Δ*pilA*::kan	*A. baumannii* strain M2 containing a deletion of *pilA* and replacement with a kanamycin resistance cassette	This study
M2Δ*pilD*::kan	*A. baumannii* strain M2 containing a deletion of *pilD* and replacement with a kanamycin resistance cassette	This study
M2Δ*pilT*::kan-*sacB*	*A. baumannii* strain M2 containing a deletion of *pilT* and replacement with the kan-*sacB* cassette	This study
M2Δ*pilT*	*A. baumannii* strain M2 containing an unmarked deletion of *pilT*	This study
M2Δ*pgyA*::kan	*A. baumannii* strain M2 containing a deletion of *pgyA* and replacement with a kanamycin resistance cassette	This study
M2Δ*pilA*::kan (*pilA+)*	M2Δ*pilA*::kan with a mini-Tn7 element containing the *pilA* gene transcribed from its predicted promoter	This study
M2Δ*pilA*::kan ($pilA_{FLAG}$+)	M2Δ*pilA*::kan with a mini-Tn7 element containing the *pilA* gene fused to a FLAG tag transcribed from its predicted promoter	This study
M2Δ*pilA*::kan *ΔpilD*::strAB($pilA_{FLAG}$+)	M2Δ*pilA* ($pilA_{FLAG}$+) containing a deletion of *pilD* and replacement with a streptomycin cassette	This study
M2Δ*pilD*::kan (*pilD*+)	M2Δ*pilD* with a mini-Tn7 element containing the *pilD* gene transcribed from its predicted promoter	This study
M2Δ*pilT* (*pilTU*+)	M2Δ*pilT* with a mini-Tn7 element containing the *pilTU* gene cluster transcribed from its predicted promoter	This study
M2Δ*pilT* Δ*pilA*::*strAB*	M2Δ*pilT* containing a deletion of *pilA* and replacement with a streptomycin cassette	This study
A. baumannii strain RUH134	Streptomycin resistant clinical isolate; source of streptomycin resistance genes used to construct pGEM-*blsA*::strep	(156)
E. coli DH5a	General cloning strain	Invitrogen
E. coli EC100D	General cloning strain, pir^+	Epicentre
E. coli DY380	Recombineering strain	(161)
E. coli DH5a(pFLP2)	Carries FLP recombinase gene under temperature control	(152)
E. coli HB101(pRK2013)	Conjugation helper strain	(162)
E. coli EC100D(pTNS2*)*	Carries transposase genes for mini-Tn*7* transposition	(163)

Primer Set		Sequence
1	F	AGAATACTTGCATAGTGACAGGTTACAG
	R	GTTATGGCGGCGGTGGAGGTC
2	F	CAAAAAGCTTATATAAAAACATACATACAATCTTTGGGGAAAAGGC TATGATTCCGGGGATCCGTCGACC
	R	GGATTGACCTCTCTTTTTTATTTCTAAAATTACGATGCTACAAATGA TTGTGTAGGCTGGAGCTGCTTCG
3	F	TTCATGGCGTATTTGTTGTTATTA
	R	GTTCAGAGTGTCCGACCAATACGA
4	F	TATGTATCGGTAGCTTTCTTAATGTAGTGATTTACCGCACGCCAAA AATGATTCCGGGGATCCGTCGACC
	R	CACCTGTGATTCCCAGAATAAAAGCCATCTTAACCTCCCAAATAAA TTTTTGTAGGCTGGAGCTGCTTCG
5	F	GCATCCAAATCGCCTGACATCC
	R	GCGAATTCTTAGTTACGGTTCCAGTTCCATCA
6	F	ATAATTGTATTCTCGCTATTTTGTTATTTTTATAGGAATGATTCAGG CTGTGTAGGCTGGAGCTGCTTCG
	R	TATTATTCTACAAAATAATGACATATTTTGATTTACTTGGGGAAATT ATGATTCCGGGGATCCGTCGACC
7	F	GCGGGATCCGCAAATTGGTGATGTGATGTCTCG
	R	GCGGGTACCTCGTATTGTGAACTAGACCATCCT
8	F	GCGGATCCGTCATGCAGAGCTACTATTTTATCCA
	R	GCGAATTCTGTTAGAGCAAGGGGAAGATGTC
9	F	CATGGTCGCTGCCGACACATG
	R	CAAATGGGCTCAGTTGTATAATG
10	F	GCGGGTACCTGTATGACGCGCTTGTGGATT
	R	GCGGGATCCCGAACCCGACATACTGCTCACCTT
11	F	TAATTTTAGAAATAAAAAAGAGAGGTCA
	R	CTTGTCGTCATCGTCCTTGTAGTCcgatgctacaaatgattgagga
12	F	CGCTACACCCAGTTCCCATCTA
	R	CCTAACTTGTTCAGCAGCATTCA
13	F	GTCGATTAGAGGAAGGCACAGTAG
	R	AGCCGATGTTACTTTTTGTTATTTG
14	F	TAAACATTCATCTGCTACTCCCGA
	R	TGCCCGTCACTCCCACTC

Continued

Table 3.2 Primers used in this study

Table 3.2 Continued

15	F	GCGGGATCCAAAATTTATTTGGGAGGTTAAGATGGC
	R	GCGGGATCCCATTATACAACTGAGCCCATTTGGA
16	F	CATAGCCTTTTCCCCAAAGATTG
	R	CAATCATTTGTAGCATCGTAATTT

Chapter 4: *Acinetobacter* strains carry two functional oligosaccharyltransferases, one devoted exclusively to type IV pilin, and the other one dedicated to *O*-glycosylation of multiple proteins

4.1 Introduction

Acinetobacter baumannii and *A. nosocomialis* are clinically relevant members of the *Acinetobacter calcoaceticus- A. baumannii* (Acb) complex and important opportunistic nosocomial pathogens (27).These species have emerged as troublesome pathogens due in part to their remarkable resistance to disinfection, desiccation, as well as their ability to acquire multiply drug resistant phenotypes, all of which promote their survivability in the hospital setting. Furthermore, pan-resistant strains within the Acb are continuously being isolated from hospitals worldwide (164, 165).While the mechanisms of antibiotic resistance of Acb members has been intensively studied (166), our understanding of their virulence mechanisms is unclear. Identified virulence factors include capsule, protein glycosylation systems, exopolysaccharide, the ability to form biofilms, and lipopolysaccharide (LPS) (49, 54, 55, 105, 166, 167). A type VI secretion system (T6SS) has been also identified, although a role in pathogenesis has not been demonstrated (127, 168).

A. baylyi is a non-pathogenic member of the genus *Acinetobacter*, characterized by its genetic tractability and natural competence. For these properties, *A. baylyi* is widely used as a model organism for molecular and genetic studies of the genus *Acinetobacter* (22, 86, 169) and is also utilized in bioremediation(170, 171). All members of the *Acinetobacter* genus, independent of their pathogenicity, carry a protein glycosylation system (105).

Protein glycosylation, the covalent attachment of carbohydrate moieties to protein substrates, is the most abundant post-translational modification of proteins (172) and occurs in all domains of life(173-175). The major types of protein glycosylation are *N*- and *O*-glycosylation. Both processes can be classified as oligosaccharyltransferase (OTase)-dependent and OTase-independent (96, 98). OTases are enzymes that catalyze the transfer of a glycan, previously assembled by cytoplasmic glycosyltransferases (GT) onto an undecaprenylpyrophosphate lipid carrier, to target proteins. The development of sensitive analytical techniques has led to the identification of OTase-dependent protein glycosylation in numerous bacterial species. These include members of the genera *Bacteroides*, *Neisseria, Burkholderia, Vibrio, Francisella, Pseudomonas,* and *Campylobacter* (106, 107, 115, 176-179). Glycosylation frequently affects protein stability, bacterial adhesion, flagellar filament assembly, biofilm formation, and virulence in general (98, 180). An OTase-dependent, ubiquitous *O*-linked protein glycosylation system has been recently discovered

within the genus *Acinetobacter*. This system was required for biofilm formation and pathogenicity of *A. baumannii* (105). The glycan structures for several strains of *A. baumannii* have also been characterized and extensive carbohydrate diversity has been established (111).

OTases involved in *O*-glycosylation (*O*-OTases) do not share extensive primary amino acid sequence homologies; yet, all *O*-Otases contain domains from the Wzy_C superfamily (181). Orthologs of PglL general *O*-Otases and WaaL O-antigen ligases are two of the most well characterized enzymes from the Wzy_C superfamily. It has proven challenging to identify *O*-OTases based solely on bioinformatic methodologies as *O*-OTases and WaaL ligases catalyze similar reactions, i.e. the transfer of lipid-linked glycans to acceptor proteins or lipid A respectively (103). The two enzymes appear to be evolutionarily and mechanistically related as mutagenesis of topologically similar conserved histidine residues of the *E. coli* O-antigen ligase (H337) and *N. meningitidis O*-OTase (H349) results in the loss of glycan transfer activities (182-184). Recently, the PglL_A and PglL_B hidden Markov models (HMM) were defined to better resolve orthologs of PglL *O*-OTases from other enzymes of the Wzy_C superfamily (110, 181).

O-OTases are often encoded downstream of their cognate target protein. This genetic arrangement is often found in Gram-negative organisms encoding type

IV pili (Tfp) systems, where the major pilin subunit gene is immediately 5' of the cognate OTase gene (110). For example, in *P. aeruginosa* strain 1244 the major pilin, PilA, is glycosylated by PilO (later renamed TfpO), an *O*-OTase encoded immediately downstream of *pilA* (113, 185). This modification is believed to play a role in virulence as glycosylation-deficient mutants showed decreased twitching motility and were out-competed by the wild type in a mouse respiratory infection model (185, 186). The same genetic arrangement and glycosylation phenotype has also been found in *P. syringae* (187).

Pilin post-translational modification has also been identified in *Acinetobacter* spp. In *A. baylyi* ADP1, two Wzy_C superfamily domain-containing proteins are encoded in the genome. One gene is found immediately downstream of the gene encoding the pilin-like protein ComP, whereas the other gene is found within a distant glycan biosynthesis gene cluster. Mutation of the predicted OTase encoded downstream of the *comP* gene affected the electrophoretic mobility of ComP, indicating this gene may encode for a ComP-specific OTase (88, 110). Additionally, during the course of our previous study demonstrating the functional production of Tfp by the medically relevant *A. nosocomialis* strain M2, we also identified two molecular forms of PilA differing by apparent molecular weight leading us to hypothesize that the pilins of Acb members may also be post-translationally modified (6, 127)

A genomic analysis of sequenced genomes of *Acinetobacter* spp. revealed that, in addition to *A. baylyi* ADP1, multiple strains within the genus *Acinetobacter* encode two OTases. In this work we employed genetic and proteomic techniques to demonstrate that both OTases are functional and that one of these enzymes acted as a pilin-specific OTase, whereas the other OTase was able to glycosylate a wide range of proteins. In addition, using mass spectrometry, we characterized the glycan structure of *A. nosocomialis* strain M2 and defined the glycoproteome of *A. baylyi*.

4.2 Materials and methods

Strains, plasmids, and growth conditions. A list of bacterial strains and plasmids can be found in table 4.3. All bacteria were grown on L-agar or in LB-broth at 37˚C unless otherwise noted. When appropriate, antibiotics were added to the *A. nosocomialis* or *A. baumannii* cultures at the following concentrations except when noted otherwise: 100 µg ampicillin/mL, 20 µg kanamycin/mL, or 12.5 µg chloramphenicol/mL. When appropriate, *E. coli* cultures were supplemented with antibiotics at the following concentrations: 50 µg ampicillin/mL for *E. coli* strains containing plasmids other than pGEM derivatives, 100 µg ampicillin/mL for *E. coli* strains containing pGEM derivatives, or 20 µg kanamycin/mL. *R. solanacearum* was grown at 30˚C in BG media (Boucher *et al*.,1985).

Bioinformatic analysis of *Acinetobacter* OTases. Protein sequences for *Acinetobacter* specific OTases were analyzed using NCBI's Basic Local Alignment Search Tool (BLAST) and protein domains identified using the Conserved Domain Database for the annotation of proteins (188-190).

Generation of a strain with an in-frame deletion of *pilA*. The Δ*pilA* mutant was constructed, generating an in-frame deletion of *pilA*, according to the methodology published previously by our group (6). Primer sets 1 and 2 were used and can be found in the primer table located in table 4.4.

Construction of the Δ*tfpO*::kan mutant. We constructed the Δ*tfpO*::kan mutant for our previous publication (6), however, at the time the gene was designated as the *pgyA* gene, not the *tfpO* gene.

Complementation of the Δ*tfpO*::kan mutant. To complement the Δ*tfpO*::kan mutant, we cloned the *tfpO* gene with the predicted *pilA* promoter into a mini-Tn7 element as previously described. Briefly, gDNA from the Δ*pilA* mutant was used as template with primer set 3 to generate an amplicon containing the predicted *pilA* promoter, the ATG start codon of the *pilA* open reading frame, a FLP scar, the last 21bp of *pilA*, the 53bp intergenic region, and the entire *tfpO* open reading frame. A four-parental mating strategy was used to introduce the mini-Tn7 element containing *tfpO* driven off the predicted *pilA* promoter into the Δ*tfpO*::kan

mutant as previously described (6). A correct clone was verified by sequencing and designated as the *tfpO*+ complement.

Plasmid construction and transfer into *E. coli* and *Acinetobacter* isolates. The *pilA* gene from strain M2 was PCR amplified from gDNA using primer set 4 and cloned into the EcoRV site of pWH1266. A correct clone containing the pWH-$pilA_{M2}$ plasmid was verified by restriction digestion and sequencing. pWH-$pilA_{M2}$ was purified from *E. coli* harboring the plasmid, then electroporated into *Acinetobacter* isolates. *Acinetobacter* isolates were made electrocompetent according to the methods previously described (191).

The pBAV-*comP*-His and pBAV-$pilA_{17978}$ plasmids were built by using primer sets 32 and 33 respectively. The sticky-ended amplicons were digested with the respective restriction enzymes and ligated into the vector pBAVmcs in the same sites. The ligation was then electroporated into DH5α-E with transformants being selected for on L-agar plates supplemented with kanamycin.

The pEXT-$pglL_{ComP}$, pEXT-$pglL_{ADP1}$, pEXT-$tfpO_{19606}$ and pEXT-$pglL_{19606}$ plasmids were built using primer sets 34, 35, 36 and 37 respectively. The resulting amplicons were digested with BamHI and SalI and inserted in the same sites of pEXT20. Ligations were electroporated into DH5α-E and transformants were selected for on L-agar plates supplemented with ampicillin.

Construction of a strain M2 ∆*pglL*::kan mutant. The entire *pilA-tfpO-pglL* locus along with 1kb of flanking DNA from *A. nosocomialis* strain M2 was amplified using primer set 6. The PCR product was ligated to pCC1 (Epicentre) and transformed into *E. coli* EPI300. A correct clone containing the pCC1-*pilA-tfpO-pglL* vector was verified by restriction digestion and sequencing. To replace the *pglL* gene with a kanamycin cassette, a modified recombineering protocol was used as previously described (6). To introduce the mutation into *A. nosocomialis* strain M2, the plasmid pCC1-∆*pgl*::kan was linearized and transformed via natural transformation. Transformants were selected on L-agar supplemented with kanamycin. The M2∆*pglL*::kan region in the mutant was verified by sequencing.

Generation of strains containing point mutations in *pilA* in strain M2. To generate a strain with a carboxy-terminal serine to alanine point mutation in the *pilA* gene of strain M2, the M2∆*pilA* mutant was complemented with a mini-Tn*7* element containing a variant of the *pilA* allele, where the carboxy-terminal serine was mutated to an alanine (pRSM3510-*pilA*[S136A]). The pRSM3510-*pilA*[S136A] plasmid was constructed using the Quikchange Site Directed Mutagenesis Kit (Stratagene) according to the manufacturer's protocol using primer set 8. A correct clone carrying the pRSM3510-*pilA*[S136A] plasmid was verified by restriction digest and sequencing. The mini-Tn*7* construct containing the *pilA*[S136A] allele was transposed into the *att*Tn7 of strain M2 via a four-

parental mating strategy previously described above. The same protocol was used to generate the *pilA*[S132A] except primer set 38 was used.

Construction of glycosyl-transferase mutants in the strain M2 background. In order to replace each glycosyl-transferase gene with a kanamycin resistance cassette, an In-Fusion HD EcoDry cloning kit was used according to the manufacturers protocol (ClonTech). The following protocol describing the construction of the M2Δ*weeH*::kan mutation was used for each glycosyl-transferase mutant, except the 15bp overhangs were added to the primers which amplified the 5' and 3' flanking regions of each respective gene. Briefly, the upstream and downstream flanking DNA regions around *weeH* were PCR amplified with primer sets 9 and 10 respectively. The Tn*5* kanamycin cassette and pGEM vector were PCR amplified with 15bp overhangs homologous to the DNA in which they were to be recombined using primer sets 11 and 12 respectively. The PCR amplicons were gel extracted and ethanol precipitated. One hundred nanograms of each product was added to the In-fusion EcoDry cloning tube according to the manufacturer's protocol and incubated at 37˚C for 15 mins then at 50˚C for 15 mins. The newly generated vector was transformed into chemically competent Stellar cells (Clontech) according to the manufacturer's protocol. Transformants were selected for on L-agar plates supplemented with kanamycin. A correct clone containing the pGEM-*weeH*::kan plasmid was sequence verified. The *weeH*::kan cassette was PCR amplified

using the forward primer of primer set 9 with reverse primer of primer set 10. The amplicon was DpnI treated, ethanol precipitated, then transformed into strain M2 according to our previously published methodologies. A correct clone designated M2Δ*weeH*::kan was sequence verified.

The upstream and downstream regions of *wafY* were amplified using primer sets 17 and 18, linearized pGEM was amplified using primer set 15, and the kanamycin cassette was amplified with primer set 16. The above protocol was used to In-Fuse all four PCR products. pGEM-*wafY*::kan was linearized with EcoRI and introduced into *A. nosocomialis* strain M2 via natural transformation as previously described. A correct clone designated M2Δ*wafY*::kan was sequence verified.

The upstream and downstream regions of *wafZ* were amplified using primer sets 19 and 20 and the upstream and downstream regions of *wagB* were amplified using primer sets 21 and 22. Mutants were then constructed as described for the *wafY* mutant. Clones designated M2Δ*wafZ*::kan and M2Δ*wagB*::kan were identified and sequence verified.

Construction of pRSM4063. To generate the pRSM4063 vector, we first introduced an empty mini-Tn*7* element into strain M2 via a four-parental mating strategy previously described. Transposition of the empty mini-Tn*7* element into

the *att*Tn*7* was sequence verified generating the strain M2attTn*7*::MCS_Empty. Genomic DNA was purified from this strain and used as a template in a PCR using primer set 13. The forward primer of primer set 13 is approximately 2kb upstream of the mini-Tn7 element and the reverse primer of primer set 13 is approximately 2kb downstream of the mini-Tn7 element. The ensuing PCR product was ligated into the pSMART-LCKan vector, sequence verified, and designated pRSM4063.

Construction of the *weeH* complemented mutant. To complement the ∆*weeH*::kan mutant, *weeH* plus 375bp of upstream DNA was PCR amplified using primer set 14. The amplicon was digested with XmaI and KpnI, cloned into pRSM4063 and electroporated into DH5α. To complement the ∆*weeH*::kan mutant, pRSM4063-*weeH* was linearized with NdeI and introduced into M2∆*weeH*::kan via natural transformation according to our previously published procedure (6).

Construction of the *wafY, wafZ*, and *wagB* complemented mutants. Given the lack of an obvious promoter driving expression of each of the glycosyl-transferase genes and the over-lapping nature of the open reading frames, the upstream *wxy* promoter was selected to drive expression of each of the three genes. Each glycosyl-transferase mutant was complemented by returning the deleted gene driven off the predicted *wxy* promoter to the chromosome using the

mini-Tn*7* system. Briefly, the glycosyl-transferase locus was PCR amplified using primer set 23, End-It repaired (Epicentre) and ligated into pCC1 (Epicentre). Transformants were selected on chloramphenicol and the pCC1-GT plasmid was verified by restriction digest. The pCC1-GT plasmid contained the predicted promoter of the *wxy* gene (329 bp upstream), *wxy*, *wafY*, *wafZ*, *wagA*, *gnaB*, and *wagB*. To generate the *wxy* promoter-*wafY* construct, an inverse PCR strategy was employed to remove the *wxy* gene and join the *wxy* promoter to the ATG start codon of the *wafY* gene using primer set 24 and pCC1-GT as template. The subsequent PCR product was End-It repaired (Epicentre) and ligated to itself generating the pCC1-wxy^P-*wafY* construct. The wxy^P-*wafY* DNA fragment was PCR amplified using primer set 27, which contained XmaI and KpnI restriction overhangs. The PCR product was digested and ligated to pre-digested pRSM3510 then transformed into EC100D cells. Transformants were selected for on L-agar supplemented with kanamycin. The mini-Tn*7* element containing wxy^P-*wafY* was introduced into the M2Δ*wafY*::kan mutant using a four-parental mating strategy previously described.

The same process was used to generate pRSM3510- wxy^P-*wafY* except primer set 25 and primer set 28 were used. The mini-Tn7 element containing wxy^P-*wafY* was introduced to the M2Δ*wafZ*::kan mutant via a four-parental mating strategy.

The wxy^P-*wagB* fragment was generated using primer set 26 and primer set 29; but, was cloned into pRSM4063. The pRSM4063- wxy^P-*wagB* vector was

linearized with XhoI and introduced into M2Δ*wagB*::kan via natural transformation as previously described.

Construction and transfer of p4063-A1S_1193-5X into *Acinetobacter* strains. The A1S_1193 open reading frame along with its predicted promoter was PCR amplified to include a C-terminal 5X His tag using primer set 30, which also contained XmaI and KpnI restriction overhangs. The PCR product was digested and ligated to pre-digested pRSM4063. The pRSM4063-A1S_1193-5X vector was linearized with XhoI and introduced to *Acinetobacter* strains via natural transformation as previously described.

Construction of pET-15b-rsPilA$_{M2}$. A truncated His-tagged **r**ecombinant, **s**oluble derivative of *pilA* (rsPilA$_{M2}$) was amplified using gDNA from *A. nosocomialis* strain M2 as template with primer set 31 deleting the first 28 amino acids of the PilA protein. This PCR product was then used as template for a second PCR where the forward primer of primer set 15 contained an NdeI site and the reverse contained a BamHI site to aid in directional cloning into pET-15b. The amplicon was digested with NdeI and BamHI then ligated into the expression vector pET-15b, which was digested with NdeI and BamHI generating a first codon fusion driven off of the T7 promoter with an N-terminal His tag followed by a thrombin cleavage site. Ligation products were electroporated into DH5α-E (Invitrogen), transformants were subcloned and verified to contain the vector with

insert by restriction digestion and sequencing. A correct clone was transformed into *E. coli* strain Origami B (DE3) (Novagen) for expression of the recombinant protein.

rsPilA$_{M2}$ purification. Origami B(DE3) (Millipore) containing pET15b-rsPilA$_{M2}$ was inoculated into 100 mL of LB broth to an A_{600nm} optical density of 0.05 and grown at 37˚C with 180 rpm to mid-log phase at which point rsPilA$_{M2}$ expression was induced with IPTG at a final concentration of 500 µM. Cells were transitioned to 19˚C with 180 rpm and grown for 18 h. Cells were harvested by centrifugation into two equal pellets and resolved in 4 mL each of 1X Ni-NTA Bind Buffer (Novagen) with protease inhibitors (Roche). Resuspended pellets were added to 15 mL TeenPrep Lysing matrix B tubes (MP Biomedicals) and lysed in a Fast Prep 24 homogenizer (MP Biomedicals) with two rounds at 6.0 m/s for 40 seconds with a 5 minute incubation on ice between each round. Supernatants were separated from the unlysed bacteria and the lysing matrix by centrifugation at 4000 rpm for 10 mins at 4˚C. Supernatants were further clarified with 1 hour of ultracentrifugation at 100,000 x *g* for 1 hour at 4˚C. Clarified supernatants were incubated with 1 mL of Ni-NTA His bind resin (Novagen) for 2 hours at 4˚C with gentle rocking followed by two 4 mL washes with 1X Ni-NTA wash buffer. His-tag rsPilA$_{M2}$ was eluted from the resin with three washes of Ni-NTA elution buffer and dialyzed overnight in phosphate buffered saline. The N-terminal His tag on rsPilA$_{M2}$ was thrombin cleaved with 0.04 units/µL of biotinylated-thrombin (Novagen) for 2 hours at room temperature. The biotinylated-thrombin was

captured with streptavidin-agarose beads for 30 minutes and the rsPilA$_{M2}$ was collected with a centrifugation in a spin filter at 500 x *g* for 5 minutes. To remove any small peptides containing the cleaved His-tag or uncleaved His-tag rsPilA$_{M2}$, the filtrate was run over Ni-NTA bind resin and the flow through was collected as pure, cleaved rsPilA$_{M2}$. The pure protein was dialyzed in phosphate buffer saline with 50% glycerol then normalized to 1 mg/mL using a BCA total protein assay kit (Pierce).

Generation of polyclonal antiserum against rsPilA$_{M2}$. Polyclonal antiserum against rsPilA$_{M2}$ was raised following our previously described methods (141). Briefly, 100 µg of purified rsPilA$_{M2}$ emulsified in one milliliter of Freund's complete adjuvant was injected using a 23 gauge needle at ten intracutaneous sites into the haunch of a 6-month old female New Zealand white rabbit (Charles River Laboratories International, Inc., Wilmington, MA). Injections consisting of 100 µg rsPilA$_{M2}$ emulsified in Freund's incomplete adjuvant were subsequently delivered at 15-day intervals, and serum was collected at 10-day intervals following the initial injection. The specificity and reactivity of the anti-rsPilA$_{M2}$ antibodies were confirmed by immunoblotting rsPilA$_{M2}$ and *A. nosocomialis* strain M2 whole-cell lysates after proteins were size-fractionated by SDS-PAGE.

Transformation efficiency assays. Natural transformation was assayed as described previously (6) Transformation efficiency was calculated by dividing the

CFU of transformants by the total CFU. Experiments were conducted on at least three separate occasions. Each bar represents the mean of three separate experiments and with two technical replicates, and error bars represent the standard errors of the means.

Western blot analyses. Western blot analyses were preformed according to our previously described methodologies (6). Primary antibodies used were Anti-rsPilA$_{M2}$ or Penta-His Antibody (Qiagen). Secondary antibodies used were Goat anti-rabbit IgG (H+L), alkaline phosphatase antibody (Molecular Probes) and Goat-anti-mouse IgG (H+L), alkaline phosphatase antibody (Molecular Probes). Membranes were developed with the BCIP/NBT Liquid Substrate System (Sigma). For each experiment utilizing western blot analysis, a minimum of three separate blotting experiments were performed and a representative image was selected for publication.

Pili Shear Preparations. Pili shear preparations were prepared as previously described with the following modifications. Briefly, bacterial lawns were removed from the agar surface and resuspended in 5 mL of ice cold DPBS supplemented with 1X protease inhibitors (Roche). The bacterial suspensions were normalized to an optical density at A_{600nm} equal to 70. To shear surface exposed proteins, bacterial suspension were vortexed on high for 1 minute. Bacteria were pelleted at 10,000 x *g* for 10 minutes at 4˚C. The supernatants were collected and again

centrifuged at 10,000 x *g* for 10 minutes at 4˚C. The supernatants were collected and further clarified by centrifugation at 20,000 x *g* for 5 mins at 4˚C. The sheared surface proteins were precipitated with ammonium sulfate at a final concentration of 30%. Precipitated proteins were pelleted by centrifugation at 20,000 x *g* for 10 minutes at 4˚C. The supernatants were discarded and the pellets were resuspended in 100 µL of 1X Laemmli buffer. Preparations were boiled for 10 minutes, run on SDS-PAGE, coomassie-stained, and bands were excised and prepared for mass spectrometric analysis according to Shevchenko *et al* (2006). Briefly, bands were washed with water and dehydrated with acetonitrile (ACN) repeatedly. Disulfide bonds were reduced with 10mM DTT in 50mM NH_4HCO_3 for 60 minutes at 37°C followed by alkylation of cysteine thiol groups with 50mM iodoacetamide in 50mM NH_4HCO_3 for 60 minutes in the dark at room temperature. Gel pieces were then washed with 50mM NH_4HCO_3, dehydrated with 100% ACN and dried. Pilin was digested with 0.02mg/mL trypsin in 50mM NH_4HCO_3 (Promega) at 37^{o}C for 16 hours. Peptides were eluted with 100% ACN and water and lyophilized. Tryptic peptides were resuspended in 0.1% Trifluoroacetic acid and desalted with a C18 ZipTip (Millipore, USA). 60% ACN was used to elute the peptides, which were dried in a speedvac and resuspended with 0.1% Formic Acid. The analysis was done using a Q-TOF Premier (Waters, Manchester, UK) coupled to a nanoACQUITY (Waters) ultra-performance liquid chromatography system as previously described (Wang N *et al*., 2007). MassLynx, v. 4.1 (Waters) was used to analyze the data. OmpA-His

was purified from strain M2 and prepared for ESI-QTOF-MS/MS analysis as described above.

LPS extraction and silver staining. LPS from *A. baylyi* and *R. solanacearum* was extracted from overnight cultures by the TRI-reagent method as described previously (192). Equal amounts of LPS were loaded on 12.5% SDS-PAGE gels for LPS separation followed by silver staining as previously described (193).

DsbA1 glycosylation in *E. coli*. *E. coli* CLM24 cells were co-transformed with three plasmids: one plasmid encoding the *C. jejuni* glycosylation locus, another plasmid encoding a single *O*-OTase gene, and the last plasmid, pAMF22, encoding *dsbA1-His*. Ampicillin (100 µg/ml), trimethoprim (50 µg/ml) and chloramphenicol (10 µg/ml) were added as required for plasmid selection. Cells were grown at 37˚C to an OD_{600} of 0.4-0.6 and then were induced with 0.1 mM IPTG and/or 0.2% arabinose. Cultures requiring arabinose induction were given a second dose of induction after 4 hours. Whole cell lysates were obtained at stationary phases and western blot analyses were employed to determine DsbA1 modification.

Digestion of membrane enriched samples of *A. baylyi* ADP1. Peptide lysates for glycopeptide enrichment and quantitative analysis were prepared according to Lithgow *et al*. (2014) with minor modifications. Briefly, 2 mg of dried membrane

enriched protein samples were solubilized in 6 M urea, 2 M thiourea, 40 mM NH_4HCO_3 and reduced with 10mM Dithiothreitol (DTT). Reduced, solubilized peptides were alkylated with 25mM iodoacetamide (IAA) for one hour in the absence of light. The resulting alkylated protein mixture was digested with Lys-C (1/100 w/w) for 4 hours, diluted 1:5 in 40 mM NH_4HCO_3, then digested with trypsin (1/50 w/w) overnight at 25°C. Digestion was terminated with the addition of 1% trifluoroacetic acid (TFA). Peptide digests were purified using the C_{18} empore (Sigma-Aldrich, St. Louis MO) STop And Go Extraction (STAGE) tips (Rappsilber *et al*., 2007) to remove primary amide and salts.

Enrichment of *A. baylyi* ADP1 glycopeptides using ZIC-HILIC purification. ZIC-HILIC enrichment was performed according to (Scott *et al*., 2011) with minor modifications. Micro-columns composed of 10 µm ZIC-HILIC resin (Sequant, Umeå, Sweden) packed into p10 tips containing a 1 mm^2 excised C_8 Empore™ disc (Sigma) were packed to a bed length of 0.5 cm. Prior to use, the columns were washed with ultra-pure water, followed by 95% acetonitrile (ACN), and then equilibrated with 80% ACN and 5% formic acid (FA). Samples were resuspended in 80% ACN and 5% FA and insoluble material was removed by centrifugation at 16,100 × *g* for 5 min at 4ºC. Samples were adjusted to a concentration of 3 µg/µL and 150 µg of peptide material was loaded onto a column and washed with 10 load volumes of 80% ACN, 5% FA. Unbound fractions were collected, pooled, and dried by vacuum centrifugation. ZIC-HILIC bound peptides were eluted with

3 load volumes of ultra-pure water and concentrated using vacuum centrifugation. Biological replicates were subjected to ZIC-HILIC enrichment independently using freshly prepared reagents.

Identification of glycopeptides using reversed-phase LC-MS, CID MS-MS and HCD MS-MS. Purified glycopeptides/peptides were resuspended in Buffer A (0.5% acetic acid) and separated using reversed-phase chromatography on either an Agilent 1290 Series HPLC (Agilent Technologies, Mississauga, ON) coupled to LTQ-Orbitrap Velos (Thermo Scientific, San Jose CA) for qualitative analysis of glycopeptides or an EASY-nLC1000 system coupled to a Q-exactive for quantitative studies. For qualitative analysis of *A. baylyi* ADP1 glycopeptides, a packed in-house 20 cm, 75 µm inner diameter, 360 µm outer diameter, ReproSil – Pur C_{18} AQ 1.9µm (Dr. Maisch, Ammerbuch-Entringen, Germany) column was used. For quantitative studies a house packaged 45 cm, 50 µm inner diameter, 360 µm outer diameter, ReproSil – Pur C_{18} AQ 1.9µm column was used. In both systems, samples were loaded onto a trap column, an in-house packed 2 cm, 100 µm inner diameter, 360 µm outer diameter column containing Aqua 5 µm C18 (Phenomenex, Torrance, CA), at 5 µL/min prior to gradient separation and infused for mass spectrometry. A 180 min gradient was run from 0% buffer B (80% ACN, 0.5% acetic acid) to 32% B over 140 min, next from 32% B to 40% B in the next 5 min, then increased to 100% B over 2.5 min period, held at 100% B for 2.5 min, and then dropped to 0% B for another 20 min. Unbound

fractions from ZIC-HILIC glycopeptide enrichment were subjected to analysis using the same instrumental set up as qualitative analysis of glycopeptides. Both instruments were operated using Xcalibur v2.2 (Thermo Scientific) with a capillary temperature of 275°C in a data-dependent mode automatically switching between MS, CID MS-MS and HCD MS-MS for qualitative analysis as previously described (111) and using a top 10 data-dependent approach switching between MS (resolution 70k, AGC target of $1x10^6$), and HCD MS-MS events (resolution 17.5k AGC target of $1x10^6$ with a maximum injection time of 60ms, NCE 28 with 20% stepping) for quantitative studies.

Quantitative dimethylation of *A. baylyi* ADP1 membrane extracts. Quantitative dimethylation of lysates from *A. baylyi* ADP1, the ADP1Δ*pglL*$_{ComP}$ mutant, and the ADP1Δ*pglL*$_{ADP1}$ mutant was performed as outlined previously (Boersema *et al*., 2009). Briefly, 1 mg of peptide lysate from each strain was resuspended in 30 µl of 100 mM tetraethylammonium bromide and mixed with the following combinations of 200 mM formaldehyde (30 µl) and 1M sodium cyanoborohyride (3 µl) isotopologues: ADP1 samples were labeled with light formaldehyde (CH_2O) and light sodium cyanoborohyride ($NaBH_3CN$), ADP1Δ*pglL*$_{ADP1}$ samples with medium formaldehyde (CD_2O) and light sodium cyanoborohyride, and ADP1Δ*pglL*$_{ComP}$ with heavy formaldehyde ($^{13}CD_2O$) and heavy sodium cyanoborodeuteride ($NaBD_3CN$). Reagents were mixed and samples incubated at room temperature for 1 h. Dimethylation reactions were

repeated twice to ensure complete labeling of all amine groups. Dimethylation reactions were terminated by the addition of 30 µl of 1M NH_4Cl for 20 minutes at room temperature. Samples were acidified by addition of 5% (v/v) acetic acid and allowed to equilibrate in the dark for 1 h before pooling the three samples at 1:1:1 ratio. Pooled samples were then STAGE tip purified, lyophilized, and stored at -20ºC.

Identification of *A. baylyi* ADP1 glycopeptides. Raw files for qualitative glycosylation analysis were processed as previously described (194, 195). Briefly, Proteome Discoverer v. 1.2 (Thermo Scientific) was used to search the resulting glycopeptide data using MASCOT v2.4 against the *A. baylyi* ADP1 database (obtained from UNIPROT, http://www.uniprot.org/, 2014-06-10, Taxon identifier: 62977 containing 3263 protein sequences). Mascot searches were preformed using the following parameters: peptide mass accuracy 20 ppm; fragment mass accuracy 0.02 Da; no enzyme specificity, fixed modifications - carbamidomethyl, variable modifications - methionine oxidation and deamidated N, Q. The instrument setting of MALDI-QUAD-TOF was chosen as previous studies show quadrupole–like fragmentation within HCD spectra (196). Scan events that did not result in peptide identifications from MASCOT searches were exported to Microsoft Excel (Microsoft, Redmond WA). To identify possible glycopeptides within exported non-match scans, the MS-MS module of GPMAW 8.2 called ‘mgf graph’ was used to identify HCD scan events that contained the

204.08 *m/z* oxonium of HexNAc. All scan events containing the oxonium 204.08 *m/z* ion were manually inspected to identify possible glycopeptides. To facilitate glycopeptide assignments HCD scan events containing the 204.08 oxonium were manual inspected to identify potential deglycosylated peptides ions. Within these HCD scans the MS features (*m/z*, charge and intensity), which corresponded to masses below that of the deglycosylated peptide were extracted using the Spectrum list function of Xcalibur v2.2. The resulting numerical values of the detected MS features were scripted into mgf files and the peptide mass set to that of the deglycosylated peptide mass. The resulting mgf files were then searched using the MASCOT setting described above. All spectra were searched with the decoy option enabled and no matches to this database were detected; the false discovery rate (FDR) was 0%.

Quantitative analysis of dimethylated *A. baylyi* ADP1 and mutant glycopeptides was preformed as previously reported (107). Briefly, dimethylated *A. baylyi* ADP1 glycopeptides were identified as above and quantified by manually extracting the area under the curve of the monoisotopic peak using Xcalibur v2.2. Triplex (wild type ADP1 vs ADP1Δ*pglL*$_{ComP}$ vs ADP1Δ*pglL*$_{ADP1}$).

4.3 Results

The two OTase homologs encoded by *Acinetobacter* contain different pfam domains

It was previously reported that *A. baylyi* ADP1 encodes two proteins containing domains from the Wzy_C superfamily (110). We wondered if other strains within the *Acinetobacter* genus encoded two Wzy_C superfamily domain-containing proteins. Through bioinformatic analyses we identified several *Acinetobacter* spp. with two open reading frames (ORFs) immediately downstream of the major type IVa pilin subunit *pilA* (Figure 4.1, panel A) that are predicted to encode proteins that contain evolutionarily related domains from the Wzy_C superfamily.

In *A. nosocomialis* strain M2, the *pilA* gene is immediately upstream of two genes, M215_10480 and M215_10475, both of which encode members of the Wzy_C superfamily. M215_10480 and M215_10475 contain the pfam13425 and the pfam04932 domains, respectively (Figure 4.1, panels A and B). At the time of this study, the same genetic arrangement was found in 12 of the 17 completed genomes for *A. baumannii* strains, 7 of 8 *A. nosocomialis* genomes, and 3 of 5 *A. pittii* genomes demonstrating the conservation of this locus amongst medically relevant members of the *Acb* complex (Data not shown). The remaining species and strains contain a *pilA* gene and *pglL* gene, but lack a *tfpO* gene. Previously we designated the gene encoding the pfam13425 domain-containing protein (ORF M215_10480) as the **p**utative **g**l**y**cosylase **A** (*pgyA*) (6). Given that the

gene encoding M215_10480 is immediately downstream of *pilA,* together with the functional data provided in this paper which demonstrates that this protein is a pilin glycosylase, we have renamed the gene encoding ORF M215_10480 as a **t**ype **f**our **p**ilin specific *O*-**O**ligosaccharyltransferase gene (***tfpO***).

The second ORF, M215_10475, encodes a predicted protein that contains a domain from the pfam04932 family, a domain that has been found in all previously characterized PglL orthologs as well as in O-antigen ligases. The PglL_A and the PglL_B domains were also identified in M215_10475. Together with data presented in this paper, we conclude that this protein is an ortholog of the PglL general OTases; thus, we have designated ORF M215_10475 as $pglL_{M2}$ (Figure 4.1, panels A and B).

Transcriptome analysis was performed on mid log phase M2 cells using RNA-seq (data not shown). $PilA_{M2}$ transcription was readily observed; $tfpO_{M2}$ transcription was also observed but the levels dropped precipitously beginning at the intergenic region between $pilA_{M2}$ and $tfpO_{M2}$. A predicted Rho-independent terminator is located immediately upstream of the ATG start codon of $tfpO_{M2}$. It is likely that $pilA_{M2}$ and $tfpO_{M2}$ are in an operon separated by a leaky transcriptional terminator. Downstream of the $tfpO_{M2}$ gene is the $pglL_{M2}$ gene. It is tempting to speculate that since the genes encoding both OTases are in close proximity as well as data presented later demonstrating that both OTases transfer the same

oligosaccharide to their cognate acceptor proteins, that these genes would be cotranscribed. There does appear to be some transcriptional read through but transcript levels for the *pglL*$_{M2}$ gene are markedly higher than the *tfpO*$_{M2}$ levels, suggesting that the intergenic region between *tfpO*$_{M2}$ and *pglL*$_{M2}$ contains a promoter, which also drives transcription of *pglL*$_{M2}$.

In the *A. baylyi* ADP1 genome, the *comP* gene, encoding a pilin-like protein, is followed by ACIAD3337 encoding a pfam04932-containing OTase-like protein, which was designated *pglL* by Schulz *et al*., (2013). In order to avoid confusion, we have designated ACIAD3337 as *pglL*$_{ComP}$ due to its proximity to *comP* (Figure 4.1, panels C and D) and the previously reported evidence demonstrating its requirement for post-translational modification of ComP (110).

A second pfam13425 domain containing ORF (ACIAD0103) predicted to encode a WaaL ligase ortholog was also identified. ACIAD0103 was not located near the pilin gene homolog, but instead was found within a glycan biosynthetic locus. We have designated ACIAD0103 as the *pglL*$_{ADP1}$ (Figure 4.1, panels C and D). *A. baylyi* was the only strain containing two genes encoding proteins with domains from the Wzy_C superfamily that were not encoded by adjacent genes.

In *A. baumannii* ATCC 17978, a well-studied strain with respect to its glycosylation, only one general *O*-OTase was identified, which was previously

designated PglL (55, 105). The novelty of two putative *O*-OTase homologs encoded by most *Acinetobacter* strains prompted us to investigate their function and protein specificity.

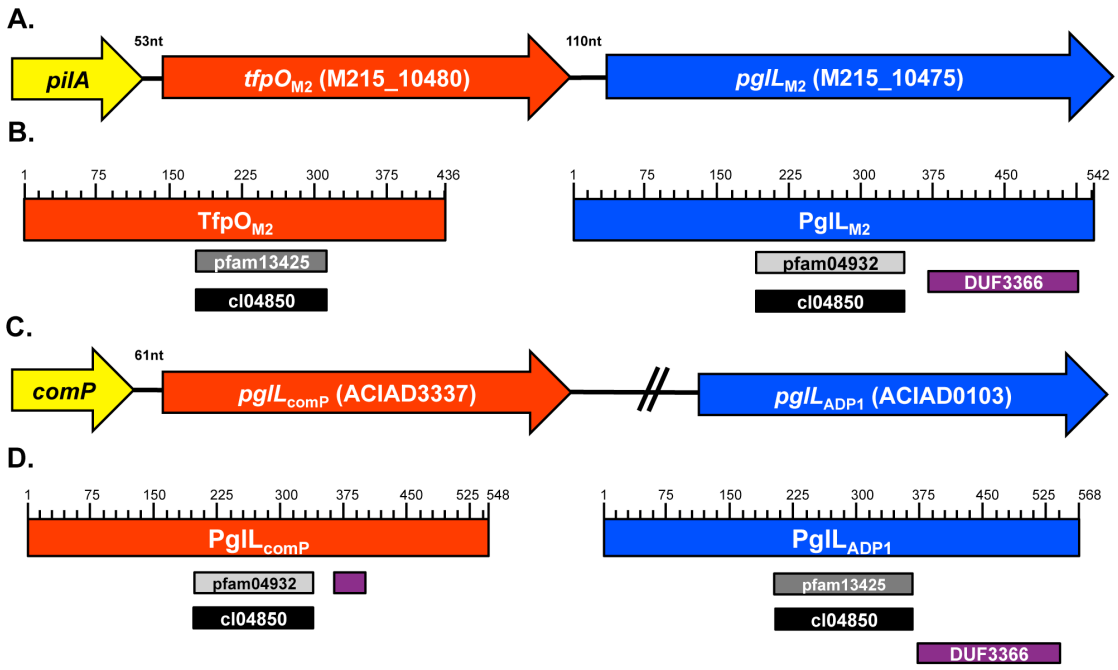

Figure 4.1 Genomic and domain organization of putative *O*-OTases of *Acinetobacter* spp. encoding two OTase genes

A) Genomic context of OTases encoded by the *A. nosocomialis* strain M2 chromosome. B) Wzy_C super family (cl04850) and DUF3366 domains present in $TfpO_{M2}$ and $PglL_{M2}$. C) Genomic context of OTases encoded by the *A. baylyi* ADP1 chromosome. D) Wzy_C super family (cl04850) and DUF3366 domains present in $PglL_{ComP}$ and $PglL_{ADP1}$. The purple rectangle below $PglL_{ComP}$ indicates a portion of the DUF3366 domain.

TfpO is required for post-translational modification of pilin in *A. nosocomialis* strain M2

Western blot analysis of whole cell lysates from strain M2, the isogenic *pilA* mutant, and the complemented *pilA* mutant strain confirmed our previous findings that PilA existed in two molecular forms differing by apparent molecular weight (Figure 4.2A). The more abundant, higher molecular weight form of PilA was likely a post-translationally modified species of PilA while the lower molecular weight form of PilA was an unmodified species. To determine the effects of TfpO on PilA post-translational modification, we constructed an isogenic *tfpO* mutant and probed for PilA expression. PilA from the strain lacking *tfpO* existed only in the lower molecular weight form (Figure 4.2A). The increase in PilA's electrophoretic mobility is consistent with the loss of a post-translational modification. Furthermore, PilA from the complemented *tfpO* mutant strain existed primarily in the higher molecular weight form confirming that TfpO was required for post-translational modification of PilA.

Immediately downstream of *tfpO* in strain M2 is $pglL_{M2}$, which encodes a homolog of the general *O*-OTases responsible for glycosylation of many membrane-associated proteins in *Neisseria gonorrhoeae* and *N. meningiditis* (197, 198). To determine if $PglL_{M2}$ also played a role in post-translational modification of PilA, we generated an isogenic mutant strain lacking $pglL_{M2}$. Western blot analysis of whole cell lysates from the $pglL_{M2}$ mutant demonstrated

that PilA existed primarily in the higher molecular weight form, indicating that $PglL_{M2}$ is not required for the post-translational modification of PilA we observed in the parental strain (Figure 4.2A).

$PilA_{M2}$ was glycosylated in a TfpO-dependent manner with a tetrasaccharide containing $(HexNAc)_2$, Hexose and N-acetyl-deoxyHexose.

To confirm that PilA was glycosylated by TfpO, PilA was purified from surface shear preparations from strain M2, a hyper-piliated M2Δ*pilT* mutant, and a hyper-piliated M2Δ*tfpO*::kanΔ*pilT*::strep mutant. The *pilT* gene encodes for the predicted retraction ATPase; therefore, mutants lacking *pilT* have a hyper-piliated phenotype, which results in an abundance of surface exposed PilA. Proteins in the shear preparations were separated by SDS-PAGE, coomassie-stained, excised and subjected to mass spectrometric analysis. MS/MS analysis of PilA from both strains M2 and M2Δ*pilT* identified the presence of a tetrasaccharide, comprised of two HexNAc residues, a Hexose and N-acetyl-deoxyHexose, on PilA (Figure 4.2B). MS/MS analysis revealed that the tetrasaccharide was present on the carboxy-terminal tryptic $_{119}$NSGTDTPVELLPQSFVAS$_{136}$ peptide. PilA from the M2Δ*tfpO*::kanΔ*pilT*::strep mutant was unmodified confirming that TfpO was required for PilA glycosylation (data not shown).

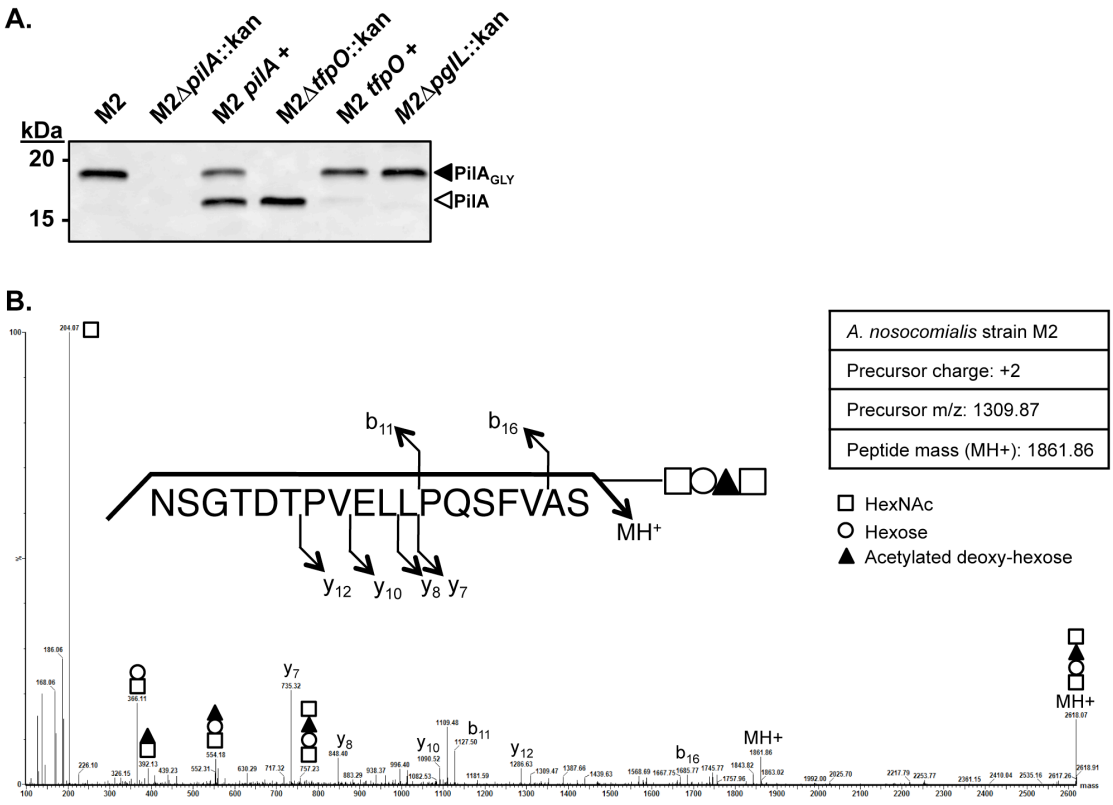

Figure 4.2 PilA$_{M2}$ was glycosylated in a TfpO-dependent manner with a tetrasaccharide containing (HexNAc)$_2$, Hexose and N-acetyl-deoxyHexose

A) Surface proteins from the indicated strains were prepared by shearing, as described in the materials and methods, followed by separation by SDS-PAGE and western blot analysis of whole cell lysates. PilA$_{M2}$ from strain M2 was identified employing rabbit anti-PilA$_{M2}$. PilA$_{M2}$ from the M2Δ*tfpO*::kan mutant existed only as a lower molecular form indicating TfpO was required for PilA$_{M2}$ post-translational modification. Strains M2 *pilA*+ and M2 *tfpO*+ were complemented *pilA* and *tfpO* mutants, respectively. B) PilA$_{M2}$ was sheared from the surface of strain M2 and a hyper-piliated mutant, precipitated, separated by SDS-PAGE, and visualized by Coomassie straining. Bands associated with PilA$_{M2}$ were excised and tryptically digested for MS/MS analysis.

The carboxy-terminal serine$_{136}$ of PilA$_{M2}$ was required for pilin modification.

In *P. aeruginosa* 1244 the pilin protein PilA is glycosylated in a TfpO-dependent manner (113). The glycosylation site was later determined to be at the carboxy-terminal serine 148 (122). Amino acid sequences of PilA proteins from *Acinetobacter* spp., including *A. nosocomialis* M2, were compared to the *P. aeruginosa* 1244 PilA (Figure 4.3A). Although the sequences share limited identity, strain M2's PilA sequence also contains a C-terminal serine, which was included in the glycopeptide identified by MS (Figure 4.2B). In fact, all *Acinetobacter* spp. containing two consecutive genes encoding *O*-OTase homologs contain a carboxy-terminal serine in their respective PilA amino acid sequences (Figure 4.3A).

In order to determine if the carboxy-terminal serine$_{136}$ was required for PilA post-translational modification we generated the M2(*pilA*[S136A])+ strain. First, we generated a strain with an in-frame deletion of the *pilA* gene so as to not affect the transcription of the downstream *tfpO* gene. We then complemented the M2Δ*pilA* strain with an allele of *pilA* where the carboxy-terminal serine was mutated to an alanine residue generating an M2(*pilA*[S136A])+ strain. Western blot analysis of whole cell lysates from the M2(*pilA*[S136A])+ strain demonstrated that PilA only existed in the unmodified, lower molecular weight form indicating that the carboxy-terminal serine was required for PilA post-translational modification (Figure 4.3B). Another highly conserved serine was found at position

132. We constructed the M2(*pilA*[S132A])+ strain in order to determine if this site was also required for glycosylation. Western blot analysis of whole cell lysates from the M2(*pilA*[S132A])+ strain demonstrated that PilA existed in the modified form indicating that serine 132 was not required for glycosylation (Figure 4.3B). Changing the carboxy terminal serine to an alanine residue did not affect Tfp functionality, as the M2(*pilA*[S136A])+ strain was naturally transformable (Figure 4.3C) and exhibited twitching motility similar to the parental strain (Data not shown).

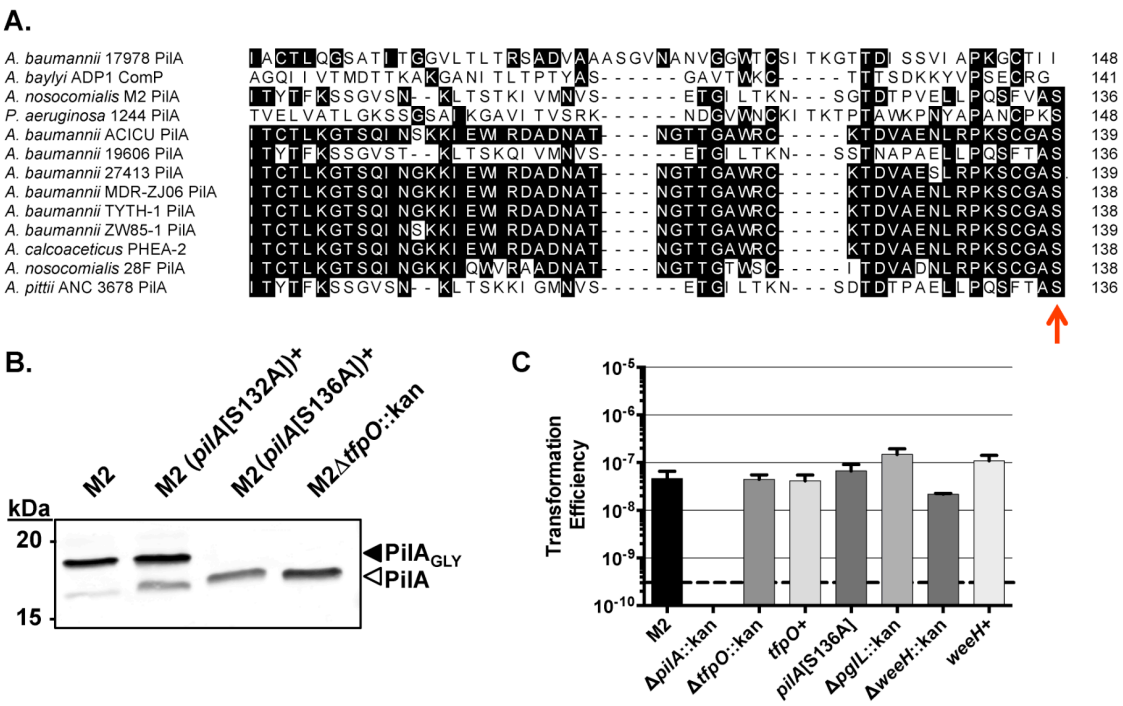

Figure 4.3 PilA$_{M2}$-like glycosylation was dependent on a conserved carboxy-terminal serine

A) Alignment of the carboxy terminal region of PilA proteins from *P. aeruginosa* strain 1244 and selected *Acinetobacter* strains. All *Acinetobacter* strains encoding *tfpO* homologs contain a carboxy-terminal serine on their respective PilA proteins. B) Western blot analysis of whole cell extracts probing for PilA$_{M2}$ expression and electrophoretic mobility. Strain M2 derivatives expressing PilA[S132A] and PilA[S136A] were constructed and extracts characterized. C) Pilin glycosylation in strain M2 is not required for natural transformation. Transformation efficiency was calculated as the total number of transformants divided by the total number of viable bacteria on non-selective media. Transformation efficiency assays were conducted on three separate occasions.

The Major Polysaccharide Antigen (MPA) Locus is required for post-translational modification of $PilA_{M2}$.

Hu *et al*. recently developed a molecular serotyping scheme for *Acinetobacter* spp. containing a major polysaccharide antigen (MPA) locus. The MPA locus, found between the conserved *fkpA* and *lldP* genes, was identified in all sequenced *Acinetobacter* strains included in their study and was also present in *A. nosocomialis* strain M2 (93, 199).

The MPA locus from *A. nosocomialis* strain M2 contains three predicted glycosyl-transferases (designated *wafY*, *wafZ*, and *wagB*) and one predicted initiating glycosyl-transferase (designated *weeH* or *pglC*) (Figure 4.4A). To determine if the MPA locus was required for post-translational modification of $PilA_{M2}$, we constructed individual isogenic mutants lacking each of the predicted glycosyltransferases. Western blot analysis of whole cell lysates from the strain lacking *weeH* demonstrated that PilA existed in the lower molecular weight form indicating that WeeH is required for glycosylation of PilA (Figure 4.4B). Deletion of the other three glycosyltransferases yielded PilA proteins with intermediate electrophoretic mobilities. PilA from the *wafY*::kan mutant migrated closest to the WT PilA mobility, then PilA from the *wafZ*::kan mutant, followed by PilA from the *wagB*::kan mutant (Figure 4.4B). Interestingly, both partially modified and unmodified forms of PilA were identified from the *wafZ*::kan and *wagB*::kan mutant backgrounds. All mutant strains were successfully complemented,

indicating that the products of *wafY*, *wafZ*, *wagB*, and *weeH* genes were all required to produce fully modified PilA.

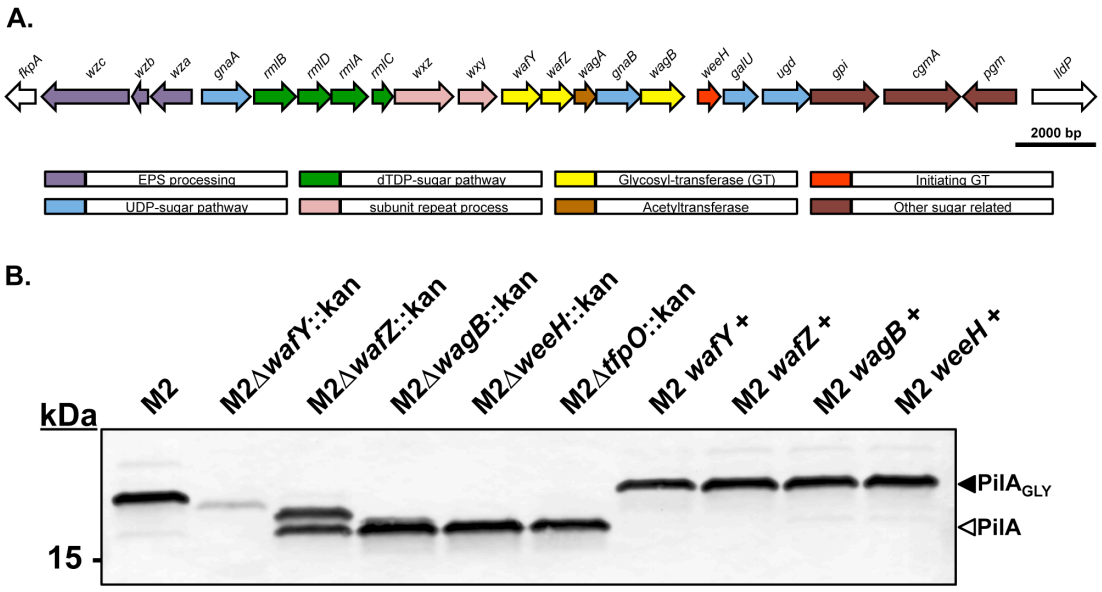

Figure 4.4 The major polysaccharide antigen locus (MPA) was required for pilin glycosylation

A) Genetic organization of the strain M2 MPA locus which is located between the conserved *fkpA* and *lldP* genes. Adapted from Hu *et al*., 2013. B) Western blot analysis of whole cell extracts probing for $PilA_{M2}$ expression and electrophoretic mobility from MPA locus mutants. $PilA_{M2}$ from the Δ*weeH*::kan mutant ran at the same electrophoretic mobility as $PilA_{M2}$ from the *tfpO*::kan mutant indicating it was not glycosylated. Deletion of the other three glycosyltransferases yielded $PilA_{M2}$ proteins with intermediate electrophoretic mobilities. PilA from the *wafY*::kan mutant migrated closest to the WT PilA mobility, then PilA from the *wafZ*::kan mutant, followed by PilA from the *wagB*::kan mutant. Mutants that were complemented all glycosylated $PilA_{M2}$.

***pglL*$_{M2}$ encodes a PglL-like *O*-OTase in *A. nosocomialis* strain M2 and uses the same tetrasaccharide precursor as a donor for general protein glycosylation.**

In figure 4.2A we showed that *pglL*$_{M2}$, the second ORF containing the Wzy_C domain, was not required for pilin glycosylation. We hypothesized that *pglL*$_{M2}$ could be a general *O*-OTase that, like the previously characterized PglL in *A. baumannii* ATCC 17978, could glycosylate non-pilin target proteins. We recently demonstrated that A1S_1193-His, encoding for the protein OmpA, could serve as a bait acceptor protein in order to isolate and identify *Acinetobacter* strain specific glycans, as it is recognized by PglLs from different strains (111). We expressed OmpA-His, containing a carboxy terminal His-tag, in strains M2, M2Δ*tfpO*::kan, M2Δ*pglL*::kan, and M2Δ*weeH*::kan. Western blot analysis demonstrated that all four strains expressed OmpA-His; however, OmpA-His from the M2Δ*pglL*::kan and the M2Δ*weeH*::kan backgrounds migrated at an increased electrophoretic mobility, consistent with the lack of a post-translational modification (Figure 4.5A). ESI-TOF-MS/MS analysis of OmpA-His purified from strain M2 revealed glycosylation with two subunits of a branched tetrasaccharide. These results indicated that M215_10475 is a general *O*-OTase providing functional evidence for the PglL$_{M2}$ designation. Furthermore, this branched tetrasaccharide was the same tetrasaccharide found on PilA, indicating that TfpO$_{M2}$ and PglL$_{M2}$ both utilize the same lipid-linked glycan precursor as the substrate for protein glycosylation (Figure 4.5B). This observation was expected given that WeeH was

required for both PilA and OmpA-His post-translational modification, indicating a common glycan precursor pathway.

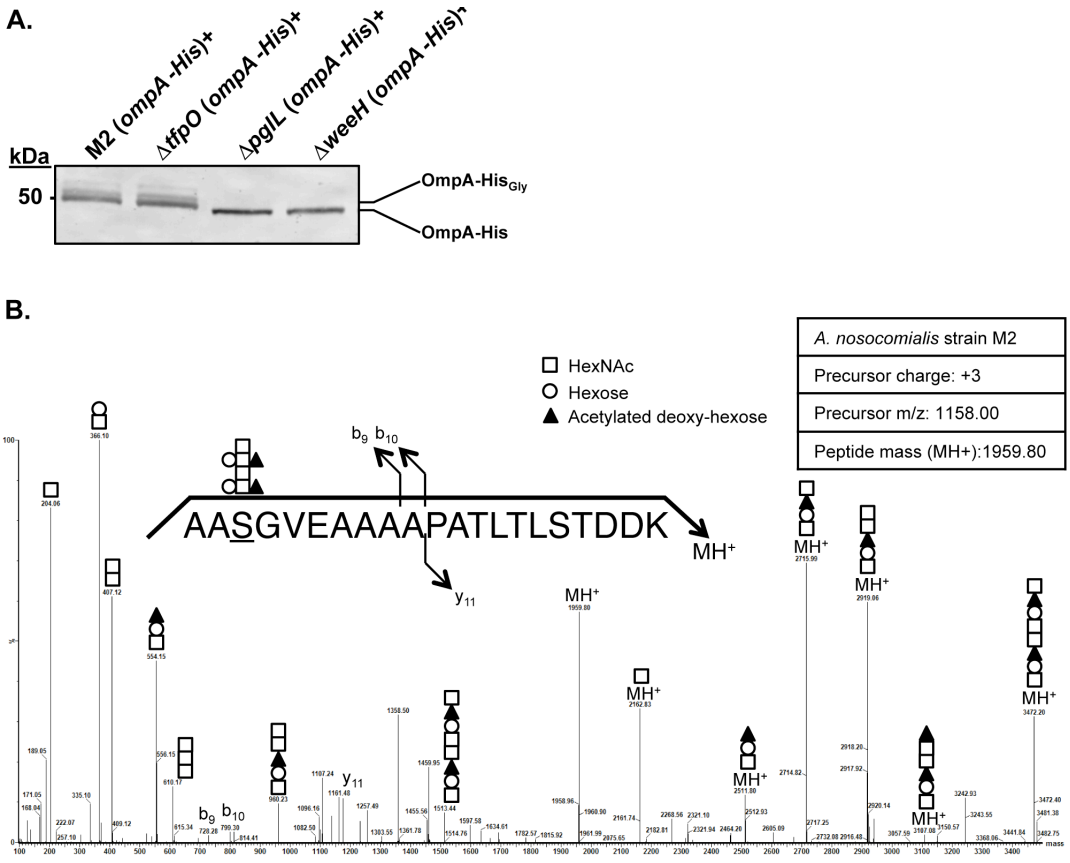

Figure 4.5 PglL$_{M2}$ is a general *O*-OTase and transfer the same core glycan to its cognate acceptor proteins as TfpO$_{M2}$

A) Western blot analysis of whole cell extracts probing for OmpA-His expression and electrophoretic mobility. OmpA-His served as bait protein for glycosylation by strain M2 as well as the isogenic *tfpO*$_{M2}$::kan and *pglL*$_{M2}$::kan mutants. All strains expressed OmpA-His; however, OmpA-His from the *pglL*$_{M2}$::kan mutant ran at an increased electrophoretic mobility indicating the lack of glycosylation. B) Glycosylated OmpA-His was purified from solubilized membranes using nickel affinity chromatography, separated by SDS-PAGE, and visualized by Coomassie staining. OmpA-His was excised from the gel and characterized by MS/MS analysis.

ACIAD0103 is not a WaaL O-antigen ligase and is not required for ComP modification.

As noted above, two OTase-like proteins containing domains from the Wzy_C superfamily are encoded in the *A. baylyi* ADP1 genome. One of these, *pglL*$_{ComP}$ (ACIAD3337), is located adjacent to *comP*. Schulz *et al.* determined, and we independently confirmed, that *pglL*$_{ComP}$ (ACIAD3337) is required for ComP modification (Figure 4.6A). Furthermore, western blot analysis probing for ComP-His expression from an isogenic *pglL*$_{ADP1}$ (ACIAD0103) mutant strain demonstrated that PglL$_{ADP1}$ is not required for ComP post-translational modification (Figure 4.6A).

Schulz *et al.* speculated that the other Wzy_C superfamily domain-containing protein, PglL$_{ADP1}$ (ACIAD0103), encoded a WaaL O-antigen ligase. For LPS biosynthesis, the O-antigen repeat unit is sequentially assembled on the same lipid carrier as the *O*-glycan on the cytoplasmic side of the inner membrane, flipped to the periplasm, polymerized to form the O-antigen chain and transferred to the lipid A-core polysaccharide by the O-antigen ligase (Hug & Feldman, 2011). Differences in the number of O-antigen subunit repeats in LPS molecules appear as a ladder-like banding pattern in LPS silver stains (200). In order to determine if *pglL*$_{ADP1}$ was acting as an O-antigen ligase, we purified LPS from *A. baylyi* ADP1, the ADP1Δ*pglL*$_{ComP}$::kan, and ADP1Δ*pglL*$_{ADP1}$::kan mutants and silver stained the SDS-PAGE-separated preparation. LPS silver stained SDS

polyacrylamide gels showed identical banding patterns, with no O-antigen subunits observed in the LOS compared to O-antigen-containing LPS obtained from the plant pathogen *Ralstonia solanacearum* (Figure 4.6B). Given that $PglL_{ADP1}$ was not acting as an O-antigen ligase, we hypothesized that $PglL_{ADP1}$ could encode a second *O*-OTase.

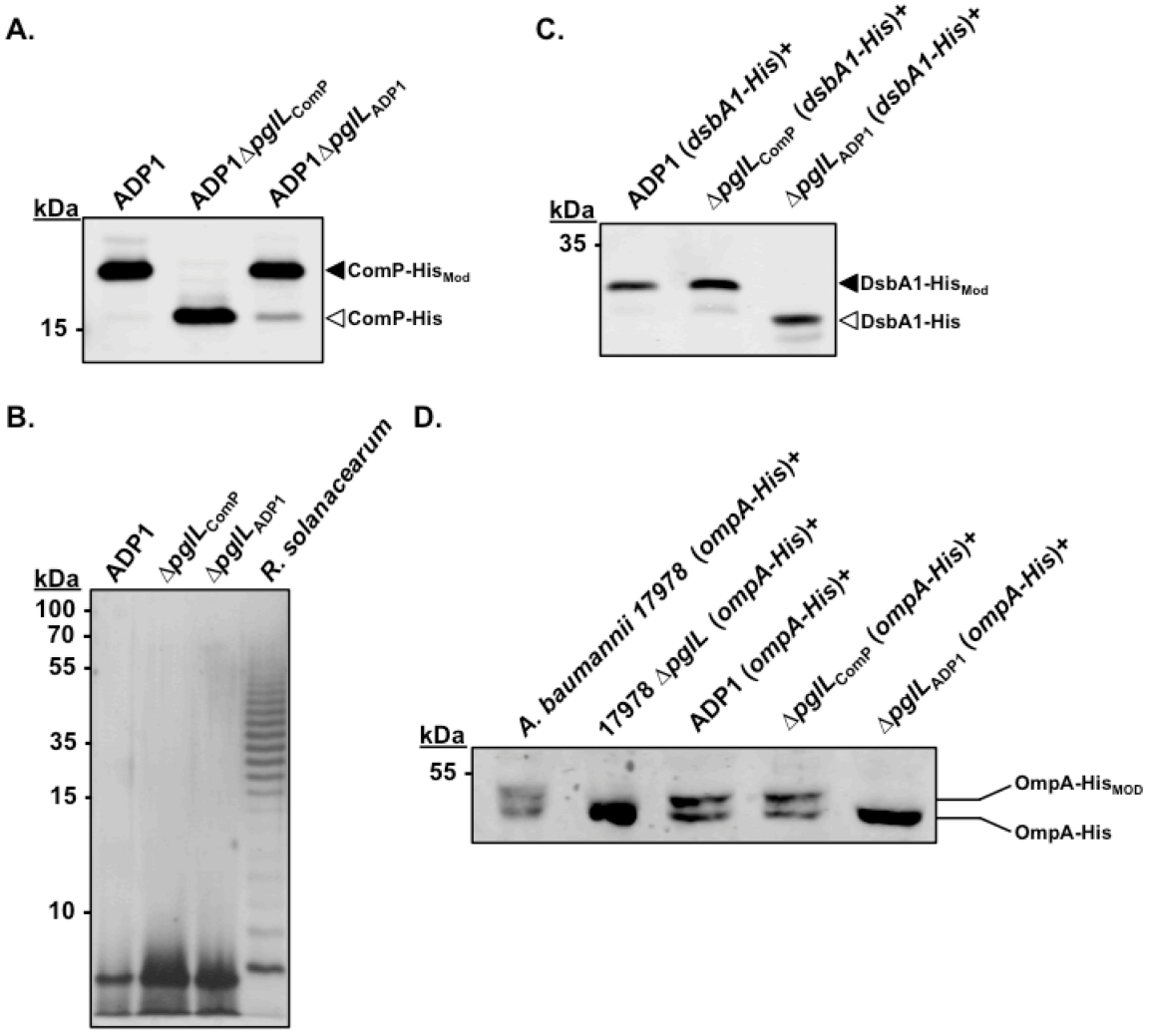

Continued

Figure 4.6 Activity of *O*-OTases in *A. baylyi* ADP1

Figure 4.6 Continued

A) Western blot analysis probing for ComP-His expression in whole cell lysates of *A. baylyi* ADP1 as well as the isogenic Δ*pglL*$_{ComP}$ and Δ*pglL*$_{ADP1}$ mutants. The increase in ComP-His electrophoretic mobility seen in the Δ*pglL*$_{ComP}$ mutant indicates the absence of pilin glycosylation in this strain. B) Silver stain of LPS obtained from *A. baylyi* ADP1, the isogenic Δ*pglL*$_{ComP}$, and Δ*pglL*$_{ADP1}$ mutants as well as *Ralstonia solanacearum*. *A. baylyi* lacks O-antigen, as seen by the lack of laddering observed with *R. solanacearum* LPS. C, D) Western blot analysis of whole cell lysates from *A. baylyi* ADP1, the isogenic , Δ*pglL*$_{ComP}$ and Δ*pglL*$_{ADP1}$ mutants recombinantly expressing his-tagged proteins Dsba1 (C) or OmpA-His (D). The increases in the relative mobility of the His-tagged proteins produced in the Δ*pglL*$_{ADP1}$ background indicate that expression of PglL$_{ADP1}$ was required for glycosylation of these proteins.

ACIAD0103 encodes the general *O*-OTase, $PglL_{ADP1}$, in *A. baylyi* ADP1

We next tested whether $PglL_{ADP1}$ was able to glycosylate DsbA1 from *N. meningitidis* and OmpA from *A. baumannii* 17978, which are also modified by general *O*-OTases in their respective strains, and were previously employed as models to study glycosylation (105, 107, 179, 197) These two proteins were independently expressed in wild-type, $\Delta pglL_{ComP}$ and $\Delta pglL_{ADP1}$ *A. baylyi* strains. DsbA1-His (Figure 4.6C) and OmpA (Figure 4.6D) displayed an increased electrophoretic mobility in the $\Delta pglL_{ADP1}$ background relative to wild-type and $\Delta pglL_{ComP}$ backgrounds. Furthermore, migration of OmpA in the $\Delta pglL_{ADP1}$ background was comparable to the migration of the unglycosylated controls, consisting of the OmpA protein expressed in *E. coli* and in the glycosylation deficient Δ*pglL A. baumannii* ATCC 17978 strain. These experiments support the role of $PglL_{ADP1}$ as a general *O*-OTase.

In vivo glycosylation assays in *E. coli* were performed to further confirm the OTase activity of $PglL_{ADP1}$ (179). We employed *E. coli* CLM24, a strain lacking the WaaL O-antigen ligase, which leads to the accumulation of lipid-linked glycan precursors that then are able to serve as substrates for heterologous *O*-OTase activity (Feldman *et al*., 2005). *E. coli* CLM24 was transformed with plasmids encoding an acceptor protein (DsbA1), a glycan donor (the *Campylobacter jejuni* lipid-linked oligosaccharide (CjLLO)), and one OTase, as previously described (177, 201). We also included $PglL_{ComP}$ and employed $TfpO_{19606}$ and $PglL_{19606,}$

encoding the pilin-specific and the general *O*-OTase from *A. baumannii* ATCC 19606, as controls. DsbAl-His was detected with an anti-histidine antibody and glycosylation was detected employing the hR6 antibody, which is reactive against the *C. jejuni* heptasaccharide. A band reacting with both antibodies, corresponding to DsbA1-His modified by the *C. jejuni* heptasaccharide, was only present in *E.coli* co-expressing DsbA1-His, the CjLLO and either $PglL_{ADP1}$ or the general *O*-OTase $PglL_{19606,}$ (Figure 4.7). Together this data supports the role of $PglL_{ADP1}$ as a general *O*-OTase.

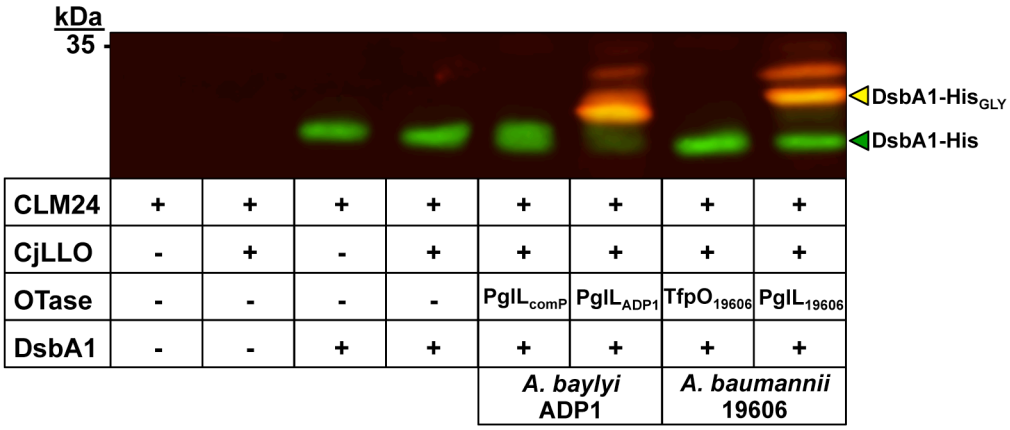

CLM24	+	+	+	+	+	+	+	+
CjLLO	-	+	-	+	+	+	+	+
OTase	-	-	-	-	PglL$_{comP}$	PglL$_{ADP1}$	TfpO$_{19606}$	PglL$_{19606}$
DsbA1	-	-	+	+	+	+	+	+
					***A. baylyi* ADP1**		***A. baumannii* 19606**	

Figure 4.7. Heterologous expression of TfpO and PglL OTases in *E. coli*

Western blot analysis of whole cell lysates of *E. coli* CLM24 expressing, as indicated, the *C. jejuni* lipid linked oligosaccharide (CjLLO) and His-tagged Dsba1 together with an *A. baylyi* or *A. baumannii* ATCC 19606 OTase. His-tagged Dsba1 was detected using the polyclonal anti-his antibody (green) and CjLLO was detected using the hR6 antibody (red). Co-localization of both signals, seen in yellow, indicates glycosylation of DsbA1 by the *Campylobacter* oligosaccharide. This is seen only when PglL$_{ADP1}$ or PglL$_{19606}$ were expressed in *E. coli* CLM24 along with CjLLO and His-tagged Dsba1.

Comparative proteomic analysis of *A. baylyi* ADP1 wild-type, Δ*pglL*$_{ComP}$ and Δ*pglL*$_{ADP1}$ strains.

To unequivocally determine the role of both putative *O*-OTases in *A. baylyi* ADP1 glycosylation, we compared the glycoproteome of *A. baylyi* ADP1 to either the ADP1Δ*pglL*$_{ComP}$ mutant or the APD1Δ*pglL*$_{ADP1}$ mutant. Using ZIC-HILIC for glycopeptide enrichment (105, 107, 111, 202) and multiple MS/MS fragmentation approaches (195), 21 unique glycopeptides from eight protein substrates were identified within *A. baylyi* ADP1 (Table 4.1). Similar to the diversity observed within other *Acinetobacter* spp. (111), *A. baylyi* ADP1 generated unique glycans with glycopeptides decorated with one of four pentasaccaride glycoforms composed of 286-217-HexNAc$_3$ (1112.41 Da, Figure 4.7A and 7D), 286-217-245-HexNAc$_2$ (1154.41 Da, Figure 4.7B and 7F), 286-217-HexNAc-245-HexNAc (1154.41 Da, Figure 4.8B and 4.8G) and 286-217-245$_2$-HexNAc (1196.41 Da, Figure 4.8C and 4.8E). Glycopeptide analysis of *A. baylyi* ADP1Δ*pglL*$_{ComP}$ enabled the identification of identical glycopeptides suggesting the glycoproteome was unaffected by the loss of this gene. In contrast none of 21 glycopeptides observed within wild type *A. baylyi* ADP1 could be detected within extracts of *A. baylyi* ADP1Δ*pglL*$_{ADP1}$, confirming that *pglL*$_{ADP1}$ was responsible for general protein glycosylation within *A. baylyi* ADP1. Furthermore, quantitative dimethylation labeling enabled comparison of all three strains simultaneously providing an internal positive control for glycopeptide enrichment and led to the detection of seven unique glycopeptides (Table 4.2). Consistent with the

requirement of $PglL_{ADP1}$ for glycosylation, no glycopeptides derived from the Δ*pglL*$_{ADP1}$ mutant (Figure 4.9 A-C) could be detected, while non-glycosylated peptides within the samples were observed at a ~1:1:1 ratio (Figure 4.9, Table 4.2).

Protein accession number	Protein name	Precursor m/z [Da]	Precursor MH+ [Da]	Precursor Charge	RT [min]	Peptide	Mascot score	Peptide mass	Glycan mass
Q6F875_ACIAD	Uncharacterized protein	703.98	2109.92	3	19.49	AAHAASAAASK	62	955.50	1154.43
Q6F875_ACIAD	Uncharacterized protein	717.98	2151.93	3	20.80	AAHAASAAASK	35	955.50	1196.43
Q6FCV1_ACIAD	Uncharacterized protein	766.33	2296.97	3	29.47	DAAHDAAASVEK	54	1184.56	1112.41
Q6FCV1_ACIAD	Uncharacterized protein;	720.06	2877.23	4	27.44	IDAAADHAAASTEHAADK	40	1764.82	1112.41
Q6FCV1_ACIAD	Uncharacterized protein;	730.57	2919.24	4	27.93	IDAAADHAAASTEHAADK	32	1764.82	1154.42
Q6FCV1_ACIAD	Uncharacterized protein;	741.07	2961.25	4	28.51	IDAAADHAAASTEHAADK	46	1764.82	1196.44
Q6FCV1_ACIAD	Uncharacterized protein;	701.72	3504.57	5	37.64	IDAAADHAAASTEHAADKAEVATR	46	2392.15	1112.42
Q6FCV1_ACIAD	Uncharacterized protein;	710.12	3546.58	5	38.00	IDAAADHAAASTEHAADKAEVATR	38	2392.15	1154.43
Q6FCV1_ACIAD	Uncharacterized protein;	897.90	3588.59	4	39.70	IDAAADHAAASTEHAADKAEVATR	21	2392.15	1196.44
Q6F7K5_ACIAD	Uncharacterized protein	1579.39	4736.14	3	83.54	IYQNTDTSSAASQTSASPTTQGLGDFLHAQEQLR	23	3623.72	1112.42
Q6F7K5_ACIAD	Uncharacterized protein	1593.39	4778.15	3	84.29	IYQNTDTSSAASQTSASPTTQGLGDFLHAQEQLR	47	3623.72	1154.43
Q6F7K5_ACIAD	Uncharacterized protein	1607.39	4820.16	3	84.77	IYQNTDTSSAASQTSASPTTQGLGDFLHAQEQLR	50	3623.72	1196.44
Q6F825_ACIAD	Uncharacterized protein	1278.95	3834.82	3	55.92	KLAEPAASAVADQNSPLSAQQQLEQK	50	2722.40	1112.42
Q6F825_ACIAD	Uncharacterized protein	1292.95	3876.83	3	55.87	KLAEPAASAVADQNSPLSAQQQLEQK	58	2722.40	1154.43
Q6F825_ACIAD	Uncharacterized protein	980.46	3918.84	4	55.74	KLAEPAASAVADQNSPLSAQQQLEQK	48	2722.40	1196.44
Q6F814_ACIAD	Putative secretion protein (HlyD family)	814.04	2440.11	3	20.96	NTAASSVAATHKK	65	1285.69	1154.42
Q6F814_ACIAD	Putative secretion protein (HlyD family)	828.05	2482.12	3	20.59	NTAASSVAATHKK	56	1285.69	1196.44
Q6F8B6_ACIAD	Uncharacterized protein	1283.91	3849.72	3	37.41	SASKPNVEASVSSQNATLSASQPQHQ	57	2653.28	1196.44
Q6F7U4_ACIAD	Uncharacterized protein	1260.88	3780.64	3	66.46	SSELEDLFNSDGGAASEPAASDKTAAK	60	2668.22	1112.41
Q6FAJ2_ACIAD	Uncharacterized protein	989.48	3954.88	4	66.33	VEQIVAQPAPASSVQFKPSNPEIDYK	26	2842.46	1112.42
Q6FAJ2_ACIAD	Uncharacterized protein	999.98	3996.89	4	66.92	VEQIVAQPAPASSVQFKPSNPEIDYK	21	2842.47	1154.43

Table 4.1 Glycopeptides identified in *A. baylyi* ADP1

Glycopeptides identified in *A. baylyi* ADP1 wild type. Identifications are grouped according to the corresponding Uniprot number. The protein name, parent m/z, charge state, glycan mass, peptide mass, glycan composition, peptide sequence and mascot ion score are provided for each identified glycopeptide.

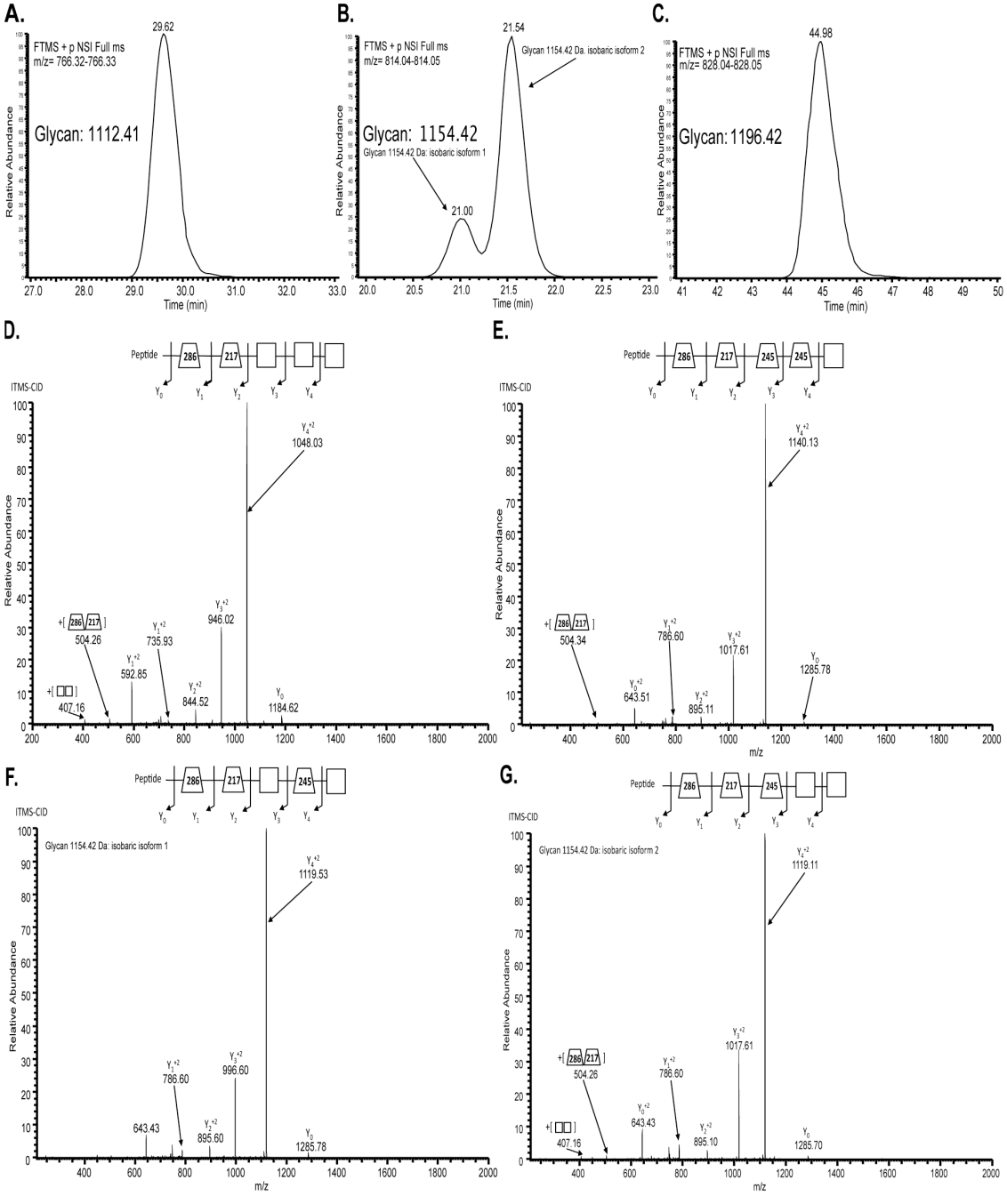

Continued

Figure 4.8 *O*-glycan structure identified using ZIC-HILIC enrichment of *A. baylyi* ADP1 glycoproteins.

Figure 4.8 Continued

ITMS-CID fragmentation results in near exclusive glycan fragmentation of *A. baylyi* ADP1 glycopeptides enabling the identification of four unique glycans on multiple protein substrates corresponding to; A and D) a pentasaccaride composed of 286-217-$HexNAc_3$ (1112.41 Da, ^{92}DAAHDAAASVEK ^{103} of Q6FCV1_ACIAD); B, F and G) two isobaric glycoforms composed of 286-217-245-$HexNAc_2$ and 286-217-HexNAc-245-HexNAc (1154.41 Da, ^{344}NTAASSVAATHKK^{356} of Q6F814_ ACIAD) and C and E) a pentasaccaride composed of 286-217-245_2-HexNAc (1196.41 Da, ^{344}NTAASSVAATHKK^{356} of Q6F814_ACIAD).

Protein	Fasta headers	peptide	Charge	Glycan mass	Precursor m/z	Precursor MH+	Mascot ion score	Number of labels
Q6F7U4	>tr|Q6F7U4|Q6F7U4_ACIAD Uncharacterized protein OS=Acinetobacter baylyi (strain ATCC 33305 / BD413 / ADP1) GN=ACIAD3186 PE=4 SV=1	SSELEDLFNSDGGAASEPAASDKTAAK	4	1112.41	966.9369	3864.7238	96	Dimethyl (K); Dimethyl (K); Dimethyl (N-term)
Q6F825	>tr|Q6F825|Q6F825_ACIAD Uncharacterized protein OS=Acinetobacter baylyi (strain ATCC 33305 / BD413 / ADP1) GN=ACIAD3092 PE=4 SV=1	KLAEPAASAVADQNSPLSAQQQLEQK	4	1112.41	980.4813	3918.9013	47	Dimethyl (K); Dimethyl (K); Dimethyl (N-term)
Q6FCV1	>tr|Q6FCV1|Q6FCV1_ACIAD Uncharacterized protein OS=Acinetobacter baylyi (strain ATCC 33305 / BD413 / ADP1) GN=ACIAD1233 PE=4 SV=1	IDAAADHAAASTEHAADKAEVATR	4	1112.41	890.9106	3560.6187	112	Dimethyl (K); Dimethyl (N-term)
Q6F8B6	>tr|Q6F8B6|Q6F8B6_ACIAD Uncharacterized protein OS=Acinetobacter baylyi (strain ATCC 33305 / BD413 / ADP1) GN=ACIAD2990 PE=4 SV=1	SASKPNVEASVSSQNATLSASQPQHQ	4	1154.43	966.6921	3863.7684	52	Dimethyl (K); Dimethyl (N-term)
Q6FCV1	>tr|Q6FCV1|Q6FCV1_ACIAD Uncharacterized protein OS=Acinetobacter baylyi (strain ATCC 33305 / BD413 / ADP1) GN=ACIAD1233 PE=4 SV=1	IDAAADHAAASTEHAADKAEVATR	4	1154.43	901.4081	3602.6325	122	Dimethyl (K); Dimethyl (N-term)
Q6F8B6	>tr|Q6F8B6|Q6F8B6_ACIAD Uncharacterized protein OS=Acinetobacter baylyi (strain ATCC 33305 / BD413 / ADP1) GN=ACIAD2990 PE=4 SV=1	SASKPNVEASVSSQNATLSASQPQHQ	4	1196.43	977.1939	3905.7756	39	Dimethyl (K); Dimethyl (N-term)
Q6FCV1	>tr|Q6FCV1|Q6FCV1_ACIAD Uncharacterized protein OS=Acinetobacter baylyi (strain ATCC 33305 / BD413 / ADP1) GN=ACIAD1233 PE=4 SV=1	IDAAADHAAASTEHAADKAEVATR	4	1196.43	911.9099	3644.6396	118	Dimethyl (K); Dimethyl (N-term)

Table 4.2 Dimethylated glycopeptides identified in *A. baylyi* ADP1

Dimethylated Glycopeptides identified in *A. baylyi* ADP1 wild type (light) and OTase complement (heavy). Identifications are grouped according to the corresponding Uniprot number. The protein name, parent m/z, charge state, glycan mass, peptide mass, glycan composition, peptide sequence and mascot ion score are provided for each identified glycopeptide. For each identified peptide the dimethylation observed is denoted to aid read distinguish glycopeptide observed from wild type (containing dimethyl N-term and K) and the complement (containing dimethyl N-term 2H(6)13C(2) and K2H(6)13C(2)).

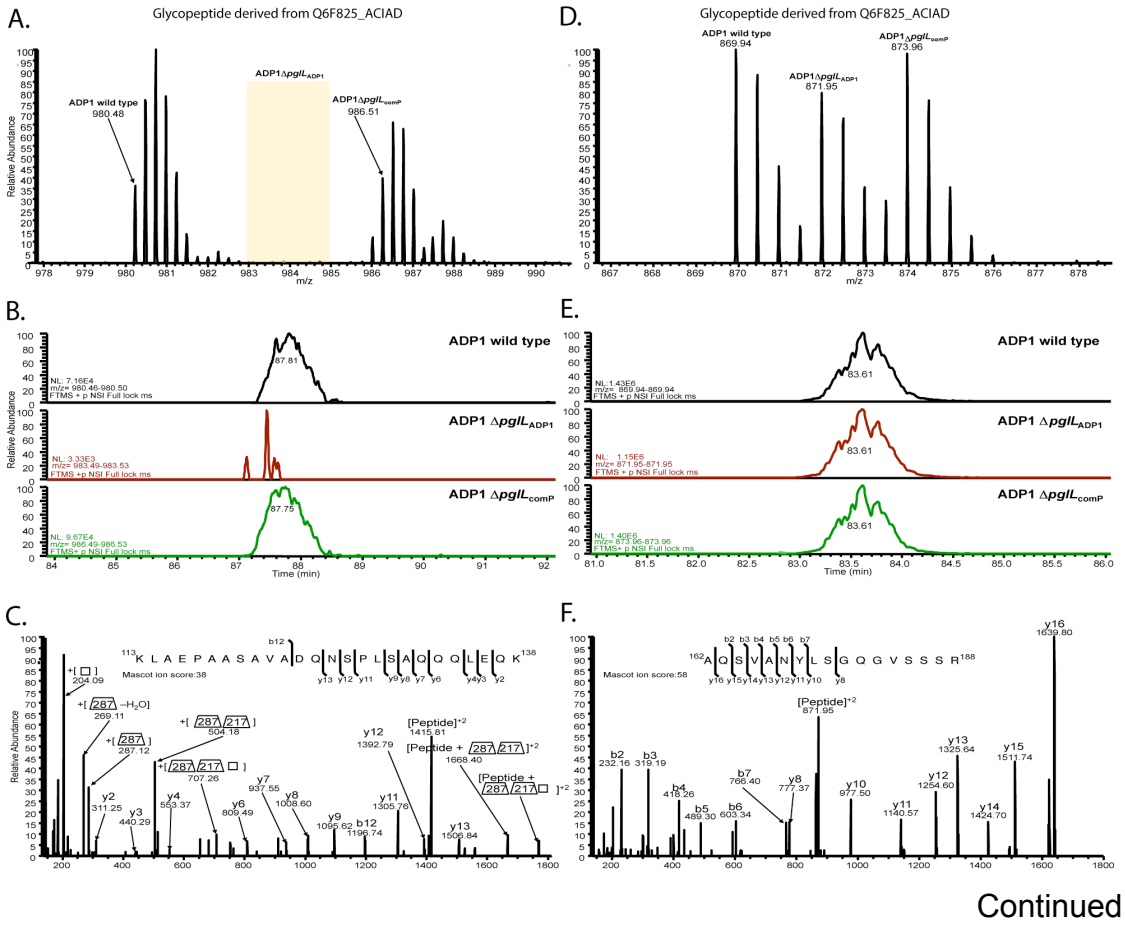

Figure 4.9 Quantitative analysis of glycosylation in *A. baylyi* ADP1 WT, *A. baylyi* ADP1Δ*pglL*$_{ADP1}$, and *A. baylyi* ADP1Δ*pglL*$_{ComP}$ using dimethyl labeling

Figure 4.9 Continued

Using dimethyl labeling and ZIC-HILIC, the *O*-OTase responsible for glycosylation of individual glycopeptides was confirmed. Glycopeptides derived from *A. baylyi* ADP1 WT, labeled with light label and *A. baylyi* ADP1Δ*pglL*$_{comP}$ labeled with heavy label, were observed at near 1:1 levels; whereas, *A. baylyi* ADP1Δ*pglL*$_{ADP1,}$ labeled with medium label, was undetectable within samples. Conversely non-glycosylated peptides were observed at a near 1:1:1 level between all three strains. **A and D)** The MS spectra of the light, medium and heavy isotopologues of the glycopeptide ^{113}KLAEPAASAVADQNSPLSAQQQLEQK^{138} (Q6F825_ACIAD) and non-glycosylated peptide ^{166}AQSVANYLSGQGVSSSR^{182} (Q6FDR2_ACIAD) enabled the comparison of glycosylation across all three strains. No glycopeptides were observed within ADP1Δ*pglL*$_{ADP1}$ while non-glycosylated peptides were observed a near 1:1:1 ratio. **B and E)** Comparison of the extracted ion chromatograms of the light, medium and heavy isotopologues confirm the absent of ADP1Δ*pglL*$_{ADP1}$ derived glycopeptides and the 1:1:1 ratio of non-glycosylated peptides. **C)** HCD fragmentation confirming the identification of the heavy isotopologues of the glycopeptide ^{113}KLAEPAASAVADQNSPLSAQQQLEQK^{138}, confirming its origins from ADP1Δ*pglL*$_{comP}$. **F)** HCD fragmentation confirming the identification of the medium isotopologues of the non-glycosylated peptide ^{166}AQSVANYLSGQGVSSSR^{182}, confirming its origins from ADP1Δ*pglL*$_{ADP1}$.

$PglL_{ComP}$, but not $TfpO_{M2}$, is specific for its cognate pilin protein

Given the strong genetic linkage between the major type IVa pilin genes and downstream *O*-OTase genes on *Acinetobacter* chromosomes, we sought to determine whether these *O*-OTases were specific for their cognate pilin protein. To test this hypothesis, we introduced a plasmid expressing $PilA_{M2}$ from *A. nosocomialis* strain M2 into different *Acinetobacter* spp., and then conducted western blot analysis probing for the expression and electrophoretic mobility of the pilin protein. $PilA_{M2}$ was modified by *A. baumannii* ATCC 19606 and *A. baumannii* 27413, both of which contain *tfpO* homologs, as evidenced by the presence of both the higher molecular weight and lower molecular forms of $PilA_{M2}$ (Figure 4.10A). We recently demonstrated that the glycan associated with *A. baumannii* ATCC 19606 was identical to the pentasaccharide identified in *A. baumannii* ATCC 17978. As expected, $PilA_{M2}$ from *A. baumannii* ATCC 19606 ran with the slowest electrophoretic mobility indicative of a larger glycan associated with $PilA_{M2}$ (111). Both *A. baumannii* ATCC 17978 and *A. baylyi* ADP1, which lack a *tfpO* homolog, were unable to glycosylate $PilA_{M2}$.

On the contrary, when we heterologously expressed ComP-His in different *Acinetobacter* spp. we found that it was glycosylated only in *A. baylyi* ADP1. Strains encoding *tfpO* homologs were unable to modify ComP-His, with the exception of. *A. baumannii* ATCC 19606, which appeared to have a marginal

capacity to modify ComP-His (Figure 4.10B). These results separate the ComP-specific OTases from the pilin TfpO *O*-OTases.

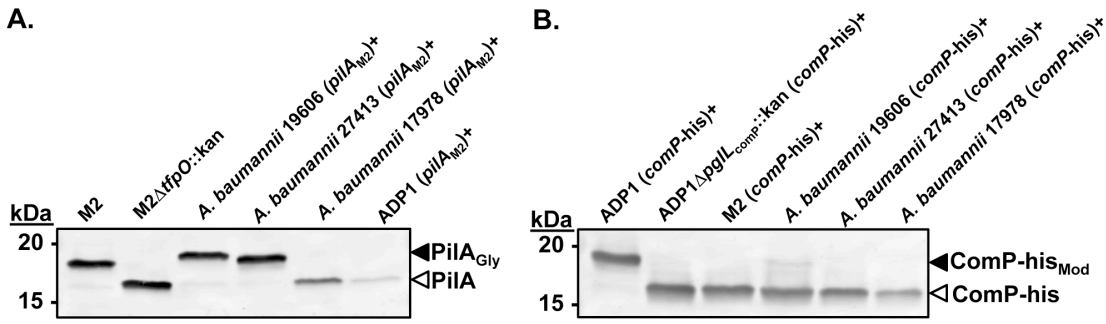

Figure 4.10 PglL$_{ComP}$, but not TfpO$_{M2}$, is specific for its cognate pilin protein

A) Western blot analysis of whole cell extracts probing for heterologous PilA$_{M2}$ expression and electrophoretic mobility. PilA$_{M2}$ was glycosylated in *A. baumannii* ATCC 19606 and *A. baumannii* 27413, both of which encode *tfpO* homologs. Strains lacking *tfpO* homologs (*A. baumannii* ATCC 17978 and *A. baylyi* ADP1) were unable to glycosylate PilA$_{M2}$. B) Western blot analysis probing for heterologous ComP-His expression and electrophoretic mobility. ComP-His was only modified in *A. baylyi* ADP1 indicating that PglL$_{ComP}$ is specific for ComP.

4.4 Discussion:

In the recent years, a panoply of glycosylation pathways have been identified in bacteria. Irrespective of the pathway utilized, both *N*- and *O*-glycans often decorate cell surface adhesins in both Gram-negative and Gram-positive bacteria. Examples of glycosylated surface-associated proteins include the *O*-glycosylation of AIDA-I and TibA in *E. coli* (203, 204), the type IV pilins of *Pseudomonas*, *Neisseria*, *Dichelobacter nodosus*, and *Fransicella tularensis* (113, 115-117, 177, 205), the flagellins in multiple species (96, 98), the serine rich adhesins in *Streptococcus* spp. (206); and the *N*-glycosylation of HMWG in *Haemophilus* (102) and *Aggregatibacter actinomycetemcomitans* (207). *Acinetobacter spp.* are not the exception and our present and previous work show that pilin and multiple outer membrane proteins are *O*-glycosylated, which could provide an adherence advantage either to host cells, in bacterial communities, or to abiotic surfaces. However, as of yet, we have not elucidated the biological role for glycosylation of *Acinetobacter* pilin subunits. Specifically, the *A. nosocomialis* strain M2Δ*tfpO*::kan mutant was equally as transformable as the parental strain (Figure 4.3C), exhibited the same twitching motility phenotype as the parent strain, and also contained similar levels of surface exposed PilA (data not shown). Furthermore, we did not find a condition in which *A. baylyi* ADP1 would attach to abiotic surfaces or form biofilms (data not shown). As mentioned earlier, pilin glycosylation in *P. aeruginosa* and *P. syringae*, mediated by PilO and TfpO, respectively, was essential for motility, biofilm formation and

virulence (186, 187). Pilin glycosylation had no effect on natural competence in *A. baylyi* (88) or *A. nosocomialis* (Figure 4.3C). Nevertheless, the ubiquitous nature of *O*-linked protein glycosylation within the genus *Acinetobacter* and the identification that all *Acinetobacter* strains encoding for *pilA* alleles with carboxy terminal serines also encode a *tfpO* homolog suggests a key, still unknown role for pilin glycosylation.

In this paper we demonstrate that some *Acinetobacter* strains encode two OTase homologs, one of which is required for general *O*-glycosylation and the other that specifically modifies pilin. The majority of the medically relevant *Acinetobacter* strains, including *A. nosocomialis* strain M2, encode two contiguous OTases, which are located immediately downstream of a type IVa major pilin subunit gene. At the time of manuscript preparation, 76% of *A. baumannii* isolates with completed genomes encoded a PilA protein containing a carboxy-terminal serine. All isolates containing a gene encoding a PilA protein with a carboxy-terminal serine also encode for a *tfpO* homolog found immediately downstream of *pilA*. This finding is congruous with findings reported for the group I pilins ($PilA_I$) found in *P. aeruginosa* (185). Thus there appears to be multiple lineages of pilin genes, specifically, a lineage that contains an allele that encodes for a PilA with a carboxy-terminal serine and the downstream accessory gene *tfpO* and lineages that are not glycosylated by a TfpO-like activity. All isolates lacking a carboxy-terminal serine on the major pilin protein, including ATCC 17978, do not encode

for a *tfpO* homolog consistent with the separate evolution of *Acinetobacter* pilin lineages.

In contrast to the contiguous organization of OTases in the medically relevant *Acinetobacter* spp., the two OTases of the environmental isolate *A. baylyi* ADP1 are distantly separated on the chromosome. We confirmed the findings of Schulz *et al.* (110), who showed that the OTase homolog *pglL*$_{ComP}$, which is encoded adjacent to *comP*, is responsible for ComP glycosylation. Mutational analysis coupled with an *in vivo* glycosylation assay as well as the characterization of the glycoproteome demonstrated that *pglL*$_{ComP}$ is a ComP-specific OTase. On the other hand, the second OTase, PglL$_{ADP1}$, is not an O-antigen ligase as previously suggested but rather a general *O*-OTase glycosylating multiple protein targets.

Our study also demonstrated that PglL$_{M2}$, encoded by M215_10475**,** is able to recognize the same motif that the general *O*-OTase PglL found in all other *A. baumannii* strains recognizes, as evidenced by the ability of *A. nosocomialis* M2 to glycosylate OmpA-His. In *A. nosocomialis* strain M2, both PglL$_{M2}$ and TfpO$_{M2}$ utilize the same lipid-linked tetrasaccharide to modify their target proteins. Recently, we demonstrated that across multiple *Acinetobacter* species, dimeric glycans were transferred to multiple peptides; thus, our finding that PglL$_{M2}$ transferred a dimeric glycan to OmpA-His is in concordance with our previous findings (111). Furthermore, we identified the MPA locus as the source of the genes encoding the proteins responsible for the synthesis of the shared lipid-

linked tetrasaccharide. Incorporating all of the data led us to propose the model depicting *O*-glycan synthesis by the MPA cluster and the shared usage of this lipid-linked glycan by $TfpO_{M2}$ and $PglL_{M2}$ (Figure 4.11).

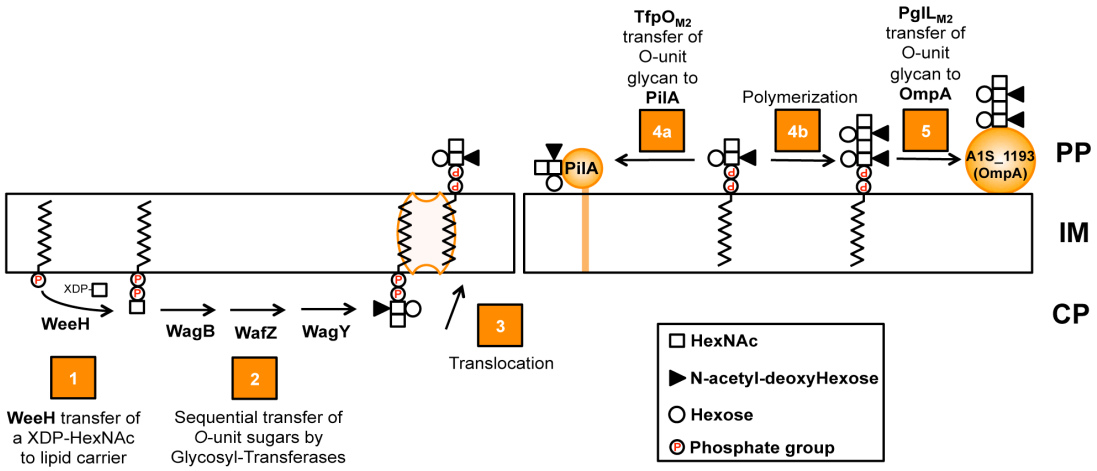

Figure 4.11 Model of lipid-linked oligosaccharide synthesis, TfpO$_{M2}$-dependent pilin glycosylation, and PglL$_{M2}$ general *O*-glycosylation in *A. nosocomialis* strain M2

The proteins encoded by the genes from the major polysaccharide antigen locus synthesize the tetrasaccharide (HexNAc)-(Hex)-(deoxy-Hex)-(HexNAc) on an undecaprenyl lipid carrier, which is then transferred to the periplasm. The lipid-linked oligosaccharide can then be transferred to the major pilin protein, PilA, by the pilin-specific OTase TfpO or further processed and transferred to other proteins, such as, OmpA by the general OTase PglL$_{M2}$.

Although many protein glycosylation systems have been identified, how *O*-OTases, such as the ones from *A. baumannii*, *Neisseria* spp. and *Burkholderia* spp., recognize the acceptor sequences in their protein targets is still not clear. It has been established that OTases recognize low complexity regions (LCR), rich in serine, alanine and proline (197). The pilin specific TfpO enzymes described here recognize a peptide of about 15 amino acids containing many serine and proline residues. Similarly to *P. aeruginosa* TfpO, our evidence suggests that the carboxy-terminal serine of $PilA_{M2}$ serves as the site of $TfpO_{M2}$-dependent glycosylation.

Bacterial species carrying two functional *O*-OTases, a PglL-general OTase and a pilin-specific OTase have not previously been identified. TfpO is the only OTase present in *Pseudomonas* (186, 187) while PglL is the only OTase identified in *Neisseria* (177), *A. baumannii* ATCC 17978 (105), *B. cenocepacia* K56-2 (107) and *R. solanacearum* (manuscript in preparation). Three possible *O*-OTases have been identified in *V. cholerae*, but the activity of only one of these has been shown in *E. coli* (179), and no glycoproteins have been identified in *V. cholerae*. In *N. meningitidis* and *N. gonorrhoeae*, the OTase PglL is able to glycosylate pilin and several other proteins (177, 205). Although PglL can recognize three glycosylation sites in pilin when the system is reconstituted in *E. coli*, none of them contain the typical LCR domain found in the remaining *Neisseria* glycoproteins, indicating that PglL can recognize more than one motif (184). In

Francisella spp. the OTase is closely related to PilO/TfpO and it appears to be responsible for both pilin and general glycosylation (Balonova *et al.,* 2012). Why *Acinetobacter* strains require two different OTases to glycosylate pilin and other proteins remains unclear as some pathogenic strains of *A. baumannii* carry only PglL, which is required for optimal biofilm formation and virulence (105).

It is important to note that non-pathogenic *A. baylyi* ADP1 also contains two *O*-OTases. However there are several differences between the ComP-specific OTase $PglL_{ComP}$ of *A. baylyi* and the pilin-specific OTases TfpO of the medically relevant *Acinetobacter* spp. Although both OTases are encoded immediately downstream of their cognate protein acceptors (Figure 4.1 panels A and C), TfpO OTases are hypothesized to be specific for the carboxy-terminal serine present on PilA, as a carboxy-terminal serine to alanine point mutant was unable to produce glycosylated pilin. Interestingly, all *Acinetobacter* strains encoding a *tfpO* gene homolog also contained the carboxy-terminal serine on their respective PilA sequences. Furthermore, our experiments demonstrated that *Acinetobacter* TfpO homologs are functionally exchangeable as $PilA_{M2}$ was modified by each *tfpO* encoding strain tested (Figure 4.10A). The variable electrophoretic mobility of $PilA_{M2}$ is likely due to glycan variability between these strains (111). Although the site of ComP glycosylation has not been identified, it is predicted to be at an internal residue as ComP does not contain a carboxy terminal serine or any carboxy-terminal residue associated with post-translational modification. BLAST

analysis of the ComP-specific OTases also demonstrated that $PglL_{ComP}$ is more closely related to the general OTase $PglL_{M2}$ than to TfpO. Although the pilin-specific TfpO OTase could cross glycosylate different pilins containing carboxy-terminal serines, $PglL_{ComP}$ was unable to glycosylate the pilins recognized by TfpO.

For these reasons we conclude that three different classes of OTases are present in *Acinetobacter*: the pilin-specific TfpO enzymes that glycosylate pilins containing carboxy-terminal serine residues; the general PglL OTases that recognize LCR in multiple proteins; and $PglL_{ComP}$, which is the first PglL-like protein that specifically glycosylates one protein. These enzymes have different biochemical characteristics, expanding our current glycoengineering toolbox for the synthesis of novel glycoconjugates with biotechnological applications. The differentiation between these enzymes is not trivial, and cannot be accurately predicted just by the presence of pfam domains. For example, despite having the highest degree of sequence similarity and being functionally homologous, PilO/TfpO from *P. aeruginosa* strain 1244 contains the pfam04932 domain, whereas *tfpO* from *A. nosocomialis* strain M2 contains the pfam13425 domain. Moreover, the general PglL OTases of the medically relevant *Acinetobacter* spp., including strain M2 and *A. baumannii* ATCC 17978, contain domains from the pfam04932 family and the *A. baylyi* general $PglL_{ADP1}$ OTases contain a pfam13425 domain. Adding to the complexity is the fact that the general PglL

OTases from medically relevant *Acinetobacter* spp. and the *A. baylyi* ComP-specific $PglL_{ComP}$ contain the same pfam04932 domains yet recognize different sequons. In addition this pfam domain is present in the WaaL O-antigen ligases. While bioinformatic analyses can be powerful tools to initially locate and identify ORFs encoding proteins predicted to be involved in glycan transfer events, our data collectively reinforces the concept that the activity of bioinformatically identified *O*-OTases must be experimentally determined and reveals a complex and fascinating evolutionary pathway for bacterial *O*-OTases.

Plasmid or strain	Relevant characteristic(s)	Source
PLASMIDS		
pFLP2	Encodes FLP recombinase	(152)
pKD13	Contains kanamycin resistance gene from Tn5 flanked by FRT sites	(150)
pRSM3542	pKD13 containing *kan-sacB*	(127)
pGEM-T-Ez	General cloning plasmid	Promega
pCC1	Single copy, general cloning plasmid	Epicentre
pSMART-LCKAN	Low copy blunt cloning vector	Lucigen
pGEM-*pilA*	pGEM containing *pilA* with 1 kb flanking DNA	(6)
pGEM-*pilA*::kan-*sacB*	pGEM-*pilA* containing *pilA*::kan	This study
pCC1-*pilA-tfpO-pglL*	pCC1 containing the *pilA-tfpO-pglL* locus with approximately 1 kb of flanking DNA	This study
pRSM3510	pKNOCK derivative with a mini-Tn*7* element containing a multiple cloning site	(6)
pRSM3510-*pilA*	pRSM3510 containing *pilA* with expression driven from the predicted *pilA* promoter	(6)
pRSM3510-*pilA*[S136A]	pRSM3510-*pilA* with a carboxy terminal serine to alanine point mutation	This study
pRSM3510-*pilA*[S132A]	pRSM3510-*pilA* with a serine 132 to alanine point mutation	This study
pRSM3510-$pilA^{P}$-*tfpO*	pRSM3510 containing the predicted *pilA* promoter, the ATG of *pilA*, a FLP scar, the last 21bp of *pilA*, and the *tfpO* gene including the 48bp intergenic region between *pilA* and *tfpO*	This study
pCC1-*pglL*::kan	pCC1-*pilA-tfpO-pglL* containing *pglL*::kan	This study
pGEM-*weeH*::kan	pGEM-T-Ez containing *weeH*::kan	This study
pRSM4063	pSMART-LCKan containing an the empty mini-Tn*7* element from pRSM3510 along with 2kb of flanking DNA up and downstream of the *att*Tn*7* from strain M2	This study
pRSM4063-*weeH*	pRSM4063 containing the *weeH* gene with its predicted promoter	This study
pWH1266	*E. coli – Acinetobacter* shuttle vector	(208)
pGEM-*wafY*::kan	pGEM-T-Ez containing *wafY*::kan	This study
pGEM-*wafZ*::kan	pGEM-T-Ez containing *wafZ*::kan	This study

Continued

Table 4.3 Plasmids and strains used in this study

Table 4.3 Continued

pGEM-*wafZ*::kan	pGEM-T-Ez containing *wafZ*::kan	This study
pGEM-*wagB*::kan	pGEM-T-Ez containing *wagB*::kan	This study
pCC1-GT	pCC1 containing the predicted promoter of the *wxy* gene (329 bp upstream), *wxy*, *wafY*, *wafZ*, *wagA*, *gnaB*, and *wagB*	This study
pCC1-*wxy*^{P}-*wafY*	pCC1-GT lacking the *wxy* open reading frame	This study
pCC1-*wxy*^{P}-*wafZ*	pCC1-GT lacking the *wxy* and *wafY* open reading frames	This study
pCC1-*wxy*^{P}-*wagB*	pCC1-GT lacking the *wxy*, *wafY*, *wagA*, and *gnaB* open reading frames	This study
pRSM4063-*wxy*^{P}-*wafY*	pRSM4063 containing *wafY* driven off the predicted *wxy* promoter	This study
pRSM4063-*wxy*^{P}-*wafZ*	pRSM4063 containing *wafZ* driven off the predicted *wxy* promoter	This study
pRSM4063-*wxy*^{P}-*wagB*	pRSM4063 containing *wagB* driven off the predicted *wxy* promoter	This study
pWH-*pilA*$_{M2}$	pWH1266 expressing *pilA*$_{M2}$ driven by the predicted *pilA* promoter	This study
pRSM3510-A1S_1193-his	pRSM3510 containing A1S_1193 driven off its predicted native promoter	This study
pET-15b	General plasmid for expression and cloning of recombinant proteins based on the T7-promoter driven system	Novagen
pET-15b-rsPilA$_{M2}$	pET-15b expressing a truncated *pilA* from the T7 promoter	This Study
pEXT20	Amp^{r} cloning and expression vector, IPTG inducible.	(209)
pBAVMCS	Km^{r} pBAV1K-T5-gfp derivative with *gfp* ORF removed. Constitutive *E.* coli/*Acinetobacter* shuttle vector	(210)
pBAVMCS-*comP*-his	Km^{r} pBAVmcs constitutively expressing C-6X His-tagged *comP* from *A. baylyi*, inserted at BamHI and SalI.	This Study
pEXT-*pglL*$_{comP}$	Amp^{r} pEXT20 expressing C-6X His-tagged *pglL*$_{ComP}$ from *A. baylyi* inserted at BamHI and SalI, IPTG inducible.	This Study
pEXT-*pglL*$_{ADP1}$	Amp^{r} pEXT20 expressing C-6X His-tagged *pglL*$_{ADP1}$ from *A. baylyi* inserted at BamHI and SalI, IPTG inducible.	This Study
pEXT-*tfpO*$_{19606}$	Amp^{r} pEXT20 expressing C-10X His-tagged *tfpO*$_{19606}$ from *A. baumannii* ATCC 19606 inserted at BamHI and SalI, IPTG inducible.	This Study
pEXT-*pglL*$_{19606}$	Amp^{r} pEXT20 expressing C-10X His-tagged *pglL*$_{19606}$ from *A. baumannii* ATCC19606 inserted at BamHI and SalI, IPTG inducible.	This Study
pAMF22	Tp^{r} C-10X His-tagged *dsbA1* from *N. meningitidis* MC58 cloned into pMLBAD, Arabinose inducible.	Feldman unpublished
pBAVMCS-*dsbA1*-His	C-6X His-tagged *dsbA1* subcloned into pBAVMCS, Km^{r}, at BamHI and HindIII. Constitutively expressing.	This Study

Continued

Table 4.3 Continued

pACYC*pglB*	Cm^r pACYC184-based plasmid encoding the *C. jejuni* protein glycosylation locus cluster with mutations W458A and D459A in PglB, IPTG inducible.	(211)
pBAVMCS-A1S_1193His10X	Km^r pBAVMCS constitutively expressing C-10X hist-tagged A1S_1193 inserted at BamHI and SalI.	(111)
STRAINS		
Acinetobacter nosocomialis strain M2	Metro Health Systems Clinical Isolate	(124)
M2Δ*pilA*::kan	Strain M2 containing a deletion of *pilA* and replacement with a kanamycin resistance cassette	(6)
M2Δ*pilA*::kan-*sacB*	Strain M2 containing a deletion of *pilA* and replacement with a kan-*sacB* cassette	This study
M2Δ*pilA*	Strain M2 containing an unmarked, in-frame deletion of *pilA*	This study
M2Δ*pilT*	Strain M2 containing an unmarked, in-frame deletion of *pilA*	(6)
M2Δ*tfpO*::kan	Strain M2 containing a deletion of *tfpO* and replacement with a kanamycin resistance cassette	This study
M2Δ*tfpO*::kanΔ*pilT*::strep	M2Δ*tfpO*::kan containing a deletion of *pilT* and replacement with a streptomycin resistance cassette	This study
M2Δ*pglL*::kan	Strain M2 containing a deletion of *pglL* and replacement with a kanamycin cassette	This study
M2Δ*pilA* (*pilA*[S136A]+)	M2Δ*pilA*::kan with a mini-Tn*7* element containing an allele of *pilA* with a carboxy-terminal serine to alanine point mutation	This study
M2Δ*wafY*::kan	Strain M2 containing a deletion of *wafY* and replacement with a kanamycin resistance cassette	This study
M2Δ*wafZ*::kan	Strain M2 containing a deletion of *wafZ* and replacement with a kanamycin resistance cassette	This study
M2Δ*wagB*::kan	Strain M2 containing a deletion of *wagB* and replacement with a kanamycin resistance cassette	This study
M2Δ*weeH*::kan	Strain M2 containing a deletion of *weeH* and replacement with a kanamycin resistance cassette	This study
M2Δ*pilA*::kan (*pilA*+)	M2Δ*pilA*::kan with a mini-Tn7 element containing the *pilA* gene transcribed from its predicted promoter	(6)
M2Δ*tfpO*::kan (*tfpO+)*	M2Δ*tfpO*::kan with a mini-Tn7 element containing the *tfpO* gene transcribed from the *pilA* predicted promoter	This study
M2Δ*wafY*::kan (*wafY*+)	M2Δ*wafY*::kan with a mini-Tn7 element containing the *wafY* gene under control of the predicted *wxy* promoter	This study
M2Δ*wafZ*::kan (*wafZ*+)	M2Δ*wafZ*::kan with a mini-Tn7 element containing the *wafY* gene under control of the predicted *wxy* promoter	This study

Continued

Table 4.3 Continued

M2Δ*wagB*::kan (*wagB*+)	M2Δ*wagB*::kan with a mini-Tn7 element containing the *wafY* gene under control of the predicted *wxy* promoter	This study
M2Δ*weeH*::kan (*weeH*+)	M2Δ*pilA*::kan with a mini-Tn7 element containing the *pilA* gene fused to a FLAG tag transcribed from its predicted promoter	This study
M2 (A1S_1193-his+)	Strain M2 with a mini-Tn*7* element containing A1S_1193-his transcribed from its predicted promoter	This study
M2Δ*tfpO*::kan (A1S_1193-his+)	M2Δ*tfpO*::kan with a mini-Tn*7* element containing A1S_1193-his transcribed from its predicted promoter	This study
M2Δ*pglL*::kan (A1S_1193-his+)	M2Δ*pglL*::kan with a mini-Tn*7* element containing A1S_1193-his transcribed from its predicted promoter	This study
A. baumannii ATCC 17978	Reference *A. baumannii* strain	ATCC
A. baumannii ATCC 19606	Reference *A. baumannii* strain	ATCC
A. baumannii 27413	*A. baumannii* clinical isolate isolated at Nationwide Children's Hospital (NCH) from body fluid	NCH
A. baylyi ADP1	Environmental isolate	(86)
A. baylyi Δ$pglL_{ComP}$::kan	Strain ADP1 with $pglL_{comP}$ deleted and replaced with a kanamycin resistance casette	(86)
A. baylyi Δ$pglL_{ADP1}$::kan	Strain ADP1 with $pglL_{ADP1}$ deleted and replaced with a kanamycin resistance casette	(86)
E. coli DH5a	General cloning strain	Invitrogen
E. coli EC100D *pir*+	General cloning strain, pir^{+}	Epicentre
E. coli DY380	Recombineering strain	(161)
E. coli DH5a(pFLP2)	Carries FLP recombinase gene under temperature control	(152)
E. coli HB101(pRK2013)	Conjugation helper strain	(162)
E. coli EC100D(pTNS2*)*	Carries transposase genes for mini-Tn*7* transposition	(163)
E. coli Origami 2(DE3)	K-12 derivative containing mutations in *trxB* and *gor* genes and a host lysogen of λDE3	Novagen
E. coli Stellar chemically competent cells	HST08 strain derivative for high transformation efficiencies	Clontech
E. coli CLM24	Constructed from E. coli W3110 (IN(rrnD-rrnE)1 rph-1). waaL mutant	(212)

Primer Set		Sequence
1	F	AGAATACTTGCATAGTGACAGGTTACAG
	R	GTTATGGCGGCGGTGGAGGTC
2	F	CAAAAAGCTTATATAAAAACATACATACAATCTTTGGGGAAAAGG CTATGATTCCGGGGATCCGTCGACC
	R	GGATTGACCTCTCTTTTTTATTTCTAAAATTACGATGCTACAAATG ATTGTGTAGGCTGGAGCTGCTTCG
3	F	GCGGGATCCGCAAATTGGTGATGTGATGTCTCG
	R	GCGGGTACCGCTGCGAGGAATAAAAAGAATACT
4	F	GCGGGATCCGCAAATTGGTGATGTGATGTCTCG
	R	GCGGGTACCTCGTATTGTGAACTAGACCATCCT
5	F	GCGGGATCCGCAAATTGGTGATGTGATGTCTCG
	R	GCGGGTACCGCTGCGAGGAATAAAAAGAATACT
6	F	AGAATACTTGCATAGTGACAGGTTACAG
	R	CGCATTTATATTTGGGGATTACTC
7	F	CTTCCATGTATAATTCTTCTCAAGTTTTTGGTCTGTAACCTGTCACT ATGATTCCGGGGATCCGTCGACC
	R	AAAATCCCCTTGAAAACAAGGGGATTTTTTTATTTATCTTTTAATA ATTGTGTAGGCTGGAGCTGCTTCG
8	F	CTTCCTCAATCATTTGTAGCAGCGTAATTTTAGAAATAAAAAAG
	R	CTTTTTTATTTCTAAAATTACGCTGCTACAAATGATTGAGGAAG
9	F	ATGAAAAAACTTGAGCACCTTGC
	R	TGTTTGCTCTTATTTCTACTG
10	F	TTGTCATTTATAAAGTTAGTCAC
	R	TGTACACCTGATTTTAATATTCTA
11	F	GAAATAAGAGCAAACAATTCCGGGGATCCGTCGACC
	R	CTTTATAAATGACAATGTAGGCTGGAGCTGCTTCG
12	F	CTCAAGTTTTTTCATCGCCATGGCGGCCGGGAGCATG
	R	AAAATCAGGTGTACAACTAGTGAATTCGCGGCCGCCTGCA
13	F	CGTCCCCAAAAGCGTGAA
	R	TTAGGCAAATTTCGAAGCGTGAT
14	F	GCGCCCGGGATAAGTGCTCAATTGATGG
	R	GGTACCGAGATCCCAAACCAGCAAC
15	F	ACTAGTGAATTCGCGGCCGCCTGCA
	R	CGCCATGGCGGCCGGGAGCATG

Continued

Table 4.4 Primers used in this study

Table 4.4 Continued

16	F	ATTCCGGGGATCCGTCGACC
	R	TGTAGGCTGGAGCTGCTTCG
17	F	CCGGCCGCCATGGCGATGACGATTGGTTTAATTTTTTC
	R	ACGGATCCCCGGAATCATACTTGTAAAAAAAAAAGTATTT
18	F	CAGCTCCAGCCTACAATGGAAGAAAATTCTTTATTAATTT
	R	CGCGAATTCACTAGTTTAAACATATTTTTCCCATTTC
19	F	CCGGCCGCCATGGCGATGACTCCTGCCGGAGG
	R	ACGGATCCCCGGAATTTAATAAAGAATTTTCTTCCATTTAC
20	F	CAGCTCCAGCCTACAATAGTAGGACTAAAAAAATGATTTCG
20	R	CGCGAATTCACTAGTTTATTTATATAACCCTTTTTCTTTC
21	F	CGGCCGCCATGGCGATGTTTAAAAATGTATTAATTACTGG
	R	ACGGATCCCCGGAATCATTTATTTATATAACCCTTTTTCT
22	F	CAGCTCCAGCCTACAATAAATTTAAAATATTCATAAATCT
	R	CGCGAATTCACTAGTTTATAATTTAAGTTCTTGAATCAAC
23	F	CTACATTGTTTATTTTTACCAGAA
	R	GAAGCTTGAAGTTATCCACGAA
24	F	CATCAAAAATACCAGCCTAAATTATC
	R	CCATTGTTTGAAATTATTTAGGG
25	F	CATCAAAAATACCAGCCTAAATTATC
	R	GAAGAAAATTCTTTATTAATTTCTG
26	F	CATCAAAAATACCAGCCTAAATTATC
	R	GAAAAAGGGTTATATAAATAAATG
27	F	GCGCCCGGGCTACATTGTTTATTTTTACCAGAA
	R	GCGGGTACCACCATCATTGACTACTAAGACCTC
28	F	GCGCCCGGGCTACATTGTTTATTTTTACCAGAA
	R	GCGGGTACCTTCTACATCCAATACCAGTCGT
29	F	GCGCCCGGGCTACATTGTTTATTTTTACCAGAA
	R	GCGGGTACCGAAGCTTGAAGTTATCCACGAA
30	F	GCGCCCGGGCCGAAGCAGGGTGGGTGTTAGT
	R	GCGGGTACCTTAGTGGTGGTGGTGGTGTTGAGCTACTGAAAACTCAATAC

Continued

Table 4.4 Continued

31	F	GCCATATGGCTTATCAAAACTATATTGCTAAATCTC
	R	GCGGATCCCTCTTTTTTATTTCTAAAATTACGATGCT
32	F	ATAGGATCCATGAATGCACAAAAGGGTTTTACC
	R	TATGTCGACTCAGTGGTGGTGGTGGTGGTGACCACGACATTCTGATGG
33	F	ATATGGATCCGTGGTTGATAGTAGTACTATATGG
	R	ATATGTCGACTCAGTGGTGGTGGTGGTGGTGATATTCTATTGAACAAAATTTTAACTTAGG
34	F	ATATGGATCCGTGGCTGGTTCCCCGCGTGTGTATAATAGC
	R	ATATGTCGACTTAGTGGTGGTGGTGGTGGTGCTTGGATGACTCTACAGCAGAAGC
35	F	ACTGGGATCCATGTTAAAAAAAATTATTCTATTTC
	R	ACTGGTCGACTAAGTGGTGGTGGTGGTGGTGGTGGTGGTGAGGAATTTTTGAGGTTGGTAC
36	F	ACTGGGATCCATGCAAGTATTCTTTCTGTTC
	R	ACTGGTCGACTAAGTGGTGGTGGTGGTGGTGGTGGTGGTGTTTATTTTTTAACAACTCTGCC
37	F	CCAGTTGAATTACTTCCTCAAGCATTTGTAGCATCGTAAT
	R	ATTACGATGCTACAAATGCTTGAGGAAGTAATTCAACTGG

Chapter 5: Discussion

5.1 Research Findings

Understanding the molecular mechanisms employed by *Acinetobacter* species to infect, colonize, and cause human disease requires robust genetic tools allowing for controlled chromosomal manipulation in order to define gene-phenotype relationships. Unfortunately, mutational analysis of medically relevant *Acinetobacter* spp. has proven to be difficult due partially to multiply drug resistant strains that limit selective marker utilization, a lack of efficient methodologies for manipulating the genome, and limited complementation systems (152).

In light of the aforementioned struggles, we sought to find a medically relevant *Acinetobacter* strain that was amenable to genetic manipulation. A previous report led by Philip Rather identified several genes in *A. nosocomialis* strain M2 (previously designated *A. baumannii* strain M2) that were partially required for surface-associated motility under the experimental conditions tested (92). During the course of the study, the *pilT* gene product was identified as a potential protein mediating surface-associated motility, which led us to further analyze and

characterize strain M2 for Tfp production and functionality (6). Utilizing methodologies adapted from *A. baylyi* ADP1, we discovered that *A. nosocomialis* strain M2 was naturally transformable, thereby, enabling rapid and efficient manipulation of strain M2's chromosome. Having a naturally transformable clinical isolate allowed us to develop and use genetic tools to further our understanding of *Acinetobacter* pathogenesis.

Using a mutational analysis approach we demonstrated that a medically relevant *Acinetobacter* spp. was capable of producing functional Tfp that were required for natural transformation and twitching motility (6). During the course of our studies, we also determined that the major pilin subunit of the Tfp fiber was glycosylated by the pilin-specific OTase TfpO. We also demonstrated that the majority of *Acinetobacter* strains carry two functional OTases, one devoted exclusively to pilin glycosylation and another dedicated to general *O*-glycosylation (Harding *et al*, 2015 Under review).

5.2 *Acinetobacter nosocomialis* strain M2 as a model system for *Acinetobacter biology*.

It has been known for decades that members of the *Acinetobacter calcoaceticus-baumannii* (Acb) complex are unreliably differentiated by phenotypic characterization alone (35). Misappropriation of a species designation can inflate the importance of one species over another; specifically, *A. baumannii* has

become the overwhelming *de facto* designation for clinical isolates that positively match to the Acb complex. As such, we sequenced the genome of *Acinetobacter* strain M2 (previously designated as *A. baumannii* strain M2) and discovered that strain M2 had been incorrectly classified as *A. baumannii* (93). Utilizing the multilocus sequence typing methodologies, we identified that strain M2 was in fact more closely related to *A. nosocomialis*; therefore, we reclassified the strain as *A. nosocomialis* strain M2 (213). However, given the highly similar genomic relationship between the medically relevant species, *A. baumannii*, *A. nosocomialis*, and *A. pittii*, and the similar clinical manifestations of human disease associated with each infection, we hypothesize that similar virulence mechanisms may be employed these species.

Our identification that *A. nosocomialis* strain M2 was naturally transformable, coupled with the strain M2 genome sequence we presented in Chapter 2, were the first steps towards establishing strain M2 as a model *Acinetobacter* organism (6, 93). We have also developed a system to introduce unmarked, in frame mutations using a modified FLP recombinase strategy. Furthermore, we identified that strain M2 was intrinsically resistant to chloramphenicol, allowing for counter selection over *E. coli* cloning strains when performing conjugal experiments. Lastly, we modified a mini-Tn*7* element system for use within strain M2 allowing for single copy, site directed integration of DNA fragments into the chromosome of strain M2. Collectively, we have developed a robust genetic

toolbox enabling reproducible genomic manipulation of *A. nosocomialis* strain M2 (6, 127).

5.3 Expression of Tfp by medically relevant *Acinetobacter* species.

Acinetobacter spp. have rapidly acquired resistance to many clinically available therapeutic agents; however, the reasons and mechanisms for this accelerated resistance acquisition is only partially understood. One mechanism of acquisition of antibiotic resistance is associated with acquisition of DNA containing genes, which encode for proteins that disrupt the action of antibiotics. Three main mechanisms have been attributed to the acquisition of DNA that facilitates antibiotic resistance: plasmid transfer, transposable elements, and integrons (214). Many *Acinetobacter* spp. have been shown to harbor plasmids, some of which have been documented to encode the genetic information that facilitate resistance to carbepenems and aminoglycosides (215), potentially mediating the adaptive evolution of the organism to clinical environments. It is tempting to speculate that functional Tfp activity has partially mediated this phenomenon as all fully sequenced medically relevant *Acinetobacter* strains contain genes that are predicted to encode proteins required for the biogenesis of Tfp. In accordance with this hypothesis is our observation that *A. nosocomialis* strain M2 is able to uptake either circular or linear plasmids and stably maintain them (Chapter 4 and data now shown).

In *N. gonorrhoeae* and *N. meningitidis*, Tfp are readily observed via electron microscopy indicating the high degree of expression by these species (61). This phenotype has not yet been observed for strain M2 as we were unsuccessful in visualizing Tfp-like appendages on strain M2; in fact, we had to utilize our *pilT* mutant, a strain predicted to be hyper-piliated, in order to find a small percentage of cells that contained structures compatible with the dimensions of Tfp (6). The lack of readily identifiable Tfp-like structures on strain M2 is consistent with our low levels of transformation frequency, as strain M2 exhibited a transformation frequency approximately 5 logs lower than some *Neisseria* spp (216). (Chapter 3); furthermore, it has been shown that filamentous Tfp appendages are not necessarily required for natural transformation (217). However, strain M2 exhibited a robust ability to exhibit twitching motility as shown in Figure 3.6, suggesting that strain M2 could readily and rapidly produce functioning Tfp capable of translocating the organisms across surfaces. Currently, we know that the growth conditions were different for natural transformation assays and twitching motility assays; however, attempts to visualize Tfp-like structures from wild-type cells grown under twitching motility conditions were unsuccessful as well (data not shown).

Although we demonstrated in Chapter 3 that strain M2 requires Tfp for natural transformation and twitching motility, it is unclear under what environmental conditions strain M2 expresses Tfp. LacZ reporter assays and western blot

analysis conducted in *A. baylyi* ADP1 demonstrated that the pilin-like competence factor ComP, orthologous to the major pilin subunit PilA of *A. nosocomialis* strain M2, was most highly expressed in stationary phase and minimally expressed during early and late exponential phase; however, the period associated with low ComP expression levels was actually the point at which ADP1 was the most transformable (88). Thus there appears to be an inverse relationship between ComP expression and transformability. Data presented in Chapter 3 partially mirrors the ADP1 data set, as strain M2 was found to only be transformable during exponential phase.

Understanding the role of Tfp in the biology and virulence of *Acinetobacter* would greatly benefit from detailed studies defining the expression profile of strain M2's Tfp associated proteins, specifically, the major pilin subunit PilA. In a recent study characterizing the motility and adherence of *A. baumannii* clinical isolates, only 18 of 50 isolates exhibited twitching motility even though all strains characterized were found to contain genes which encoded proteins predicted to be subunits of functioning Tfp (5). Therefore, regulatory elements may vary between strains resulting in differential expression profiles. Comparative genomic analyses of *Acinetobacter* strains known to exhibit twitching motility versus those strains that do not twitch might provide insight into those regulatory elements that may vary between these dichotomous populations. If genes that encode proteins previously found to modulate Tfp expression are identified, strain M2 could serve

as a model system for probing the role of target genes in *Acinetobacter* Tfp expression and regulation given the simple methodologies we have developed for mutational analysis as well as the standardized transformation and twitching motility assays we have developed for strain M2.

5.4 The role of the *Acinetobacter* pilin glycan.

Pilin glycosylation has only been identified in a handful of Gram-negative organisms, including, *Neisseria* spp., *P. aeruginosa*, *P. syringae, D. nodosus,* and *F. tularensis* (112-114, 116, 187). In Chapter 4, we described that *A. nosocomialis* strain M2 and *A. baylyi* ADP1 also glycosylate their pilin proteins. Although advancements in mass spectrometry coupled with glycopeptide enrichment strategies have facilitated the identification and characterization of glycopeptides, the role of these glycans, specifically the role of pilin glycans in Tfp associated phenotypes is poorly understand; however, both *Neisseria* and *Pseudomonas* pilin glycan functions have been partially characterized (111).

In both *N. gonorrhoeae* and *N. meningitidis*, the pilin glycosylation system is highly conserved. Furthermore, in *Neisseria* spp. the pilin glycans have been directly shown to be required for optimal binding to surfaces. Specifically, the pilin glycan of *N. meningitidis* has been shown to synergize with phosphorylcholine modifications on the meningococcal pilin fiber to mediate binding to the platelet activating factor receptor, thus, facilitating adherence to human airway epithelial

cells, colonization, and subsequent disease (218). The pilin glycan of *N. gonorrhoeae* was shown to be required for optimal cervical infection, where, glycan deficient strains were hyper-adhesive initially, but, were unable to optimally invade human cervical epithelial cells. The pilin glycan was found to mediate binding of *N. gonorrhoeae* to the I-domain region of complement receptor 3 (219). Increasing the significance of these findings is the high degree of glycan similarity between *N. meningitidis* strains as well as the high degree of glycan similarity between *N. gonorrhoeae* strains(220).

In *P.* aeruginosa, two different systems for pilin glycosylation have been identified. The first system is based on glycosylation of group I pilins ($PilA_I$) (185). Group I pilins, are glycosylated by the accessory protein TfpO at the carboxy-terminal serine of $PilA_I$. Studies led by Peter Castric found that removal of the pilin glycan from *P. aeruginosa* strain 1244 greatly increased the hydrophobicity of the TFP fiber (186). Furthermore, multiple groups have found that *P. aeruginosa* strains encoding for group I pilins had a higher frequency of being isolated from the lungs of cystic fibrosis patients (185, 186). To this end, they also found that strains unable to glycosylate their pilin subunits had an approximately four fold reduced ability to colonize the respiratory tract of mice when co infected with the parental strain (186). The data collectively indicate that the glycan of group I pilins may provide an adherence advantage *in vivo*, specifically in certain niches such as the respiratory tract. In agreement with this

hypothesis is the recent observation that the pilin glycan of *P. aeruginosa* 1244 shields the pilin from opsonins, including surfactant protein A, thereby decreasing the ability of alveolar macrophages and neutrophils to phagocytose and eliminate *P. aeruginosa* 1244 during an acute pulmonary infection (221). Similar studies could be performed to determine if the *Acinetobacter* pilin glycan contributes to *in vivo* fitness, however, first establishing a role for *Acinetobacter* Tfp in models that recapitulate human disease would need to be established.

The second pilin glycosylation system is based on studies revolving around the *P. aeruginosa* 5196 isolate (Pa5196). The Pa5196 isolate contains a group IV pilin ($PilA_{IV}$) (185) and to date is the only isolate characterized to encode $pilA_{IV}$. The Group IV pilin of Pa5196 is glycosylated by the accessory protein TfpW at multiple internal serine and threonine resides with by $_{D}$-arabinofuranose (114, 117) Studies led by Lori Burrows have shown that blocking pilin glycosylation in Pa5196 results in markedly decreased abundance of surface exposed $PilA_{IV}$, which, is coupled with a decreased ability to exhibit twitching motility (123). The authors speculated that the unmodified pilin protein might be folded into an atypical conformation resulting in aberrant processing by the Tfp biogenesis machinery. Their findings were based on the observation that heterologous, non-glycosylated pilins were processed and assembled into fibers similarly to the parental glycosylated pilin subunits in the *tfpW* mutant background indicating the

Tfp biogenesis machinery were properly functioning. This phenotype, however, appears to be exclusive to *P. aeruginosa* strains encoding group IV pilins.

To date, the biological role of pilin glycosylation in *Acinetobacter* has yet to be determined. Neither the pilin-specific OTase, TfpO, nor the pilin glycan were required for basic Tfp function as both the *tfpO* mutant and the M2(*pilA*[S136A])+ point mutant were naturally transformable and exhibited twitching motility similarly to the parental strain (Chapter 4). Even though pilin glycosylation did not alter primary Tfp function in *A. nosocomialis* strain M2 under our experimental conditions, it may alter the ability of the Tfp fiber to interact with the external environment as is the case with group I pilins of *P. aeruginosa*. Understanding more about where the medically relevant *Acinetobacter* reside outside of healthcare facilities may provide insight into the natural role of the pilin glycan; such as, blocking phages from interacting and binding the pilin subunits.

It is unlikely that the *Acinetobacter* pilin glycan recognizes a specific receptor, as is the case for *Neisseria* spp., given the high degree of glycan heterogeneity found between *Acinetobacter* strains as well as glycan microheterogeneity found within strains (111). In *Acinetobacter*, it has been shown that as many as 77 carbohydrate serotypes exist to date; furthermore, these carbohydrates are not only utilized for capsule biosynthesis but are also incorporated into the *O*-glycosylation system serving as the glycan subunit for OTases (55, 111). Thus,

although orthologous proteins, such as PilA, are glycosylated at similar regions by the same OTases in *Acinetobacter* strains, the glycan subunits from different strains will vary depending on which major polysaccharide antigen locus is encoded which will alter the biochemical signature of the glycosylated protein.

Furthermore, experiments performed but not shown (Chapter 4) demonstrated that *A. nosocomialis* strain M2 mutants unable to glycosylate their respective pilins do not have aberrant piliation phenotypes, as the M2Δ*tfpO* mutant exhibited similar levels of surface exposed PilA as compared to the parental strain indicating that glycosylation is not required for pilin stabilization or proper processing of pilin subunits into Tfp fibers.

Although the role of the *Acinetobacter* pilin glycan has yet to be deciphered, our preliminary evidence presented in Chapter 4, indicating *pilA* and *tfpO* appear to be in an operon, leads us to hypothesize that these two genes coevolved. Furthermore, all *Acinetobacter* spp. that encode a *tfpO* homolog also contain a carboxy-terminal serine on their respective PilA sequences. The coevolution of *pilA* and *tfpO* leads us to speculate that the *tfpO* gene product does provide a fitness advantage.

5.5 A Targeted approach to block glycan synthesis: future directions.

General *O*-glycosylation has been shown to directly contribute to the virulence of *Acinetobacter*; specifically, a glycosylation deficient strain had a significantly reduced ability to form biofilms and had an attenuated virulence in a murine model of peritoneal sepsis (105). Additionally, the role of the *Acinetobacter* capsular polysaccharide in virulence has also been recently described, where, loss of the capsule resulted in susceptibility to complement-mediated killing and a reduction in the *in vivo* virulence in the same septicemia model utilized above (55). It was simultaneously demonstrated that in many *Acinetobacter* spp., capsule synthesis and the general *O*-glycosylation system share a common pathway for glycan precursor synthesis (55). Furthermore, in Chapter 4 we demonstrated that the pilin-specific OTase, TfpO, also utilizes the same glycan subunit shared by the general *O*-glycosylation and capsular polysaccharide synthesis pathway (Chapter 4, Figure 10). Together all three processes, capsule production, general *O*-glycosylation, and pilin glycosylation are all linked by the same glycan subunit for a given *Acinetobacter* strain. Consequently, targeted approaches seeking to disrupt these pathways are rationally being pursued to limit the virulence of these organisms.

The glycan precursor consists of an oligosaccharide assembled onto the predicted Und-P lipid. Synthesis is initiated by the initiating glycosyl-transferase *weeH* (also known as *pglC*), which transfers a nucleotide-activated sugar onto the Und-P (103). This first step is the most critical, as blocking this step impedes

all downstream steps. Therefore, mutations in *weeH* block glycan precursor synthesis, which accordingly blocks capsule production, general *O*-glycosylation, and pilin glycosylation in *Acinetobacter* (55) (Harding *et al*., 2015 under review). WeeH is a member of the polyisoprenyl-phosphate hexose-1-phosphate transferase (PHPT) family (222). This class of proteins only exists in prokaryotes and has been studied extensively for their role in the synthesis of the repeating subunit of the O-antigen in lipopolysaccharide (223, 224). PHPT proteins are membrane proteins containing cytoplasmic domains associated with the transfer of the nucleotide-activated sugar to Und-P at the inner leaflet of the cytoplasmic membrane. Initiating glycosyl-transferases have canonically been identified to transfer hexose sugars, in accordance with this is the fact that of the 13 carbohydrate structures solved for *A. baumannii*, the reducing sugar has been identified as either 2-acetamido-2-deoxy-D-glucose (GlcNAc) or 2-acetamido-2-deoxy-D-galactose (GalNAc), both common hexoses (55, 199).

The majority of the initiating glycosyl-transferases are predicted to contain five transmembrane domains (223); however, the *Acinetobacter* initiating glycosyl-transferases are predicted to only contain a single transmembrane domain. Importantly, *weeH* homologs are highly conserved across medically relevant *Acinetobacter* species making this protein an attractive target for the development of small inhibitory molecules.

Future work regarding *Acinetobacter* glycosylation should focus on functional characterization of WeeH. Protein reporter experiments should be conducted to definitively determine which domains are cytoplasmic and various truncation constructs can begin to identify protein domains required for functionality. Identification of the catalytic domain via structure analyses will facilitate the rational design of molecules that bind the catalytic domain and could be coupled with *in vitro* assays screening for potent inhibitors.

5.6 Conclusions

Reliable genetic manipulation is the hallmark for understanding the relationships between a gene or sets of genes and a phenotype. The genome sequence we have deposited and the techniques we have developed for *A. nosocomialis* strain M2 in Chapters 2, 3, and 4 can be utilized to study any gene-phenotype relationship reliably and reproducibly. With these techniques we have laid the foundation for future work probing the role of Tfp in the biology and virulence of medically relevant *Acinetobacter* spp.; however, as mentioned above, future studies should first be directed at discerning the regulation and expression of Tfp in medically relevant *Acinetobacter* strains, especially given the disparate levels of Tfp functionality as determined by twitching motility of clinical isolates.

The pilin glycosylation system in *Acinetobacter* parallels that of *P. aeruginosa* strains encoding for group I pilins, and as such, identifying the role of the

Acinetobacter pilin glycan will probably be equally as elusive as it has been for *P. aeruginosa*; however, future work could utilize the strains we have built to probe the role of pilin glycosylation in different model systems.

This work identified for first time that a medically relevant *Acinetobacter* strain was able to produce functioning Tfp and is the first step in determining if *Acinetobacter* broadly use these surface organelles to facilitate colonization and subsequent disease.

References

1. Brisou J & Prevot AR (1954) [Studies on bacterial taxonomy. X. The revision of species under *Acromobacter* group]. *Annales de l'Institut Pasteur* 86(6):722-728.
2. Baumann P, Doudoroff M, & Stanier RY (1968) A study of the *Moraxella* group. II. Oxidative-negative species (genus *Acinetobacter*). *Journal of bacteriology* 95(5):1520-1541.
3. Juni E (1972) Interspecies transformation of *Acinetobacter*: genetic evidence for a ubiquitous genus. *Journal of bacteriology* 112(2):917-931.
4. Barker J & Maxted H (1975) Observations on the growth and movement of *Acinetobacter* on semi-solid media. *Journal of medical microbiology* 8(3):443-446.
5. Eijkelkamp BA*, et al.* (2011) Adherence and motility characteristics of clinical Acinetobacter baumannii isolates. *FEMS microbiology letters* 323(1):44-51.
6. Harding CM*, et al.* (2013) *Acinetobacter baumannii* strain M2 produces type IV pili which play a role in natural transformation and twitching motility but not surface-associated motility. *mBio* 4(4).
7. Johnson JL, Anderson RS, & Ordal EJ (1970) Nucleic acid homologies among oxidase-negative *Moraxella* species. *Journal of bacteriology* 101(2):568-573.
8. Bouvet PJM & Grimont PAD (1986) Taxonomy of the Genus *Acinetobacter* with the Recognition of *Acinetobacter baumannii* sp. nov., *Acinetobacter haemolyticus* sp. nov., *Acinetobacter johnsonii* sp. nov., and *Acinetobacter junii* sp. nov. and Emended Descriptions of *Acinetobactercalcoaceticus* and *Acinetobacter lwoffii*. *Int J Syst Bacteriol* 36(2):228-240.
9. Gerner-Smidt P, Tjernberg I, & Ursing J (1991) Reliability of phenotypic tests for identification of *Acinetobacter* species. *Journal of clinical microbiology* 29(2):277-282.
10. Tjernberg I & Ursing J (1989) Clinical strains of *Acinetobacter* classified by DNA-DNA hybridization. *APMIS : acta pathologica, microbiologica, et immunologica Scandinavica* 97(7):595-605.
11. Nemec A*, et al.* (2011) Genotypic and phenotypic characterization of the *Acinetobacter calcoaceticus-Acinetobacter baumannii* complex with the proposal of *Acinetobacter pittii* sp. nov. (formerly *Acinetobacter* genomic species 3) and *Acinetobacter nosocomialis* sp. nov. (formerly *Acinetobacter* genomic species 13TU). *Research in microbiology* 162(4):393-404.
12. Kang YS, Jung J, Jeon CO, & Park W (2011) *Acinetobacter oleivorans* sp. nov. is capable of adhering to and growing on diesel-oil. *J Microbiol* 49(1):29-34.
13. Sahl JW*, et al.* (2013) Evolution of a pathogen: a comparative genomics analysis identifies a genetic pathway to pathogenesis in *Acinetobacter*. *PloS one* 8(1):e54287.

14. Carr EL, Kampfer P, Patel BK, Gurtler V, & Seviour RJ (2003) Seven novel species of *Acinetobacter* isolated from activated sludge. *International journal of systematic and evolutionary microbiology* 53(Pt 4):953-963.
15. Elliott KT & Neidle EL (2011) *Acinetobacter baylyi* ADP1: transforming the choice of model organism. *IUBMB life* 63(12):1075-1080.
16. Juni E & Heym GA (1964) Pathways for Biosynthesis of a Bacterial Capsular Polysaccharide. Iv. Capsule Resynthesis by Decapsulated Resting-Cell Suspensions. *Journal of bacteriology* 87:461-467.
17. Taylor WH & Juni E (1961) Pathways for biosynthesis of a bacterial capsular polysaccharide. III. Syntheses from radioactive substrates. *The Journal of biological chemistry* 236:1231-1234.
18. Taylor WH & Juni E (1961) Pathways for biosynthesis of a bacterial capsular polysaccharide. I. Characterization of the organism and polysaccharide. *Journal of bacteriology* 81:688-693.
19. Taylor WH & Juni E (1961) Pathways for biosynthesis of a bacterial capsular polysaccharide. I. Carbohydrate metabolism and terminal oxidation mechanisms of a capsuleproducing coccus. *Journal of bacteriology* 81:694-703.
20. Juni E & Janik A (1969) Transformation of *Acinetobacter calco-aceticus* (*Bacterium anitratum*). *Journal of bacteriology* 98(1):281-288.
21. Patel RN, Mazumdar S, & Ornston LN (1975) Beta-ketoadipate enol-lactone hydrolases I and II from *Acinetobacter calcoaceticus*. *The Journal of biological chemistry* 250(16):6567-6567.
22. Vaneechoutte M*, et al.* (2006) Naturally transformable *Acinetobacter* sp. strain ADP1 belongs to the newly described species *Acinetobacter baylyi*. *Applied and environmental microbiology* 72(1):932-936.
23. Dijkshoorn L, Nemec A, & Seifert H (2007) An increasing threat in hospitals: multidrug-resistant Acinetobacter baumannii. *Nature reviews. Microbiology* 5(12):939-951.
24. Dijkshoorn L*, et al.* (1993) Correlation of typing methods for *Acinetobacter* isolates from hospital outbreaks. *Journal of clinical microbiology* 31(3):702-705.
25. Boo TW, Walsh F, & Crowley B (2009) Molecular characterization of carbapenem-resistant *Acinetobacter* species in an Irish university hospital: predominance of *Acinetobacter* genomic species 3. *Journal of medical microbiology* 58(Pt 2):209-216.
26. van den Broek PJ*, et al.* (2009) Endemic and epidemic acinetobacter species in a university hospital: an 8-year survey. *Journal of clinical microbiology* 47(11):3593-3599.
27. Wisplinghoff H*, et al.* (2012) Nosocomial bloodstream infections due to *Acinetobacter baumannii*, *Acinetobacter pittii* and *Acinetobacter nosocomialis* in the United States. *The Journal of infection* 64(3):282-290.
28. Wang X, Chen T, Yu R, Lu X, & Zong Z (2013) *Acinetobacter pittii* and *Acinetobacter nosocomialis* among clinical isolates of the *Acinetobacter calcoaceticus-baumannii* complex in Sichuan, China. *Diagnostic microbiology and infectious disease* 76(3):392-395.

29. Chusri S, *et al.* (2014) Clinical outcomes of hospital-acquired infection with *Acinetobacter nosocomialis* and *Acinetobacter pittii*. *Antimicrobial agents and chemotherapy* 58(7):4172-4179.
30. McConnell MJ, Actis L, & Pachon J (2013) *Acinetobacter baumannii*: human infections, factors contributing to pathogenesis and animal models. *FEMS microbiology reviews* 37(2):130-155.
31. Joly-Guillou ML (2005) Clinical impact and pathogenicity of *Acinetobacter*. *Clinical microbiology and infection : the official publication of the European Society of Clinical Microbiology and Infectious Diseases* 11(11):868-873.
32. Bernards AT, *et al.* (1998) Methicillin-resistant *Staphylococcus aureus* and *Acinetobacter baumannii*: an unexpected difference in epidemiologic behavior. *American journal of infection control* 26(6):544-551.
33. Dijkshoorn L, *et al.* (1989) Use of protein profiles to identify *Acinetobacter calcoaceticus* in a respiratory care unit. *Journal of clinical pathology* 42(8):853-857.
34. Prevention CfDCa (2013) Antibiotic Resistance Threats in the United States, 2013. (htttp://http://www.cdc.gov/drugresistance/threat-report-2013-508.pdf).
35. Viehman JA, Nguyen MH, & Doi Y (2014) Treatment options for carbapenem-resistant and extensively drug-resistant *Acinetobacter baumannii* infections. *Drugs* 74(12):1315-1333.
36. Bou G & Martinez-Beltran J (2000) Cloning, nucleotide sequencing, and analysis of the gene encoding an AmpC beta-lactamase in *Acinetobacter baumannii*. *Antimicrobial agents and chemotherapy* 44(2):428-432.
37. Hujer KM, *et al.* (2005) Identification of a new allelic variant of the *Acinetobacter baumannii* cephalosporinase, ADC-7 beta-lactamase: defining a unique family of class C enzymes. *Antimicrobial agents and chemotherapy* 49(7):2941-2948.
38. Corvec S, *et al.* (2003) AmpC cephalosporinase hyperproduction in *Acinetobacter baumannii* clinical strains. *The Journal of antimicrobial chemotherapy* 52(4):629-635.
39. Hamidian M, Hancock DP, & Hall RM (2013) Horizontal transfer of an ISAba125-activated *ampC* gene between *Acinetobacter baumannii* strains leading to cephalosporin resistance. *The Journal of antimicrobial chemotherapy* 68(1):244-245.
40. Turton JF, *et al.* (2006) The role of ISAba1 in expression of OXA carbapenemase genes in *Acinetobacter baumannii*. *FEMS microbiology letters* 258(1):72-77.
41. Mitchell JM & Leonard DA (2014) Common clinical substitutions enhance the carbapenemase activity of OXA-51-like class D beta-lactamases from *Acinetobacter* spp. *Antimicrobial agents and chemotherapy* 58(11):7015-7016.
42. Tang SS, Apisarnthanarak A, & Hsu LY (2014) Mechanisms of beta-lactam antimicrobial resistance and epidemiology of major community- and healthcare-associated multidrug-resistant bacteria. *Advanced drug delivery reviews* 78C:3-13.

43. Peleg AY, Seifert H, & Paterson DL (2008) *Acinetobacter baumannii*: emergence of a successful pathogen. *Clinical microbiology reviews* 21(3):538-582.
44. Kempf M & Rolain JM (2012) Emergence of resistance to carbapenems in *Acinetobacter baumannii* in Europe: clinical impact and therapeutic options. *International journal of antimicrobial agents* 39(2):105-114.
45. Wieczorek P*, et al.* (2008) Multidrug resistant *Acinetobacter baumannii*--the role of AdeABC (RND family) efflux pump in resistance to antibiotics. *Folia histochemica et cytobiologica / Polish Academy of Sciences, Polish Histochemical and Cytochemical Society* 46(3):257-267.
46. Moffatt JH*, et al.* (2010) Colistin resistance in *Acinetobacter baumannii* is mediated by complete loss of lipopolysaccharide production. *Antimicrobial agents and chemotherapy* 54(12):4971-4977.
47. Adams MD*, et al.* (2009) Resistance to colistin in *Acinetobacter baumannii* associated with mutations in the PmrAB two-component system. *Antimicrobial agents and chemotherapy* 53(9):3628-3634.
48. Kim Y*, et al.* (2014) In vivo emergence of colistin resistance in *Acinetobacter baumannii* clinical isolates of sequence type 357 during colistin treatment. *Diagnostic microbiology and infectious disease* 79(3):362-366.
49. Choi CH, Lee JS, Lee YC, Park TI, & Lee JC (2008) Acinetobacter baumannii invades epithelial cells and outer membrane protein A mediates interactions with epithelial cells. *BMC microbiology* 8:216.
50. Gaddy JA, Tomaras AP, & Actis LA (2009) The *Acinetobacter baumannii* 19606 OmpA protein plays a role in biofilm formation on abiotic surfaces and in the interaction of this pathogen with eukaryotic cells. *Infection and immunity* 77(8):3150-3160.
51. Kim SW*, et al.* (2009) Serum resistance of *Acinetobacter baumannii* through the binding of factor H to outer membrane proteins. *FEMS microbiology letters* 301(2):224-231.
52. Lee JS, Choi CH, Kim JW, & Lee JC (2010) Acinetobacter baumannii outer membrane protein A induces dendritic cell death through mitochondrial targeting. *J Microbiol* 48(3):387-392.
53. Gentile V*, et al.* (2014) Iron and *Acinetobacter baumannii* Biofilm Formation. *Pathogens* 3(3):704-719.
54. Choi AH, Slamti L, Avci FY, Pier GB, & Maira-Litran T (2009) The pgaABCD locus of *Acinetobacter baumannii* encodes the production of poly-beta-1-6-N-acetylglucosamine, which is critical for biofilm formation. *Journal of bacteriology* 191(19):5953-5963.
55. Lees-Miller RG*, et al.* (2013) A common pathway for O-linked protein-glycosylation and synthesis of capsule in *Acinetobacter baumannii*. *Molecular microbiology* 89(5):816-830.
56. Penwell WF, Arivett BA, & Actis LA (2012) The *Acinetobacter baumannii* entA gene located outside the acinetobactin cluster is critical for siderophore production, iron acquisition and virulence. *PloS one* 7(5):e36493.

57. Smith MG*, et al.* (2007) New insights into Acinetobacter baumannii pathogenesis revealed by high-density pyrosequencing and transposon mutagenesis. *Genes & development* 21(5):601-614.
58. Pelicic V (2008) Type IV pili: e pluribus unum? *Molecular microbiology* 68(4):827-837.
59. Melville S & Craig L (2013) Type IV pili in Gram-positive bacteria. *Microbiology and molecular biology reviews : MMBR* 77(3):323-341.
60. Burrows LL (2012) Pseudomonas aeruginosa twitching motility: type IV pili in action. *Annual review of microbiology* 66:493-520.
61. Craig L*, et al.* (2006) Type IV pilus structure by cryo-electron microscopy and crystallography: implications for pilus assembly and functions. *Molecular cell* 23(5):651-662.
62. Giltner CL, Nguyen Y, & Burrows LL (2012) Type IV pilin proteins: versatile molecular modules. *Microbiology and molecular biology reviews : MMBR* 76(4):740-772.
63. Strom MS, Bergman P, & Lory S (1993) Identification of active-site cysteines in the conserved domain of PilD, the bifunctional type IV pilin leader peptidase/N-methyltransferase of *Pseudomonas aeruginosa*. *The Journal of biological chemistry* 268(21):15788-15794.
64. Strom MS, Nunn DN, & Lory S (1993) A single bifunctional enzyme, PilD, catalyzes cleavage and N-methylation of proteins belonging to the type IV pilin family. *Proceedings of the National Academy of Sciences of the United States of America* 90(6):2404-2408.
65. Giltner CL, Habash M, & Burrows LL (2010) *Pseudomonas aeruginosa* minor pilins are incorporated into type IV pili. *Journal of molecular biology* 398(3):444-461.
66. Nguyen Y*, et al.* (2015) *Pseudomonas aeruginosa* Minor Pilins Prime Type IVa Pilus Assembly and Promote Surface Display of the PilY1 Adhesin. *The Journal of biological chemistry* 290(1):601-611.
67. Chiang P*, et al.* (2008) Functional role of conserved residues in the characteristic secretion NTPase motifs of the *Pseudomonas aeruginosa* type IV pilus motor proteins PilB, PilT and PilU. *Microbiology* 154(Pt 1):114-126.
68. Collins RF, Davidsen L, Derrick JP, Ford RC, & Tonjum T (2001) Analysis of the PilQ secretin from *Neisseria meningitidis* by transmission electron microscopy reveals a dodecameric quaternary structure. *Journal of bacteriology* 183(13):3825-3832.
69. Berry JL*, et al.* (2012) Structure and assembly of a trans-periplasmic channel for type IV pili in *Neisseria meningitidis*. *PLoS pathogens* 8(9):e1002923.
70. Satyshur KA*, et al.* (2007) Crystal structures of the pilus retraction motor PilT suggest large domain movements and subunit cooperation drive motility. *Structure* 15(3):363-376.
71. Merz AJ, So M, & Sheetz MP (2000) Pilus retraction powers bacterial twitching motility. *Nature* 407(6800):98-102.

72. Maier B*, et al.* (2002) Single pilus motor forces exceed 100 pN. *Proceedings of the National Academy of Sciences of the United States of America* 99(25):16012-16017.
73. O'Toole GA & Kolter R (1998) Flagellar and twitching motility are necessary for *Pseudomonas aeruginosa* biofilm development. *Molecular microbiology* 30(2):295-304.
74. Hahn HP (1997) The type-4 pilus is the major virulence-associated adhesin of *Pseudomonas aeruginosa*--a review. *Gene* 192(1):99-108.
75. Palmen R & Hellingwerf KJ (1997) Uptake and processing of DNA by *Acinetobacter calcoaceticus*--a review. *Gene* 192(1):179-190.
76. Cehovin A*, et al.* (2013) Specific DNA recognition mediated by a type IV pilin. *Proceedings of the National Academy of Sciences of the United States of America* 110(8):3065-3070.
77. Wolfgang M*, et al.* (1998) PilT mutations lead to simultaneous defects in competence for natural transformation and twitching motility in piliated *Neisseria gonorrhoeae*. *Molecular microbiology* 29(1):321-330.
78. Graupner S, Weger N, Sohni M, & Wackernagel W (2001) Requirement of novel competence genes *pilT* and *pilU* of *Pseudomonas stutzeri* for natural transformation and suppression of *pilT* deficiency by a hexahistidine tag on the type IV pilus protein PilAI. *Journal of bacteriology* 183(16):4694-4701.
79. Henrichsen J (1983) Twitching motility. *Annual review of microbiology* 37:81-93.
80. Conrad JC*, et al.* (2011) Flagella and pili-mediated near-surface single-cell motility mechanisms in *P. aeruginosa*. *Biophysical journal* 100(7):1608-1616.
81. Antunes LC, Imperi F, Carattoli A, & Visca P (2011) Deciphering the multifactorial nature of Acinetobacter baumannii pathogenicity. *PloS one* 6(8):e22674.
82. Metzgar D*, et al.* (2004) *Acinetobacter* sp. ADP1: an ideal model organism for genetic analysis and genome engineering. *Nucleic acids research* 32(19):5780-5790.
83. de Berardinis V, Durot M, Weissenbach J, & Salanoubat M (2009) *Acinetobacter baylyi* ADP1 as a model for metabolic system biology. *Current opinion in microbiology* 12(5):568-576.
84. Young DM, Parke D, & Ornston LN (2005) Opportunities for genetic investigation afforded by *Acinetobacter baylyi*, a nutritionally versatile bacterial species that is highly competent for natural transformation. *Annual review of microbiology* 59:519-551.
85. de Vries J, Meier P, & Wackernagel W (2001) The natural transformation of the soil bacteria *Pseudomonas stutzeri* and *Acinetobacter* sp. by transgenic plant DNA strictly depends on homologous sequences in the recipient cells. *FEMS microbiology letters* 195(2):211-215.
86. de Berardinis V*, et al.* (2008) A complete collection of single-gene deletion mutants of *Acinetobacter baylyi* ADP1. *Molecular systems biology* 4:174.

87. Porstendorfer D, Drotschmann U, & Averhoff B (1997) A novel competence gene, *comP*, is essential for natural transformation of *Acinetobacter* sp. strain BD413. *Applied and environmental microbiology* 63(11):4150-4157.
88. Porstendorfer D, Gohl O, Mayer F, & Averhoff B (2000) ComP, a pilin-like protein essential for natural competence in *Acinetobacter* sp. Strain BD413: regulation, modification, and cellular localization. *Journal of bacteriology* 182(13):3673-3680.
89. Busch S, Rosenplanter C, & Averhoff B (1999) Identification and characterization of ComE and ComF, two novel pilin-like competence factors involved in natural transformation of *Acinetobacter* sp. strain BD413. *Applied and environmental microbiology* 65(10):4568-4574.
90. Link C, Eickernjager S, Porstendorfer D, & Averhoff B (1998) Identification and characterization of a novel competence gene, *comC*, required for DNA binding and uptake in *Acinetobacter* sp. strain BD413. *Journal of bacteriology* 180(6):1592-1595.
91. Eijkelkamp BA, Hassan KA, Paulsen IT, & Brown MH (2011) Investigation of the human pathogen Acinetobacter baumannii under iron limiting conditions. *BMC genomics* 12:126.
92. Clemmer KM, Bonomo RA, & Rather PN (2011) Genetic analysis of surface motility in Acinetobacter baumannii. *Microbiology* 157(Pt 9):2534-2544.
93. Carruthers MD*, et al.* (2013) Draft Genome Sequence of the Clinical Isolate *Acinetobacter nosocomialis* Strain M2. *Genome announcements* 1(6).
94. Tucker AT*, et al.* (2014) Defining gene-phenotype relationships in *Acinetobacter baumannii* through one-step chromosomal gene inactivation. *mBio* 5(4):e01313-01314.
95. Ramirez MS*, et al.* (2010) Naturally competent Acinetobacter baumannii clinical isolate as a convenient model for genetic studies. *Journal of clinical microbiology* 48(4):1488-1490.
96. Nothaft H & Szymanski CM (2010) Protein glycosylation in bacteria: sweeter than ever. *Nature reviews. Microbiology* 8(11):765-778.
97. Apweiler R, Hermjakob H, & Sharon N (1999) On the frequency of protein glycosylation, as deduced from analysis of the SWISS-PROT database. *Biochimica et biophysica acta* 1473(1):4-8.
98. Iwashkiw JA, Vozza NF, Kinsella RL, & Feldman MF (2013) Pour some sugar on it: the expanding world of bacterial protein *O*-linked glycosylation. *Molecular microbiology* 89(1):14-28.
99. Schirm M*, et al.* (2004) Structural and genetic characterization of glycosylation of type a flagellin in *Pseudomonas aeruginosa*. *Journal of bacteriology* 186(9):2523-2531.
100. Thibault P*, et al.* (2001) Identification of the carbohydrate moieties and glycosylation motifs in *Campylobacter jejuni* flagellin. *The Journal of biological chemistry* 276(37):34862-34870.
101. Twine SM*, et al.* (2008) Flagellar glycosylation in *Clostridium botulinum*. *The FEBS journal* 275(17):4428-4444.

102. Gross J, *et al.* (2008) The *Haemophilus influenzae* HMW1 adhesin is a glycoprotein with an unusual N-linked carbohydrate modification. *The Journal of biological chemistry* 283(38):26010-26015.
103. Hug I & Feldman MF (2011) Analogies and homologies in lipopolysaccharide and glycoprotein biosynthesis in bacteria. *Glycobiology* 21(2):138-151.
104. Rahn A, Beis K, Naismith JH, & Whitfield C (2003) A novel outer membrane protein, Wzi, is involved in surface assembly of the *Escherichia coli* K30 group 1 capsule. *Journal of bacteriology* 185(19):5882-5890.
105. Iwashkiw JA, *et al.* (2012) Identification of a general O-linked protein glycosylation system in Acinetobacter baumannii and its role in virulence and biofilm formation. *PLoS pathogens* 8(6):e1002758.
106. Coyne MJ, *et al.* (2013) Phylum-wide general protein O-glycosylation system of the Bacteroidetes. *Molecular microbiology* 88(4):772-783.
107. Lithgow KV, *et al.* (2014) A general protein *O*-glycosylation system within the *Burkholderia cepacia* complex is involved in motility and virulence. *Molecular microbiology* 92(1):116-137.
108. Power PM, *et al.* (2000) Genetic characterization of pilin glycosylation in *Neisseria meningitidis*. *Microbiology* 146 (Pt 4):967-979.
109. Vanterpool E, Roy F, & Fletcher HM (2005) Inactivation of *vimF*, a putative glycosyltransferase gene downstream of *vimE*, alters glycosylation and activation of the gingipains in *Porphyromonas gingivalis* W83. *Infection and immunity* 73(7):3971-3982.
110. Schulz BL, *et al.* (2013) Identification of bacterial protein O-oligosaccharyltransferases and their glycoprotein substrates. *PloS one* 8(5):e62768.
111. Scott NE, *et al.* (2014) Diversity within the O-linked protein glycosylation systems of *Acinetobacter* species. *Molecular & cellular proteomics : MCP* 13(9):2354-2370.
112. Jennings MP, *et al.* (1998) Identification of a novel gene involved in pilin glycosylation in *Neisseria meningitidis*. *Molecular microbiology* 29(4):975-984.
113. Castric P (1995) pilO, a gene required for glycosylation of Pseudomonas aeruginosa 1244 pilin. *Microbiology* 141 (Pt 5):1247-1254.
114. Voisin S, *et al.* (2007) Glycosylation of *Pseudomonas aeruginosa* strain Pa5196 type IV pilins with mycobacterium-like alpha-1,5-linked d-Araf oligosaccharides. *Journal of bacteriology* 189(1):151-159.
115. Egge-Jacobsen W, *et al.* (2011) O-linked glycosylation of the PilA pilin protein of *Francisella tularensis*: identification of the endogenous protein-targeting oligosaccharyltransferase and characterization of the native oligosaccharide. *Journal of bacteriology* 193(19):5487-5497.
116. Cagatay TI & Hickford JG (2008) Glycosylation of type-IV fimbriae of *Dichelobacter nodosus*. *Veterinary microbiology* 126(1-3):160-167.
117. Kus JV, *et al.* (2008) Modification of *Pseudomonas aeruginosa* Pa5196 type IV Pilins at multiple sites with D-Araf by a novel GT-C family Arabinosyltransferase, TfpW. *Journal of bacteriology* 190(22):7464-7478.

118. Aas FE, Vik A, Vedde J, Koomey M, & Egge-Jacobsen W (2007) *Neisseria gonorrhoeae O*-linked pilin glycosylation: functional analyses define both the biosynthetic pathway and glycan structure. *Molecular microbiology* 65(3):607-624.
119. Power PM*, et al.* (2003) Genetic characterization of pilin glycosylation and phase variation in *Neisseria meningitidis*. *Molecular microbiology* 49(3):833-847.
120. Chamot-Rooke J*, et al.* (2007) Alternative *Neisseria* spp. type IV pilin glycosylation with a glyceramido acetamido trideoxyhexose residue. *Proceedings of the National Academy of Sciences of the United States of America* 104(37):14783-14788.
121. Castric P, Cassels FJ, & Carlson RW (2001) Structural characterization of the *Pseudomonas aeruginosa* 1244 pilin glycan. *The Journal of biological chemistry* 276(28):26479-26485.
122. Comer JE, Marshall MA, Blanch VJ, Deal CD, & Castric P (2002) Identification of the *Pseudomonas aeruginosa* 1244 pilin glycosylation site. *Infection and immunity* 70(6):2837-2845.
123. Harvey H, Kus JV, Tessier L, Kelly J, & Burrows LL (2011) *Pseudomonas aeruginosa* D-arabinofuranose biosynthetic pathway and its role in type IV pilus assembly. *The Journal of biological chemistry* 286(32):28128-28137.
124. Niu C, Clemmer KM, Bonomo RA, & Rather PN (2008) Isolation and characterization of an autoinducer synthase from Acinetobacter baumannii. *Journal of bacteriology* 190(9):3386-3392.
125. Stacy DM, Welsh MA, Rather PN, & Blackwell HE (2012) Attenuation of quorum sensing in the pathogen *Acinetobacter baumannii* using non-native N-Acyl homoserine lactones. *ACS chemical biology* 7(10):1719-1728.
126. Saroj SD, Clemmer KM, Bonomo RA, & Rather PN (2012) Novel mechanism for fluoroquinolone resistance in *Acinetobacter baumannii*. *Antimicrobial agents and chemotherapy* 56(9):4955-4957.
127. Carruthers MD, Nicholson PA, Tracy EN, & Munson RS, Jr. (2013) Acinetobacter baumannii utilizes a type VI secretion system for bacterial competition. *PloS one* 8(3):e59388.
128. Maragakis LL & Perl TM (2008) Acinetobacter baumannii: epidemiology, antimicrobial resistance, and treatment options. *Clinical infectious diseases : an official publication of the Infectious Diseases Society of America* 46(8):1254-1263.
129. Towner KJ (2009) Acinetobacter: an old friend, but a new enemy. *The Journal of hospital infection* 73(4):355-363.
130. Weber DJ, Rutala WA, Miller MB, Huslage K, & Sickbert-Bennett E (2010) Role of hospital surfaces in the transmission of emerging health care-associated pathogens: norovirus, Clostridium difficile, and Acinetobacter species. *American journal of infection control* 38(5 Suppl 1):S25-33.
131. Houang ET, Sormunen RT, Lai L, Chan CY, & Leong AS (1998) Effect of desiccation on the ultrastructural appearances of Acinetobacter baumannii and Acinetobacter lwoffii. *Journal of clinical pathology* 51(10):786-788.

132. Lockhart SR*, et al.* (2007) Antimicrobial resistance among Gram-negative bacilli causing infections in intensive care unit patients in the United States between 1993 and 2004. *Journal of clinical microbiology* 45(10):3352-3359.
133. Rice LB (2008) Federal funding for the study of antimicrobial resistance in nosocomial pathogens: no ESKAPE. *The Journal of infectious diseases* 197(8):1079-1081.
134. Hsueh PR*, et al.* (2002) Pandrug-resistant Acinetobacter baumannii causing nosocomial infections in a university hospital, Taiwan. *Emerging infectious diseases* 8(8):827-832.
135. Giamarellou H, Antoniadou A, & Kanellakopoulou K (2008) Acinetobacter baumannii: a universal threat to public health? *International journal of antimicrobial agents* 32(2):106-119.
136. Jacobs AC*, et al.* (2010) Inactivation of phospholipase D diminishes Acinetobacter baumannii pathogenesis. *Infection and immunity* 78(5):1952-1962.
137. Brossard KA & Campagnari AA (2012) The Acinetobacter baumannii biofilm-associated protein plays a role in adherence to human epithelial cells. *Infection and immunity* 80(1):228-233.
138. Bentancor LV, Camacho-Peiro A, Bozkurt-Guzel C, Pier GB, & Maira-Litran T (2012) Identification of Ata, a multifunctional trimeric autotransporter of Acinetobacter baumannii. *Journal of bacteriology* 194(15):3950-3960.
139. Tomaras AP, Dorsey CW, Edelmann RE, & Actis LA (2003) Attachment to and biofilm formation on abiotic surfaces by Acinetobacter baumannii: involvement of a novel chaperone-usher pili assembly system. *Microbiology* 149(Pt 12):3473-3484.
140. Gaddy JA*, et al.* (2012) Role of acinetobactin-mediated iron acquisition functions in the interaction of Acinetobacter baumannii strain ATCC 19606T with human lung epithelial cells, Galleria mellonella caterpillars, and mice. *Infection and immunity* 80(3):1015-1024.
141. Actis LA, Potter SA, & Crosa JH (1985) Iron-regulated outer membrane protein OM2 of *Vibrio anguillarum* is encoded by virulence plasmid pJM1. *Journal of bacteriology* 161(2):736-742.
142. Ayers M, Howell PL, & Burrows LL (2010) Architecture of the type II secretion and type IV pilus machineries. *Future microbiology* 5(8):1203-1218.
143. Mattick JS (2002) Type IV pili and twitching motility. *Annual review of microbiology* 56:289-314.
144. Chen I & Dubnau D (2004) DNA uptake during bacterial transformation. *Nature reviews. Microbiology* 2(3):241-249.
145. Carruthers MD*, et al.* (2012) Biological roles of nontypeable Haemophilus influenzae type IV pilus proteins encoded by the pil and com operons. *Journal of bacteriology* 194(8):1927-1933.
146. Skerker JM & Berg HC (2001) Direct observation of extension and retraction of type IV pili. *Proceedings of the National Academy of Sciences of the United States of America* 98(12):6901-6904.

147. Skiebe E*, et al.* (2012) Surface-associated motility, a common trait of clinical isolates of Acinetobacter baumannii, depends on 1,3-diaminopropane. *International journal of medical microbiology : IJMM* 302(3):117-128.
148. Wolfgang M, Park HS, Hayes SF, van Putten JP, & Koomey M (1998) Suppression of an absolute defect in type IV pilus biogenesis by loss-of-function mutations in pilT, a twitching motility gene in Neisseria gonorrhoeae. *Proceedings of the National Academy of Sciences of the United States of America* 95(25):14973-14978.
149. Whitchurch CB & Mattick JS (1994) Characterization of a gene, pilU, required for twitching motility but not phage sensitivity in Pseudomonas aeruginosa. *Molecular microbiology* 13(6):1079-1091.
150. Datsenko KA & Wanner BL (2000) One-step inactivation of chromosomal genes in Escherichia coli K-12 using PCR products. *Proceedings of the National Academy of Sciences of the United States of America* 97(12):6640-6645.
151. Tracy E, Ye F, Baker BD, & Munson RS, Jr. (2008) Construction of non-polar mutants in Haemophilus influenzae using FLP recombinase technology. *BMC molecular biology* 9:101.
152. Kumar A, Dalton C, Cortez-Cordova J, & Schweizer HP (2010) Mini-Tn7 vectors as genetic tools for single copy gene cloning in Acinetobacter baumannii. *Journal of microbiological methods* 82(3):296-300.
153. Tramont EC*, et al.* (1981) Gonococcal pilus vaccine. Studies of antigenicity and inhibition of attachment. *The Journal of clinical investigation* 68(4):881-888.
154. Schoolnik GK (1994) Purification of somatic pili. *Methods in enzymology* 236:271-282.
155. Kelley LA & Sternberg MJ (2009) Protein structure prediction on the Web: a case study using the Phyre server. *Nature protocols* 4(3):363-371.
156. Mussi MA*, et al.* (2010) The opportunistic human pathogen Acinetobacter baumannii senses and responds to light. *Journal of bacteriology* 192(24):6336-6345.
157. McQueary CN*, et al.* (2012) Extracellular Stress and Lipopolysaccharide Modulate Acinetobacter baumannii Surface-Associated Motility. *Journal of Microbiology* 50(3):434-443.
158. Rudel T*, et al.* (1995) Role of pili and the phase-variable PilC protein in natural competence for transformation of Neisseria gonorrhoeae. *Proceedings of the National Academy of Sciences of the United States of America* 92(17):7986-7990.
159. Baynham PJ, Ramsey DM, Gvozdyev BV, Cordonnier EM, & Wozniak DJ (2006) The Pseudomonas aeruginosa ribbon-helix-helix DNA-binding protein AlgZ (AmrZ) controls twitching motility and biogenesis of type IV pili. *Journal of bacteriology* 188(1):132-140.
160. Henrichsen J (1972) Bacterial surface translocation: a survey and a classification. *Bacteriological reviews* 36(4):478-503.
161. Lee EC*, et al.* (2001) A highly efficient Escherichia coli-based chromosome engineering system adapted for recombinogenic targeting and subcloning of BAC DNA. *Genomics* 73(1):56-65.

162. Figurski DH & Helinski DR (1979) Replication of an origin-containing derivative of plasmid RK2 dependent on a plasmid function provided in trans. *Proceedings of the National Academy of Sciences of the United States of America* 76(4):1648-1652.
163. Choi KH*, et al.* (2005) A Tn7-based broad-range bacterial cloning and expression system. *Nature methods* 2(6):443-448.
164. Arroyo LA, Mateos I, Gonzalez V, & Aznar J (2009) In vitro activities of tigecycline, minocycline, and colistin-tigecycline combination against multi- and pandrug-resistant clinical isolates of *Acinetobacter baumannii* group. *Antimicrobial agents and chemotherapy* 53(3):1295-1296.
165. Gottig S*, et al.* (2014) Detection of pan drug-resistant *Acinetobacter baumannii* in Germany. *The Journal of antimicrobial chemotherapy* 69(9):2578-2579.
166. Gordon NC & Wareham DW (2010) Multidrug-resistant *Acinetobacter baumannii*: mechanisms of virulence and resistance. *International journal of antimicrobial agents* 35(3):219-226.
167. Walzer G, Rosenberg E, & Ron EZ (2006) The *Acinetobacter* outer membrane protein A (OmpA) is a secreted emulsifier. *Environmental microbiology* 8(6):1026-1032.
168. Weber BS*, et al.* (2013) Genomic and functional analysis of the type VI secretion system in *Acinetobacter*. *PloS one* 8(1):e55142.
169. Brzoska AJ, Hassan KA, de Leon EJ, Paulsen IT, & Lewis PJ (2013) Single-step selection of drug resistant *Acinetobacter baylyi* ADP1 mutants reveals a functional redundancy in the recruitment of multidrug efflux systems. *PloS one* 8(2):e56090.
170. Abd-El-Haleem D, Moawad H, Zaki EA, & Zaki S (2002) Molecular characterization of phenol-degrading bacteria isolated from different Egyptian ecosystems. *Microbial ecology* 43(2):217-224.
171. Mara K*, et al.* (2012) Molecular and phenotypic characterization of *Acinetobacter* strains able to degrade diesel fuel. *Research in microbiology* 163(3):161-172.
172. Varki A (1993) Biological roles of oligosaccharides: all of the theories are correct. *Glycobiology* 3(2):97-130.
173. Neuberger A (1938) Carbohydrates in protein: The carbohydrate component of crystalline egg albumin. *The Biochemical journal* 32(9):1435-1451.
174. Sleytr UB (1975) Heterologous Reattachment of Regular Arrays of Glycoproteins on Bacterial Surfaces. *Nature* 257(5525):400-402.
175. Mescher MF & Strominger JL (1976) Structural (shape-maintaining) role of the cell surface glycoprotein of *Halobacterium salinarium*. *Proceedings of the National Academy of Sciences of the United States of America* 73(8):2687-2691.
176. Szymanski CM, Yao RJ, Ewing CP, Trust TJ, & Guerry P (1999) Evidence for a system of general protein glycosylation in *Campylobacter jejuni*. *Molecular microbiology* 32(5):1022-1030.
177. Faridmoayer A, Fentabil MA, Mills DC, Klassen JS, & Feldman MF (2007) Functional characterization of bacterial oligosaccharyltransferases involved in *O*-linked protein glycosylation. *Journal of bacteriology* 189(22):8088-8098.

178. Balonova L*, et al.* (2012) Characterization of protein glycosylation in *Francisella tularensis* subsp. *holarctica*: identification of a novel glycosylated lipoprotein required for virulence. *Molecular & cellular proteomics : MCP* 11(7):M111 015016.
179. Gebhart C*, et al.* (2012) Characterization of exogenous bacterial oligosaccharyltransferases in *Escherichia coli* reveals the potential for O-linked protein glycosylation in *Vibrio cholerae* and *Burkholderia thailandensis*. *Glycobiology* 22(7):962-974.
180. Logan SM (2006) Flagellar glycosylation - a new component of the motility repertoire? *Microbiology* 152(Pt 5):1249-1262.
181. Power PM, Seib KL, & Jennings MP (2006) Pilin glycosylation in *Neisseria meningitidis* occurs by a similar pathway to wzy-dependent *O*-antigen biosynthesis in *Escherichia coli*. *Biochemical and biophysical research communications* 347(4):904-908.
182. Perez JM, McGarry MA, Marolda CL, & Valvano MA (2008) Functional analysis of the large periplasmic loop of the *Escherichia coli* K-12 WaaL O-antigen ligase. *Molecular microbiology* 70(6):1424-1440.
183. Ruan X, Loyola DE, Marolda CL, Perez-Donoso JM, & Valvano MA (2012) The WaaL O-antigen lipopolysaccharide ligase has features in common with metal ion-independent inverting glycosyltransferases. *Glycobiology* 22(2):288-299.
184. Musumeci MA, Faridmoayer A, Watanabe Y, & Feldman MF (2014) Evaluating the role of conserved amino acids in bacterial *O*-oligosaccharyltransferases by in vivo, in vitro and limited proteolysis assays. *Glycobiology* 24(1):39-50.
185. Kus JV, Tullis E, Cvitkovitch DG, & Burrows LL (2004) Significant differences in type IV pilin allele distribution among *Pseudomonas aeruginosa* isolates from cystic fibrosis (CF) versus non-CF patients. *Microbiology* 150(Pt 5):1315-1326.
186. Smedley JG, 3rd*, et al.* (2005) Influence of pilin glycosylation on *Pseudomonas aeruginosa* 1244 pilus function. *Infection and immunity* 73(12):7922-7931.
187. Nguyen LC*, et al.* (2012) Type IV pilin is glycosylated in *Pseudomonas syringae* pv. *tabaci* 6605 and is required for surface motility and virulence. *Molecular plant pathology* 13(7):764-774.
188. Marchler-Bauer A*, et al.* (2009) CDD: specific functional annotation with the Conserved Domain Database. *Nucleic acids research* 37(Database issue):D205-210.
189. Marchler-Bauer A & Bryant SH (2004) CD-Search: protein domain annotations on the fly. *Nucleic acids research* 32(Web Server issue):W327-331.
190. Marchler-Bauer A*, et al.* (2011) CDD: a Conserved Domain Database for the functional annotation of proteins. *Nucleic acids research* 39(Database issue):D225-229.
191. Aranda J*, et al.* (2010) A rapid and simple method for constructing stable mutants of *Acinetobacter baumannii*. *BMC microbiology* 10:279.
192. Yi EC & Hackett M (2000) Rapid isolation method for lipopolysaccharide and lipid A from gram-negative bacteria. *The Analyst* 125(4):651-656.

193. Tsai CM & Frasch CE (1982) A sensitive silver stain for detecting lipopolysaccharides in polyacrylamide gels. *Analytical biochemistry* 119(1):115-119.
194. Scott NE*, et al.* (2012) Modification of the *Campylobacter jejuni N*-linked glycan by EptC protein-mediated addition of phosphoethanolamine. *The Journal of biological chemistry* 287(35):29384-29396.
195. Scott NE*, et al.* (2011) Simultaneous glycan-peptide characterization using hydrophilic interaction chromatography and parallel fragmentation by CID, higher energy collisional dissociation, and electron transfer dissociation MS applied to the *N*-linked glycoproteome of *Campylobacter jejuni*. *Molecular & cellular proteomics : MCP* 10(2):M000031-MCP000201.
196. Olsen JV*, et al.* (2007) Higher-energy C-trap dissociation for peptide modification analysis. *Nature methods* 4(9):709-712.
197. Vik A*, et al.* (2009) Broad spectrum *O*-linked protein glycosylation in the human pathogen *Neisseria gonorrhoeae*. *Proceedings of the National Academy of Sciences of the United States of America* 106(11):4447-4452.
198. Borud B*, et al.* (2011) Genetic and molecular analyses reveal an evolutionary trajectory for glycan synthesis in a bacterial protein glycosylation system. *Proceedings of the National Academy of Sciences of the United States of America* 108(23):9643-9648.
199. Hu D, Liu B, Dijkshoorn L, Wang L, & Reeves PR (2013) Diversity in the major polysaccharide antigen of *Acinetobacter baumannii* assessed by DNA sequencing, and development of a molecular serotyping scheme. *PloS one* 8(7):e70329.
200. Whitfield C (1995) Biosynthesis of lipopolysaccharide O antigens. *Trends in microbiology* 3(5):178-185.
201. Ielmini MV & Feldman MF (2011) *Desulfovibrio desulfuricans* PglB homolog possesses oligosaccharyltransferase activity with relaxed glycan specificity and distinct protein acceptor sequence requirements. *Glycobiology* 21(6):734-742.
202. Nothaft H*, et al.* (2012) Diversity in the protein N-glycosylation pathways within the *Campylobacter* genus. *Molecular & cellular proteomics : MCP* 11(11):1203-1219.
203. Charbonneau ME*, et al.* (2007) *O*-linked glycosylation ensures the normal conformation of the autotransporter adhesin involved in diffuse adherence. *Journal of bacteriology* 189(24):8880-8889.
204. Cote JP, Charbonneau ME, & Mourez M (2013) Glycosylation of the *Escherichia coli* TibA self-associating autotransporter influences the conformation and the functionality of the protein. *PloS one* 8(11):e80739.
205. Aas FE*, et al.* (2006) *Neisseria gonorrhoeae* type IV pili undergo multisite, hierarchical modifications with phosphoethanolamine and phosphocholine requiring an enzyme structurally related to lipopolysaccharide phosphoethanolamine transferases. *The Journal of biological chemistry* 281(38):27712-27723.
206. Zhou M & Wu H (2009) Glycosylation and biogenesis of a family of serine-rich bacterial adhesins. *Microbiology* 155(Pt 2):317-327.

207. Tang G & Mintz KP (2010) Glycosylation of the collagen adhesin EmaA of *Aggregatibacter actinomycetemcomitans* is dependent upon the lipopolysaccharide biosynthetic pathway. *Journal of bacteriology* 192(5):1395-1404.
208. Hunger M, Schmucker R, Kishan V, & Hillen W (1990) Analysis and nucleotide sequence of an origin of DNA replication in *Acinetobacter calcoaceticus* and its use for *Escherichia coli* shuttle plasmids. *Gene* 87(1):45-51.
209. Dijkshoorn L*, et al.* (1996) Comparison of outbreak and nonoutbreak *Acinetobacter baumannii* strains by genotypic and phenotypic methods. *Journal of clinical microbiology* 34(6):1519-1525.
210. Nakar D & Gutnick DL (2001) Analysis of the *wee* gene cluster responsible for the biosynthesis of the polymeric bioemulsifier from the oil-degrading strain *Acinetobacter lwoffii* RAG-1. *Microbiology* 147(Pt 7):1937-1946.
211. Wacker M*, et al.* (2002) N-linked glycosylation in *Campylobacter jejuni* and its functional transfer into *E. coli*. *Science* 298(5599):1790-1793.
212. Feldman MF*, et al.* (2005) Engineering N-linked protein glycosylation with diverse O antigen lipopolysaccharide structures in *Escherichia coli*. *Proceedings of the National Academy of Sciences of the United States of America* 102(8):3016-3021.
213. Bartual SG*, et al.* (2005) Development of a multilocus sequence typing scheme for characterization of clinical isolates of *Acinetobacter baumannii*. *Journal of clinical microbiology* 43(9):4382-4390.
214. Esterly J, Richardson CL, Eltoukhy NS, Qi C, & Scheetz MH (2011) Genetic Mechanisms of Antimicrobial Resistance of *Acinetobacter baumannii* (February). *The Annals of pharmacotherapy*.
215. Gifford B, Tucci J, McIlroy SJ, & Petrovski S (2014) Isolation and characterization of two plasmids in a clinical *Acinetobacter nosocomialis* strain. *BMC research notes* 7:732.
216. Duffin PM & Seifert HS (2012) Genetic transformation of *Neisseria gonorrhoeae* shows a strand preference. *FEMS microbiology letters* 334(1):44-48.
217. Seitz P & Blokesch M (2013) DNA-uptake machinery of naturally competent *Vibrio cholerae*. *Proceedings of the National Academy of Sciences of the United States of America* 110(44):17987-17992.
218. Jen FE*, et al.* (2013) Dual pili post-translational modifications synergize to mediate meningococcal adherence to platelet activating factor receptor on human airway cells. *PLoS pathogens* 9(5):e1003377.
219. Jennings MP, Jen FE, Roddam LF, Apicella MA, & Edwards JL (2011) *Neisseria gonorrhoeae* pilin glycan contributes to CR3 activation during challenge of primary cervical epithelial cells. *Cellular microbiology* 13(6):885-896.
220. Gault J*, et al.* (2014) Complete posttranslational modification mapping of pathogenic *Neisseria meningitidis* pilins requires top-down mass spectrometry. *Proteomics* 14(10):1141-1151.

221. Tan RM*, et al.* (2015) Type IV Pilus Glycosylation Mediates Resistance of *Pseudomonas aeruginosa* to Opsonic Activities of the Pulmonary Surfactant Protein-A. *Infection and immunity*.
222. Stevenson G, Andrianopoulos K, Hobbs M, & Reeves PR (1996) Organization of the *Escherichia coli* K-12 gene cluster responsible for production of the extracellular polysaccharide colanic acid. *Journal of bacteriology* 178(16):4885-4893.
223. Patel KB, Ciepichal E, Swiezewska E, & Valvano MA (2012) The C-terminal domain of the *Salmonella enterica* WbaP (UDP-galactose:Und-P galactose-1-phosphate transferase) is sufficient for catalytic activity and specificity for undecaprenyl monophosphate. *Glycobiology* 22(1):116-122.
224. Merino S*, et al.* (2011) A UDP-HexNAc:polyprenol-P GalNAc-1-P transferase (WecP) representing a new subgroup of the enzyme family. *Journal of bacteriology* 193(8):1943-1952.